



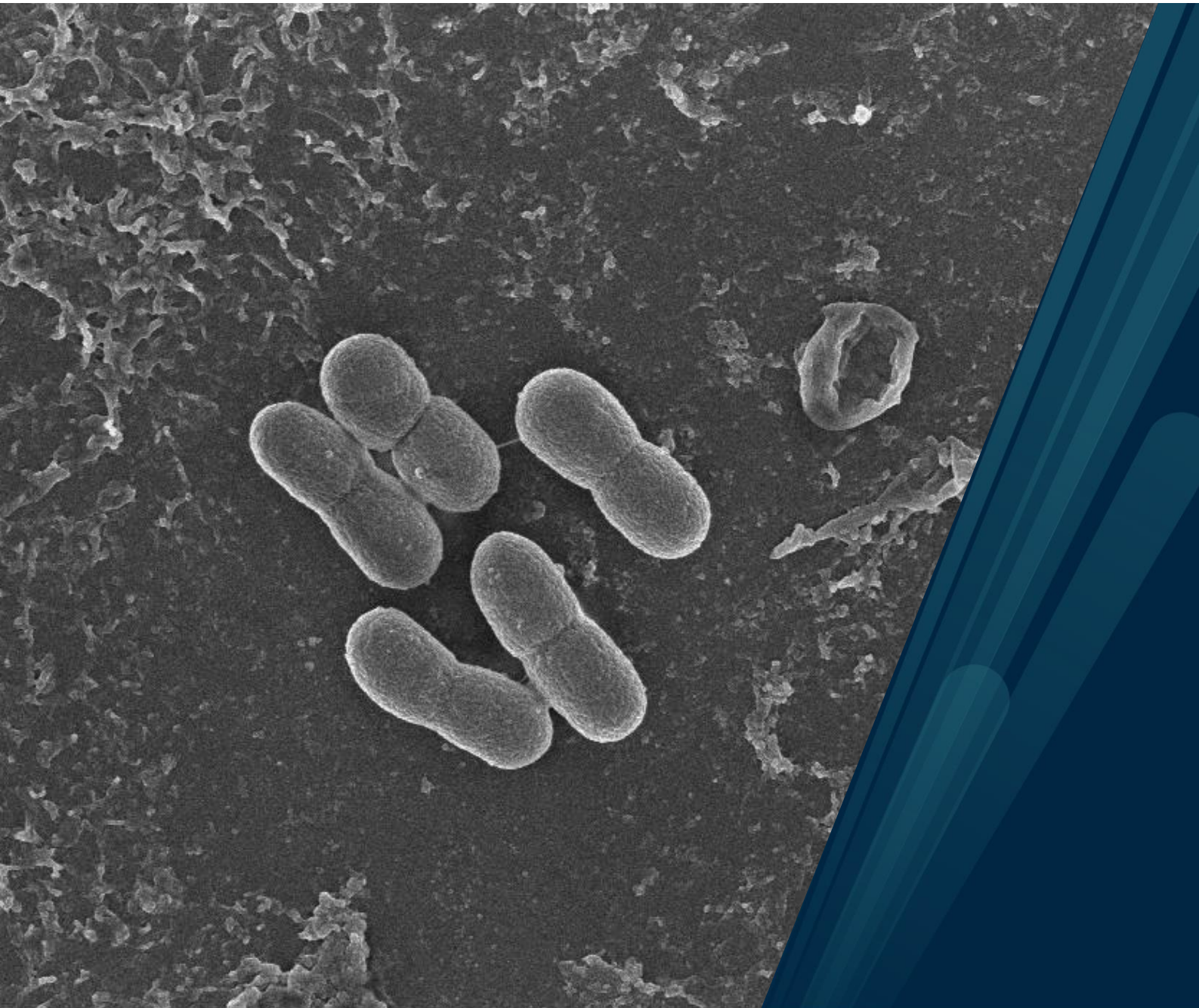
UiT The Arctic University of Norway

NFH – The Norwegian College of Fisheries

The effect of microplastic on natural transformation and biofilm formation using *Acinetobacter baylyi* as a model organism

Marte Strømmen

Master's thesis in Marine Biotechnology, BIO-3901, May 2022



Acknowledgements

This master thesis in Marine Biotechnology at UiT – The Arctic University of Norway was conducted at NORCE and NFH – The Norwegian College of Fisheries from August 2021 until May 2022. I would like to start by thanking all of my supervisors Odd-Gunnar Wikmark, Klara Stensvåg and Klaus Harms for all of your guidance and encouragement, and helping me with laboratory work and analysis, and for always answering my emails.

I am also grateful for the warm welcome from everyone working at NORCE and your good company in stressful periods. A special thanks to Idun Grønsberg for all of your kind help at the lab, and to my fellow biotechnology students and office mates Trygve Strømsnes, Elise Heimland, Mitra Azad, Sebastian Schmidke, and Maria Pham for a really great time and for all your support, understanding and kindness. I also want to thank Randi Olsen and Tom-Ivar Eilertsen at AMCF – The Advanced Microscopy Core Facility for all your help regarding the biofilm fixation and scanning electron microscopy.

I have to thank my friends for a great time outside the master office - for memorable hikes and conversations, and for always supporting me. A big thanks to my family for your encouragement and for pretending to understand what I have been doing and talking about for the last couple of months.

Tromsø, May 2022

Marte Strømmen

Abstract

Microplastic pollution is a big and rapidly increasing environmental problem in the world. Although the direct effects of microplastic pollution are well-studied the indirect effects are hardly investigated, especially in the context of spreading antibiotic resistance genes. Antibiotic resistance is a natural phenomenon, but the misuse and overuse of antibiotics has led to a rapid development and spread globally, and the result is that antibiotics become ineffective, and infections become more difficult or almost impossible to treat. Antibiotic resistance is now considered as one of the biggest threats to global health, and therefore it is necessary and highly important to investigate and evaluate the impact of microplastics in the aquatic environment. The major aim of this study was to evaluate how the presence of microplastics affects the potential for DNA uptake via natural transformation in the naturally competent bacteria *Acinetobacter baylyi*, to obtain a better understanding of horizontal gene transfer of antibiotic resistant genes within microplastic-associated communities in the aquatic environment. One important subgoal was to evaluate how DNA uptake via transformation in *A. baylyi* can be affected by the presence of different concentrations of microplastic polymers, including high density polystyrene (HDPS), high density polyethylene (HDPE), polypropylene (PP), polyvinyl chloride A (PVC A), and polyvinyl chloride B (PVC B). The results obtained in this study revealed that the transformation frequency alters in the presence and absence of different concentrations of polymers. The results indicate small effects, but the trend is clear; the DNA uptake is most efficient in the presence of PP and PVC B. Additional analysis of natural transformation of *A. baylyi* biofilms grown on microplastics for 96 h, showed that natural transformation on PP was most efficient. The effect of weathering processes on the virgin microplastic surface morphology revealed that weathering processes changes the surface, with an increase in surface roughness, pores and cracks. The early biofilm formation of *A. baylyi* on the different polymers were found to differ and revealed that most biofilm formation was found on the polymers PVC A, PVC B and PP. Scanning electron microscopic analysis revealed that the bacterial colonization of *A. baylyi* started in the formed cracks and wells before colonizing smooth surfaces. The results provide new insight into evaluating the risks caused by plastic wastes in the environment, and this study is laying the foundation for further investigations of the interactions between microplastics associated with antibiotic resistant bacteria.

Abbreviations

ABR	Antibiotic resistance
ARGs	Antibiotic resistance genes
ARB	Antibiotic resistant bacteria
CFU	Colony forming unit
DNA	Deoxyribonucleic acid
dsDNA	Double stranded DNA
EPS	Extracellular polymeric substances
HGT	Horizontal gene transfer
LB	Luria Bertani
MDR	Multidrug resistance
MP	Microplastic
OD	Optical density
PBS	Phosphate-buffered saline
PE	Polyethylene
PP	Polypropylene
PS	Polystyrene
PVC	Polyvinylchloride
QS	Quorum sensing
RIC	Recycle identification code
RNA	Ribonucleic acid
SEM	Scanning electron microscopy
ssDNA	Single stranded DNA
UV	Ultraviolet
WHO	World health organization
WWTP	Wastewater treatment plant

Table of Contents

Acknowledgements	I
Abstract	II
Abbreviations	III
1 Introduction	1
1.1 Background.....	1
1.2 Plastics.....	1
1.3 Microplastics	3
1.3.1 Microplastics as important vectors for bacteria	4
1.4 The plastisphere concept	5
1.5 Bacterial biofilm formation	6
1.6 Horizontal gene transfer	7
1.6.1 Natural transformation	8
1.7 The competent bacterium <i>A. baylyi</i>	9
1.7.1 Twitching motility.....	9
1.8 Antibiotics	10
1.8.1 Antibiotic resistance	10
1.9 Interactions between microplastics and antibiotic resistance genes.....	12
1.10 The MicroPlastResist project.....	13
2 Principles of methods	14
2.1 <i>A. baylyi</i> as a model organism.....	14
2.2 Culture media	14
2.2.1 Liquid media	14
2.2.2 Solid media.....	15
2.3 DNA extraction.....	15
2.4 Methodology of biofilm research	15
2.4.1 Crystal violet staining.....	15

2.4.2	Scanning electron microscopy	16
2.5	Aim of the study	17
3	Materials and Methods	18
3.1	Workflow.....	18
3.2	Biological material	19
3.3	Chemicals and antibiotics.....	19
3.4	Microplastic polymers	20
3.5	Kanamycin stock solution	21
3.6	Culture media	21
3.6.1	Liquid culture media	21
3.6.2	Solid culture media.....	21
3.7	DNA extraction with the peqGOLD bacterial DNA kit	21
3.8	Measuring DNA concentrations with NanoDrop	22
3.9	Transformation of <i>A. baylyi</i> in the presence of MP polymers.....	22
3.10	Quantification of biofilm formation on MP surfaces.....	23
3.11	Bacterial biofilm detachment methods	23
3.12	Transformation of <i>A. baylyi</i> biofilms on MP polymers	23
3.13	Characterization of MP surface morphology and bacterial biofilm formation with SEM	24
3.14	Statistical analysis.....	24
4	Results	25
4.1	DNA concentrations and purity	25
4.2	Natural transformation and twitching motility	26
4.3	Natural transformation of <i>A. baylyi</i> under influence of different concentrations of microplastic polymers	26
4.4	The early biofilm formation of <i>A. baylyi</i> on MP polymers	27
4.5	Natural transformation of <i>A. baylyi</i> biofilms grown on microplastic polymers for 96 h	28

4.6	Morphology characteristics of virgin and aged microplastic polymers with SEM...	29
4.7	Characterization of early biofilm formation of <i>A. baylyi</i> on microplastic polymers with SEM.....	31
5	Discussion	34
5.1	Use <i>A. baylyi</i> as a model organism.....	34
5.1.1	Twitching motility of <i>A. baylyi</i>	35
5.2	Effect of selected microplastic polymers.....	36
5.3	Natural transformation.....	36
5.3.1	Natural transformation of <i>A. baylyi</i> with microplastic polymers	36
5.4	<i>A. baylyi</i> biofilm formation on microplastic polymers studied with optical density.	38
5.4.1	Natural transformation of <i>A. baylyi</i> biofilm grown on microplastic polymers for 96 h	39
5.5	Scanning electron microscopy	40
5.5.1	Virgin and aged microplastic polymers characteristics.....	40
5.5.2	Early <i>A. baylyi</i> biofilm formation on microplastic polymers.....	40
5.6	Further studies	41
6	Conclusion.....	42
7	References	43
	Appendix	

1 Introduction

1.1 Background

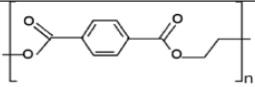



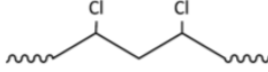



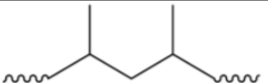

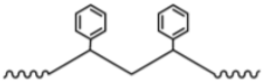

Today it is difficult to imagine a world without plastics since it is used in a number of different applications. The steady increase in use of plastics has led to an increasing accumulation in the environment, and this accumulation has become a big global concern (Kim, 2021). A large part of the concern is the fact that plastics can degrade into smaller pieces called microplastics (MPs), resulting from physical and biological degradation (Arias-Andres et al., 2018). Microplastic provides a new microbial niche, collectively known as the plastisphere, due to the hydrophobic surface that readily supports the attachment of bacteria and formation of bacterial biofilm (Yang et al., 2020b, Zettler et al., 2013). Although the direct effects of MP pollution are increasingly studied, the indirect effects are hardly investigated, especially the fact that MP can serve a vector for transport and spread of antibiotic resistance genes (ARGs) (Liu et al., 2021, Marathe and Bank, 2022). Antibiotic resistance (ABR) is a natural phenomenon, but the misuse and overuse of antibiotics has led to a rapid development and spread globally (Aminov, 2010). ARGs can be transferred from pathogenic bacteria to other bacteria species through horizontal gene transfer (HGT), and the result is that antibiotics become ineffective, and infections become more difficult or almost impossible to treat (Willey, 2017). World Health Organization (WHO) are now considering the spread of ABR, especially multidrug resistance (MDR), as one of the biggest threats to global health, and therefore it is important and necessary to look at the impact of microplastics in the environment (Talebi Bezzmin Abadi et al., 2019).

1.2 Plastics

Plastics are synthetic or semi-synthetic material made from long chains of polymeric molecules that are created from organic and inorganic raw materials such as carbon, silicon, hydrogen, oxygen and chloride (Ivar do Sul and Costa, 2014). Their plasticity makes it possible to be shaped into various objects, and this adaptability, plus a wide range of other properties, such as being lightweight, durable, flexible, corrosion-resistant, strong and inexpensive to produce, has led to its widespread use (Thompson et al., 2009). The breakthrough came in 1907, when Leo Baekeland invented Bakelite, the first fully synthetic mass-produced plastic (Crespy et al., 2008). Since then, plastics has revolutionized our daily lives, but at the same time resulted in detrimental consequences for ecosystems, global health and food security worldwide (Costa et al., 2020).

The production of plastics have increased drastically worldwide over the last 60 years, and is still increasing, with the current global production at approximately 300 million tons yearly (Nerland et al., 2014). It is estimated that over 2 billion people still don't have access to solid waste management services, and in the absence of changes to current waste management services, the flux of land-sourced plastics into the ocean is projected to continue increasing exponentially over the next decade, driven by the global population growth and plastic consumption trends (Sebille et al., 2016). Around 70% of the global production of plastics is concentrated in 6 major polymer types, and unlike most other plastics, these can be identified by their recycle identification code (RIC). Geyer et al. (2017) presented the first global analysis of all mass-produced plastics ever made by developing and combining global data on production, use, and end-of-life fate of polymer resins, synthetic fibers, and additives into a comprehensive material flow model. According to the study, the abundant categories in worldwide production, shown in Table 1, include low density polyethylene (15.7%), high density polyethylene (12.8%), polypropylene (16.7%), polyvinyl chloride (9.3%), polystyrene (6.1%), and polyethylene terephthalate (6.1%). These plastics have stable carbon-hydrogen bonds with no side groups (PE), with methyl group (PP), with phenyl group (PS), with chloride group (PVC), and with two carboxylic and two hydroxyl groups (PET).

Table 1: Some of the major MP polymers produced and found in the aquatic environment. The polymers PET, HDPE, PVC, LDPE, PP, and PS presented with short, chemical formula, molecular structure and RIC.

Polymer type	Short	Chemical formula	Molecular structure	Recycle ID code
Polyethylene terephthalate	PET	$(C_{10}H_8O_4)_n$		
High Density Polyethylene	HDPE	$(C_2H_4)_n$		
Polyvinyl chloride	PVC	$(C_2H_3Cl)_n$		
Low Density Polyethylene	LDPE	$(C_2H_4)_n$		
Polypropylene	PP	$(C_3H_6)_n$		
Polystyrene	PS	$(C_8H_8)_n$		

1.3 Microplastics

Microplastics are small pieces of plastic (<5 mm) that occurs in the environment as a consequence of plastic pollution (Law and Thompson, 2014). MP pollution is a widespread and global environmental problem that is projected to increase in upcoming decades creating significant challenges for its management and prevention (Marathe and Bank, 2022). MP are present in a variety of products, such as bottles, plastic bags, cosmetics, tires and synthetic clothing, and many of these products find their way into the environment via land-based sources such as illegal dumping and inadequate waste management, industrial activity, unfiltered wastewater, coastal littering, and storm water runoffs, or maritime activities such as commercial fishing, shipping, offshore oil platforms, and illegal dumping (Nerland et al., 2014, Sebille et al., 2016). MP can be classified as either primary or secondary based on their original size (Yang et al., 2020b) as shown in Figure 1. Primary MP are directly released into the environment as small particles, for instance via personal care products such as toothpaste (Nerland et al., 2014). Secondary MP are derived from weathering processes and the abiotic breakdown of larger plastics, for instance via photodegradation, mechanical breakup, aquatic immersion and erosion (Boucher and Friot, 2017). A third category, which is often kept separate from the others, is industrial plastic which refers to resin pellets used as precursors in plastic manufacturing processes (Nerland et al., 2014). MP's small size makes it difficult to remove once present in the environment, and it is also hard to avoid that it enters at all, since it is easily lost, and it has the ability to escape the filters of wastewater treatment plants (WWTPs).



Figure 1: **Examples of microplastic found in the marine environment.** Including primary microplastic, secondary microplastic and resin pellets. Modified from Nerland et al. (2014).

Since 2004, there has been a steady increase in the knowledge available about MP contamination in the ocean (Thompson et al., 2004), and this is reflected by the increasing number of publications the recent years. Eriksen et al. (2014) estimated by data obtained from surface net tows from 2007-2013 that at least 5.25 trillion particles weighting 268,940 tons are floating at sea, but this estimate does not account for the amount present on shorelines, on the seabed, suspended in the water column, and within organisms. Despite the growing plastic production and discharge into the environment, researchers have struggled to detect expected increases of marine plastic debris in sea surfaces, which has caused discussion about possible marine plastic debris sinks (Erni-Cassola et al., 2019). Earlier studies have assumed that MP float and therefore focused sampling on the surface layers, but a meta-analysis by Erni-Cassola et al. (2019) confirmed the presence of marine plastic debris also in subsurface layers in the ocean. Once MP enters the ocean, polymers with low-density tend to float on the sea surface or in the water column, and polymers with high-density tend to accumulate on the ocean floor (Rochman et al., 2016). Floating polymers have the potential to be transported via currents and other hydrodynamic processes (Nerland et al., 2014) or reach the sea floor as marine snow, where it is produced as a biologically enhanced aggregation, including organic and inorganic particles such as bacteria, phytoplankton and zooplankton (Van Cauwenberghe et al., 2013).

1.3.1 Microplastics as important vectors for bacteria

Recent studies have highlighted the role of MP as important vectors for bacteria (Yang et al., 2020b). Arias-Andres et al. (2018) have studied interactions between MP and their associated bacterial biofilms, and the results revealed that MP represents an artificial surface for bacterial colonization, development of interactions, and gene exchange, which distinguish from the microbial composition of free-living communities in the surrounding water. Critical factors controlling microbial biofilm formation on MP polymers are: (I) the polymer type, where the polymer type affects biofilm formation directly; (II) roughness, surface area, and hydrophobicity, where aged MP exposed to UV irradiation and other weathering processes usually have increased surface area, roughness and polarity compared to virgin samples; (III) microbial growth, which represents a temporal succession process that can be divided into early, mid and late colonization period; (IV) microbial community composition, which depends on the surrounding microbial communities; and (V) environmental conditions including nutrient availability (carbon, phosphorus etc.), pollutants (antibiotics, toxic metals etc.), physicochemical parameters (light, pH, temperature, salinity etc.) and aquatic biota (animals, plants and other microbes) (Yang et al., 2020b, Tu et al., 2020).

Marine plastic debris represent a novel artificial substrate and vector for bacteria, and the presence of MP in the marine environment has shown to enhance horizontal gene transfer in bacteria and thus, may serve as a reservoir for metal resistance and antibiotic resistance genes (Marathe and Bank, 2022). Therefore, microplastic polymers can be regarded as a new microbial niche in the marine environment (Yang et al., 2020b). The role of MP in the spread of antibiotic resistant genes is a relatively new research topic that has been of great interest to scientists who aim to investigate whether or not microplastic polymers are enriching antibiotic resistant bacteria, and if so, learn more about the microbial communities involved. The indirect effects of microplastics have not been well studied especially in the context of seafood safety and global food security, and these effects may pose a significant hazard for human health regarding the spread of pathogenic microbes and antibiotic resistance genes.

1.4 The plastisphere concept

One of the critical mechanisms of the microplastic antibiotic resistance connection is the plastisphere concept (Marathe and Bank, 2022). The plastisphere is a term used to refer to ecosystems that have evolved to live in human-made plastic environments. The concept was first presented by Zettler et al. (2013) who collected marine plastic debris at multiple locations in the North Atlantic and used scanning electron microscopy (SEM) and next-generation sequencing to characterize the attached microbial communities. MP surfaces in the marine ecosystems are novel ecological habitats for marine organisms, and the composition and diversity of biofilm communities have been investigated in various studies (Tu et al., 2020, McCormick et al., 2014, Reisser et al., 2014). The study by Zettler et al. (2013) reported that microbial communities attached to plastic debris were diverse and composed of heterotrophs, autotrophs, predators, symbionts, and pathogens, and were distinct from the surrounding marine waters (Yang et al., 2020b). Modern molecular methods, especially high-throughput DNA sequencing, have increased the understanding of microbes that colonize marine plastic debris (Amaral-Zettler et al., 2020), and recent studies have revealed that many of the bacteria that colonize plastic particles are natural biofilm formers that prefer an attached lifestyle over a free-living one. The understanding of the plastisphere is an important factor for forming scientific questions regarding the overall direct and indirect impacts of MP pollution. Primarily because of the long residence time of MPs in the environment and the potential for long-range transport and the associated risks of transfer of pathogens and disease.

1.5 Bacterial biofilm formation

Bacterial biofilms are complex, diverse and dynamic microbial communities that are attached to a surface or to each other, and play a significant role in the persistence of bacterial infections (Rabin et al., 2015). Biofilm formation enables single-cell bacteria to assume a temporary multicellular lifestyle in a self-produced matrix, mainly composed of secreted proteins, extracellular DNA and polysaccharides, collectively referred to as extracellular polymeric substances (EPS) (Muhammad et al., 2020, Kostakioti et al., 2013). The matrix acts as a protective coating, and protects bacteria from various environmental factors such as high and low temperatures and pH, UV-radiation, high salinity, poor nutrients availability and antibiotics (Yin et al., 2019). In the matrix, bacterial interactions can promote the spread of ARGs and other drug-resistant markers, and as a result, biofilm-forming pathogens persist for instance antibiotics, and establishing infections that could be difficult or impossible to treat (Kostakioti et al., 2013). Bacterial biofilm formation includes 5 main phases, shown in Figure 2: (I) the attachment phase where bacteria attach to the surface; (II) the colonization phase where bacteria interact with the surface using bacterial adhesins; (III) the development phase where bacteria produces extracellular polymeric substances; (IV) the mature phase where bacteria use quorum sensing to synthesize and release signalling molecules; and (V) the dispersal phase where bacteria detach and the biofilm disperses (Muhammad et al., 2020; Yin et al., 2019).

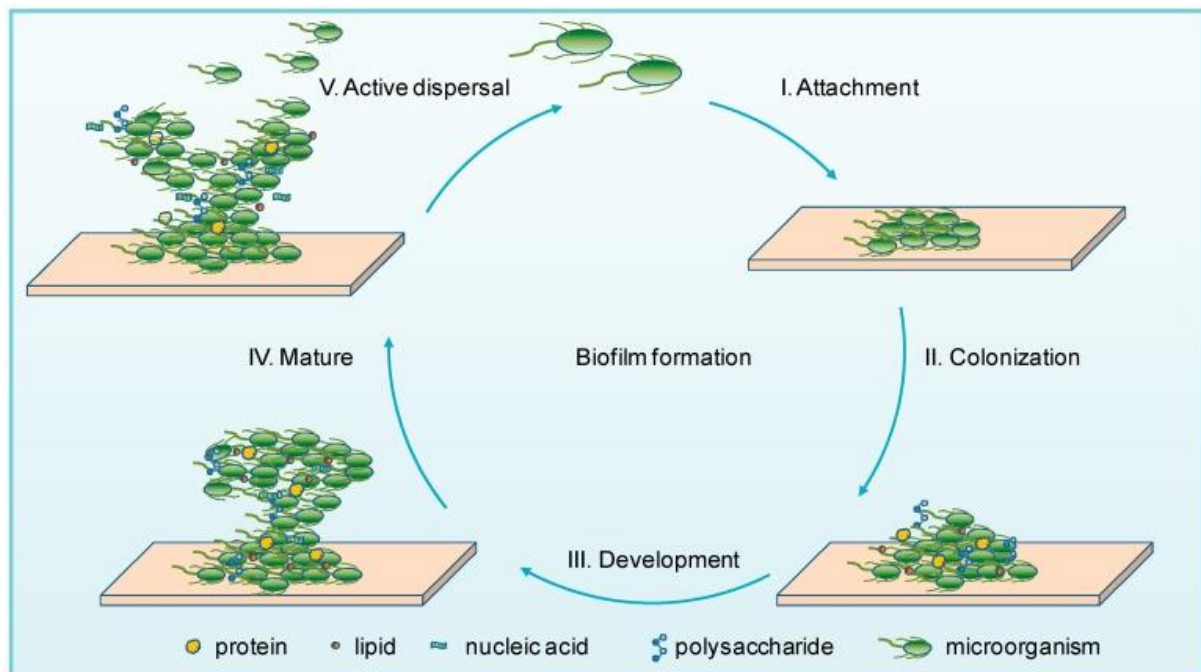


Figure 2: A schematic representation of biofilm formation of bacteria (Muhammad et al., 2020, Yin et al., 2019).

1.6 Horizontal gene transfer

Bacteria have evolved different mechanisms for taking up DNA from the environment and incorporating it into their genomes through horizontal gene transfer (HGT). HGT plays an important role in evolution of bacteria (Emamalipour et al., 2020). It may provide a potential advantage for the bacterium because it enables an individual cell to accumulate advantageous mutations originating from separate individuals or even acquire genetic material from other species, and this is therefore of primary concern in the medical field (Sun, 2018, Andam et al., 2011). The spread and transfer of ARGs plays an important role in the development of ABR bacteria. Although bacteria are able to establish ABR through spontaneous mutations, development of multidrug resistance in the bacteria would take a long time if it only relies on self-adaptive mutation (Sun et al., 2019). HGT allows bacteria to exchange ARGs, and the genes can be transferred to other bacteria species through 3 different natural mechanisms shown in Figure 3: (I) natural transformation, where the bacteria take up DNA from the environment and adds it to the genomic material into the recipient cell; (II) transduction, where bacteriophages transfer a fragment of DNA from one bacterium to another; and (III) conjugation, where there is a transfer of DNA from a living donor bacterium to a living recipient bacterium by cell-to-cell contact (Burmeister, 2015, Zamani Dahaj, 2015). Once transferred, the genes and pathogens continue to evolve, often resulting in bacteria with greater resistance (Burmeister, 2015).

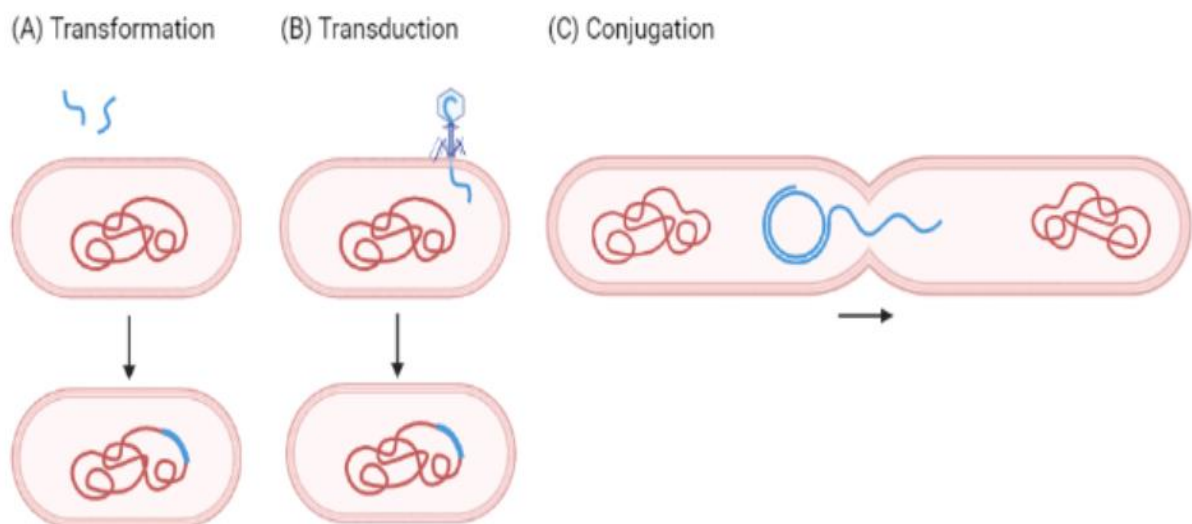


Figure 3: **The major pathways in horizontal gene transfer for bacteria.** (A) Bacterial transformation, (B) bacterial transduction, and (C) bacterial conjugation. Modified from Vernikos and Medini (2014).

1.6.1 Natural transformation

Natural transformation was discovered in *Streptococcus pneumoniae* in 1928 by the bacteriologist Fred Griffith, who observed that *S. pneumoniae* could become infectious after being exposed to a heat-killed infectious bacteria strain (Willey, 2017). He discovered that there were transformation mechanisms from the heat-killed strain that made the apathogenic strain infectious, and this process was in 1944 identified as natural transformation by Oswald Avery (Zamani Dahaj, 2015). Natural transformation involves bacterial DNA uptake from the surrounding environment and incorporation of the genomic material into the recipient cell (Sun, 2018), and for natural transformation to occur, bacterial cells must first develop a regulated physiological state of competence (Thomas and Nielsen, 2005). Competence is a complex phenomenon that is induced at a certain stage of growth, and some bacteria become competent during early exponential phase, while others become competent in stationary phase.

Natural transformation is a multistep process that can be divided into 4 distinct phases, shown in Figure 4: (I) a cell in competent state; (II) binding of exogenous dsDNA from the surrounding environment to cell-surface located receptors; (III) uptake of one of the two strands of the transforming dsDNA into the competent cell; and (IV) integration of the ssDNA into the bacterial chromosome, providing that sufficient homology is present, and its expression, due to the presence of specific membrane proteins that import the DNA (Palmen and Hellingwerf, 1997). Gram-negative and Gram-positive bacteria use similar proteins as the main components of their DNA uptake machinery, but the major differences arise from the need for Gram-negative bacteria to move dsDNA across the outer membrane prior to its translocation as ssDNA across the cytoplasmic membrane.

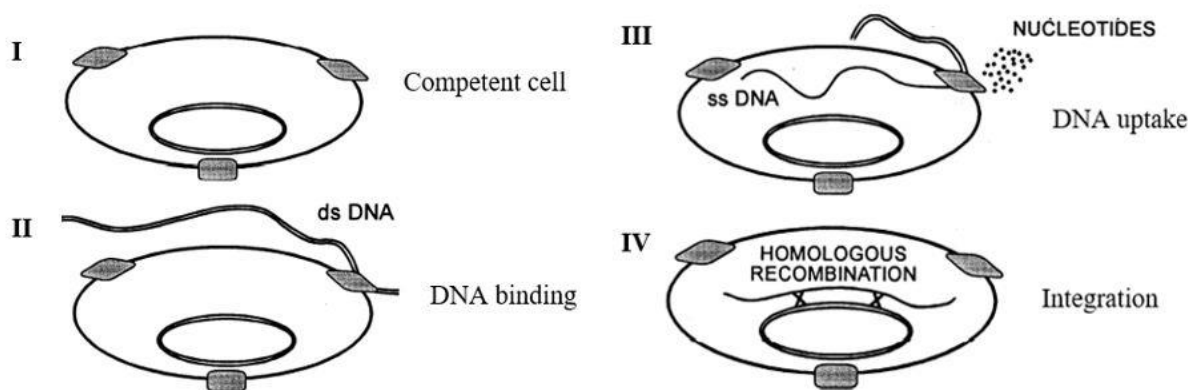


Figure 4: A schematic representation of the natural transformation processes. Modified from Palmen and Hellingwerf (1997).

1.7 The competent bacterium *A. baylyi*

Members of the genus *Acinetobacter* are widely distributed in nature, and *A. baylyi* is a model strain to study the molecular basis of natural transformation and competence in Gram-negative bacteria (Zeidler and Müller, 2019). *A. baylyi* are widespread in nature and can be obtained from soil, water and living organisms (Barbe et al., 2004). The *A. baylyi* strain ADP1, previously known as *A. calcoaceticus* BD413 or LMD 82.3, is a non-pathogenic model for the Gram-negative *Acinetobacter* genus, that are tolerant of wide temperature ranges and desiccation, and can use a diverse array of carbon sources (Leong et al., 2017). The strain is suitable as a model organism in laboratory experiments, and it has been used for more than 35 years because it is well characterized, but also due to its genetic characteristics, robust physiological properties such as nutritional versatility, fast growth and easy culturing (Elliott and Neidle, 2011, Santala and Santala, 2021, Kannisto et al., 2014). The interest in ADP1 as a model organism stems from genetic opportunities afforded by its transformation and recombination capabilities (Elliott and Neidle, 2011). *A. baylyi* is convenient for studying the possible benefits of natural transformation for three reasons: (I) competence is expressed upon dilution into new medium; (II) the bacteria stay competent during most of the log phase; and (III) most of the cells in a population are competent for DNA uptake at the same time (Utne et al., 2015). ADP1 is highly competent for transformation, and has the potential for the uptake and chromosomal incorporation of exogenous DNA, including foreign and linear DNA (Barbe et al., 2004). As an example of the strain's competence, every cell in the population could take up more than 60 molecules of DNA at peak transformation efficiency (Leong et al., 2017).

1.7.1 Twitching motility

Five major methods of bacterial movement have been observed and bacteria use the motility to move toward nutrients such as sugars and amino acids, and away from many harmful substances and bacterial waste products (Willey, 2017). Twitching motility, which is one method for bacterial movement in *A. baylyi*, is a special kind of bacterial surface translocation that may lead to the production of spreading zones, or swarming, on solid surfaces (Henrichsen, 1983). The name "*Acinetobacter*" comes from the Greek word "akineto" and means "non-motile", because an early taxonomic study suggested that a non-motile phenotype was a common characteristic for this genus (Corral et al., 2021). However, many strains of *Acinetobacter* are motile, through twitching and surface-associated motility. The phenomenon twitching was already discovered and reported in 1961 by Lautrop in *A. calcoaceticus*, and is characterized by short, intermittent, jerky motions of up to several micrometers in length (Willey, 2017). It is

mediated by the extension and retraction of the IV pili to a surface using the distal end of the pili (Clemmer et al., 2011), and when the pilus retracts, the cell is pulled forward. Henrichsen (1972) concluded that twitching on solid agar plates are normally dependent on the availability of a surface film of liquid and moist.

1.8 Antibiotics

Antibiotics are a class of secondary metabolites produced by microorganisms, such as soil bacteria and fungi, as well as chemically synthesized or semi-synthesized analogous compounds, which kill or inhibit growth of other microorganisms, such as bacteria (Clardy et al., 2009, Ben et al., 2019). In 1928, Fleming discovered penicillin which was one of the greatest medical advances of the 20th century since antibiotics could cure patients with bacterial infections while leaving human cells and tissues unaffected (O'Neill, 2014). In addition to treat infectious diseases, antibiotics made many modern medical interventions possible, including organ transplantation, open-heart surgeries and cancer treatments (Hutchings et al., 2019). Antibiotics are classified into 5 major groups, according to their mode of action: (I) cell wall synthesis inhibition; (II) protein synthesis inhibition; (III) nucleic acid synthesis inhibition; (IV) antimetabolites; and (V) cell membrane disintegration (Uluseker et al., 2021). Antibiotics are not only used in the treatment of humans, but nowadays antibiotics are also extensively used in the animal husbandry industry, aquaculture, agriculture, bee-keeping, horticulture, food preservation, and veterinary use (Mann et al., 2021, Al-Waili et al., 2012, Meek et al., 2015), and therefore antibiotics can enter the marine environment through a various pathways, for instance via the discharge of municipal and industry wastewater (Ben et al., 2019).

1.8.1 Antibiotic resistance

The discovery of antibiotics revolutionised healthcare, but since then, a gradual decline in antibiotic discovery and development, and the evolution of drug resistance in many human pathogens has become an increasing global health problem (Hutchings et al., 2019). Antibiotic resistance is the ability of bacteria to overcome and resist exposure to antibiotic substances, and this is possible by the acquisition of ARGs (Yang et al., 2020a). Bacteria have developed 4 main types of resistance mechanisms against antibiotics: (I) the efflux pumps, which effectively excrete antibiotics from the cell; (II) inactivation of antibiotics by hydrolysis or by conversion of functional groups; (III) target by-pass which includes new pathways to circumvent the originally targeted enzyme, overproduction of the target compound, structural changes in the cell wall, and prevention of the antibiotic to bind to its target; and (IV) modification of the

antibiotic targets themselves (Uluseker et al., 2021). Multiple types of resistance mechanisms may simultaneously confer resistance against the same family of antibiotics, and conversely, one type of resistance mechanism can also confer resistance against more than one type of antibiotics.

These processes occur naturally, but the misuse and overuse of antibiotics is accelerating the processes (Davies and Davies, 2010). The result is that antibiotics become ineffective, and infections become more difficult or almost impossible to treat (Willey, 2017). The World Health Organization has named antibiotic resistance as one of the three most important public health threats of the 21st century (Munita and Arias, 2016). WHO is now warning of a return to the pre-antibiotic era if the world does not urgently change the use of antibiotics. In 2017, they published a list of antibiotic resistance bacteria priority pathogens, shown in Table 2, to guide and promote research and development of new antibiotics (Tacconelli et al., 2018). The list is divided into three categories (critical, high and medium priority) which includes 12 different bacteria families that pose a large threat to human health because of the diseases they can cause and the loss of effective antibiotics to treat them (Ismail et al., 2021). Part of the issue is to understand how antibiotic resistance genes spread in different environments to prevent the spread existing and the development of new ARGs (Uluseker et al., 2021).

Table 2: **The list of ABR priority pathogens by WHO** (Tacconelli et al., 2018).

Priority	Bacteria species	Antibiotic resistance
Critical	<i>Acinetobacter baumannii</i>	Carbapenem-resistant
	<i>Pseudomonas aeruginosa</i>	Carbapenem-resistant
	<i>Enterobacteriaceae</i>	Carbapenem-resistant, ESBL-producing
High	<i>Enterococcus faecium</i>	Vancomycin-resistant
	<i>Staphylococcus aureus</i>	Methicillin-resistant, vancomycin-intermediate and resistant
	<i>Helicobacter pylori</i>	Clarithromycin-resistant
	<i>Campylobacter</i> spp.	Fluoroquinolone-resistant
	<i>Salmonellae</i>	Fluoroquinolone-resistant
	<i>Neisseria gonorrhoeae</i>	Cephalosporin-resistant, fluoroquinolone-resistant
Medium	<i>Streptococcus pneumoniae</i>	Penicillin-non-susceptible
	<i>Haemophilus influenzae</i>	Ampicillin-resistant
	<i>Shigella</i> spp.	Fluoroquinolone-resistant

1.9 Interactions between microplastics and antibiotic resistance genes

Recent studies have shown that the enrichment of ARGs on MPs depends on the MP composition and properties, surface charge, ARG subtypes, surrounding environment, and incubation time (Dong et al., 2021). ARGs on MP related to WWTPs, landfill leachate, the aquatic environment and soil samples have been studied with the use of conventional quantitative polymerase chain reaction (qPCR), high throughput qPCR (HT-qPCR) and metagenomics methods (Liu et al., 2021). Yang et al. (2019) investigated the diversity and abundance of ARGs on MP debris compared to seawater, and the results reported that ARGs were found in all of the plastic samples, which includes 64 ARG subtypes that provide resistance to 13 different antibiotics (vancomycin, tetracycline, rifamycin, MLS, multidrug, kasugamycin, fosmidomycin, fosfomycin, chloramphenicol, beta-lactam, bacitracin and aminoglycoside). ARGs were only found in 4 of the 17 seawater samples and only 6 ARG subtypes that provide resistance to 2 antibiotics, which indicates that MPs are an important reservoir for ARGs, and that ARGs on plastics are more abundant and more diverse.

The polymer type is also an important influence when it comes to ARG enrichment on MPs (Liu et al., 2021), and therefore the surface charge, functional groups, polarity, and molecular arrangement need to be studied to understand the sorption process of ARGs. In general, polymers containing monomers with C and H atoms are considered non-polar, and polymers containing monomers as -Cl and benzene are considered polar polymers. The strong C-C and C-H bonds impart a high structural strength and chemical resistance, while the polar polymers are easily capable of interacting with reactive compounds (Atugoda et al., 2021). Studies have mainly been focusing on the most common MP polymers (PE, PP, PS and PVC) in the marine environment (Martínez-Campos et al., 2021), and a study by Guo et al. (2020) revealed different preferences for ARGs on the different MP polymers, where a higher abundance of ARGs were located on PE than the others. Another study investigated the sorption process of tylosin on PE, PP, PS and PVC, and the study revealed that PVC had the highest sorption capacity for tylosin (Guo et al., 2018). Pham et al. (2021) investigated the abundance of ARGs on the widely used MP polymers PE and PS, and the results revealed that almost all of the ABR target genes (*sul1* and *sul2*) and the *int11* integrase gene of integrons often carrying resistance genes were found in PE biofilms. In comparison, PS had fewer target genes which indicates that PE is likely more potent in enriching these genes than PS.

Another important factor that affects the fate of ARGs in the aquatic environment is the polymer aging process. Strongly aged MPs are shown to have higher ARG abundance compared to weakly ones (Lu et al., 2020). The oxidation process during the weathering of MPs yields oxygen-containing functional groups (carboxyl, hydroxyl, ketone and ester) to the polymer structure introducing hydrophilic properties (Atugoda et al., 2021). The sorption capacity to aged MPs are higher, due to the increase in surface areas, hydrophilic properties at the surface, higher contents of oxygen-containing groups, and increase in surface roughness, cracks and wells (Agboola and Benson, 2021). Li et al. (2018) studied the sorption of the antibiotic oxytetracycline on PS in the coastal beaches of North China and observed that the adsorption capacity of aged MPs was twice of that of virgin PS. Simultaneously, Yuan et al. (2022) investigated how UV-aged PS affected the ARG transfer efficiency from various ARG vectors to recipient bacteria, and the results revealed that the adsorption capacity of 20 days UV-aged PS increased compared to virgin PS, due to increased specific surface area and affinity for these ARG vectors. Su et al. (2021) showed that the aging process of MPs compared to virgin MPs clearly changed the MPs surface properties and morphology, which further increased the probability of bacterial colonization. Another study showed that the adsorption abilities of aged PS and PVC were respectively more than 123.3% and 20.4% higher, than the corresponding virgin MPs (Liu et al., 2019). Hence, weathering and aging processes can render the MP hydrophilic, thereby increasing the sorption of hydrophilic compounds (Atugoda et al., 2021), however, more studies are still needed to understand the enrichment, transport, and transfer of ARGs on MPs and provide a fundamental basis for evaluating their exposure health risk.

1.10 The MicroPlastResist project

This master thesis, in collaboration with NORCE, is a part of the MicroPlastResist project, co-founded by The Research Council of Norway and the National Research Foundation of South Africa by the SANOCEAN program. The overall project aims to achieve new knowledge about the effects of plastic pollution, especially in micro size, and the connection between microplastic particles and the spread of antibiotic resistance genes. The project can be divided into two subcategories: (I) to understand the biofilms associated with the MP pollution at different locations and countries, and (II) investigate the biofilms potential for HGT of ARGs.

2 Principles of methods

2.1 *A. baylyi* as a model organism

The strains *A. baylyi* JV26 (recipient strain) and JV31 (donor strain), are derivatives of the *A. baylyi* strain ADP1, and both of the bacterial strains were constructed using standard molecular biology techniques by The Arctic University of Norway (UiT). Both strains are near-isogenic, and therefore they have good incorporation of DNA from the donor cell into the genome of the recipient cell via homologous recombination (Overballe-Petersen et al., 2013, de Vries et al., 2003). JV26 was derived from the DSMZ strain collection name DSM 588, which was a *trpE* mutant of BD413. By transformation with *trpE*⁺ DNA, the mutation was reverted back to the ADP1 wildtype, resulting in the JV26 mutant. So far, there is found no difference in the DNA sequence between JV26 and the published genome of ADP1 (NC_005966.1). JV31 is identical with the *A. baylyi* strain JV28 *nptIII*⁺ in the paper by de Vries et al. (2003), which is derived from ADP1 (Hülter et al., 2017). The JV31 strain was constructed by inserting the *nptIII*⁺ *tg4* construct: a kanamycin resistance [10 mg/l] gene (*nptIII*), followed by a eukaryotic terminator (*tg4*), into the *alkM* gene in the *A. baylyi* chromosome. In addition, the strain carries the *trpE27* mutation which makes the strain require tryptophan for growing in minimal medium, and the *rpoBI* allele which confers rifampicin resistance.

2.2 Culture media

Culturing bacteria can be possible if suitable culture media, also known as growth media, are available (Willey, 2017). A culture media is a solid, semi-solid or liquid preparation used to grow, transport and store microorganisms, and it contains all the nutrients the microbes require for growth (Bonnet et al., 2019). The knowledge of a bacteria's normal habitat is often useful when selecting an appropriate medium because its nutrient requirements reflect its natural surroundings. Selective compounds can be added to influence growth, such as antibiotics.

2.2.1 Liquid media

Liquid culture media is often referred to as broth (nutrient broth), and does not contain any solidifying agents (Willey, 2017). Liquid media is used for various purposes such as propagation of a large number of cells, fermentation studies and various other tests. After inoculation and incubation, the cells become visible in the form of turbidity. Culturing in liquid medium is suitable to use in test tubes to grow bacteria, but the properties of bacteria are not visible and the presence of more than one type of bacteria cannot be detected.

2.2.2 Solid media

Solid culture media is often agar plates that are sterile Petri dishes containing solidified sulfated polymer composed mainly of D-galactose, 3,6-anhydro-L-galactose, and D-glucuronic acid extracted from red algae (Willey, 2017). Agar plates can be used to either estimate the concentration of microorganisms in a liquid culture by counting the number of colony forming units per volume or to establish pure cultures from a mixed culture by plating a sample on an agar plate that will grow into individual colonies.

2.3 DNA extraction

DNA extraction is a method to obtain and purify DNA by using physical or chemical methods from a sample separating DNA from other cellular components (Gupta, 2019). The purification of DNA from bacterial cultures provides the basis for downstream molecular analysis, and this is often achieved using commercially available kits (Wright et al., 2017). DNA isolation techniques should lead to efficient extraction with good quantity and quality of DNA, which is pure and is lacking contaminants. The extraction of bacterial DNA can be performed in 5 steps: (I) disruption of the cellular structure to create a lysate, releasing the DNA into solution (II) separation of the soluble DNA from cell debris and other insoluble material, (III) binding the DNA of interest to a purification matrix, (IV) washing proteins and other contaminants away from the matrix, and (V) elution of the DNA (Tan and Yiap, 2009).

2.4 Methodology of biofilm research

2.4.1 Crystal violet staining

Crystal violet is used in Gram staining to differentiate Gram-positive and -negative bacteria. This staining technique also determines the amount of biofilm indirectly by measuring the optical density (OD) of crystal violet-stained biofilm (Ebert et al., 2021). Crystal violet binds to DNA in the nucleus and binds to negatively charged surface molecules and polysaccharides in the extracellular matrix, while at the same time allowing proteins to be stained (Tu et al., 2020). The staining provides a good measure of bacterial biofilm mass, but it does not give a measure of biofilm viability as it cannot distinguish the living status of cells (Welch et al., 2012). The OD can be measured with an absorbance microplate reader, which is capable of detecting and quantifying the light photons absorbed by a liquid sample present in a microplate when exposed to light at a specific wavelength (Zhang and Hoshino, 2014).

2.4.2 Scanning electron microscopy

SEM is a tool for observing the surface morphology of samples using secondary electron signal imaging (Tu et al., 2020). SEM can be used to visually identify microbial morphology and posture, characterizing the biodiversity on MP surface or to analyze the surface morphology of MPs to understand the process of change for weathering and fragmentation of MPs in the environment. Commercial SEM systems were introduced in the 1960s, and the new and detailed structural information changed the view of cell biology and microbiology dramatically (Grin et al., 2011). Further development over the past 70 years allowed researchers to push the resolution limit further, and today, the resolution of electron microscopes has reached sub-nanometer scale. As SEM visualizes surfaces directly, it has been shown to be a suitable tool not only to observe in detail the substratum morphology, but also to follow the bacterial adhesion and biofilm formation on abiotic surfaces (Gomes and Mergulhão, 2017). When observing objects containing biofilm, the SEM sample preparation is usually subjected to cell fixation, dehydration where cells lose water and undergo structural changes, drying, and sputter-coated with a thin metal layer to create a conductive surface and to increase the signal (Tu et al., 2020). This signal is provided by the number of secondary electrons released from the outer shell of the atoms hit by the primary beam of electrons.

2.5 Aim of the study

The main aim of this study was to evaluate how the presence and absence of the microplastic polymers high density polystyrene (HDPS), high density polyethylene (HDPE), polypropylene (PP), polyvinyl chloride A (PVC A), and polyvinyl chloride (PVC B) affects the potential for DNA uptake of the kanamycin resistance marker (*nptII*) via natural transformation in the naturally competent bacterium *Acinetobacter baylyi*.

Sub-goals related to this aim are:

- Evaluate how DNA uptake via natural transformation in *A. baylyi* can be affected by the presence of different concentrations of microplastic polymers.
- Evaluate how colonization on the microplastic surface, in biofilms, may affect the transformation frequency in *A. baylyi*.
- Evaluate the effect of weathering processes on the microplastic surface morphology with scanning electron microscopy.
- Evaluate how the early stage of biofilm formation of *A. baylyi* on microplastic polymers builds up over time with scanning electron microscopy.

3 Materials and Methods

3.1 Workflow

The workflow is presented in Figure 5 and addresses the use of the competent bacteria *Acinetobacter baylyi* JV26 and the kanamycin resistant gene (*nptII*) from JV31 to perform natural transformation assays in the presence and absence of the MP polymers HDPE, HDPS, PP, PVC A, and PVC B, and the use of scanning electron microscopy and optical density to investigate the early biofilm formation on the MP polymers. Also, SEM was used to investigate the morphology differences of virgin and aged polymers.

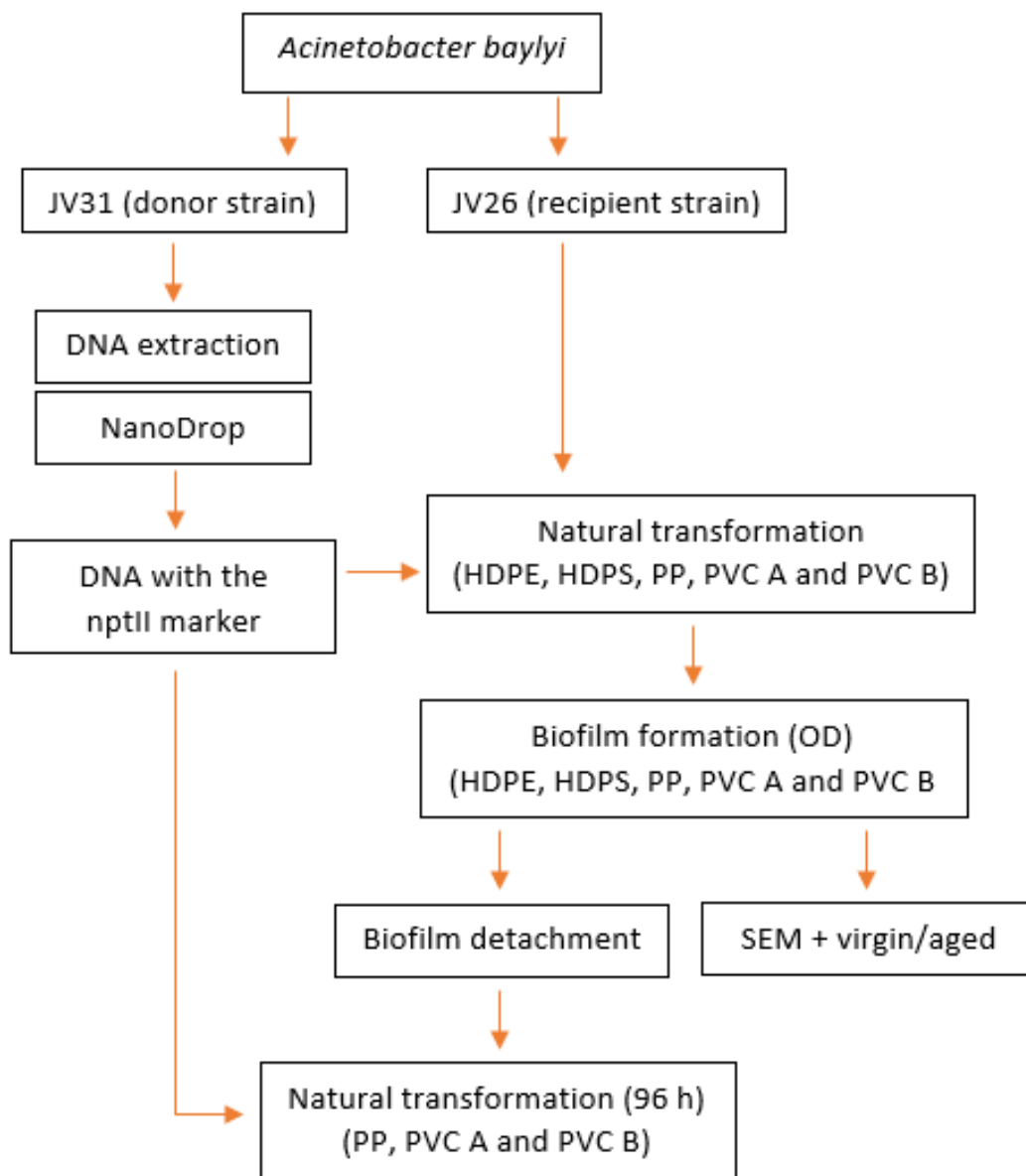


Figure 5: A schematic illustration of the workflow in this project.

3.2 Biological material

Both of the *A. baylyi* strains JV26 (the recipient strain) and JV31 (the donor strain), shown in Table 3, was provided by the Department of Pharmacy at UiT. Liquid cultures of the strains were grown overnight (16 h) at 30°C with shaking (200 rpm) in Luria-Bertani broth (10 g of tryptone, 5 g of yeast extract, 10 g of NaCl, 1 L MilliQ water [pH 7.5]). Hence, 40% glycerol stocks for preservation of isolates were made and stored at -80°C in 1-mL aliquots. To recover the bacterial isolates, a sterile inoculating needle was used to scrape the frozen surface of the culture, before plating on LB agar and incubating at 30°C.

Table 3: *Bacterial strains used in this thesis.*

Strain	Genotype	Reference
JV26	ADP1 wildtype	(Barbe et al., 2004)
JV31	ADP1 <i>trpE27 rpoB1 alkM::(nptII⁺ tg4)</i>	(de Vries et al., 2003)

3.3 Chemicals and antibiotics

The chemicals and antibiotics used in this study are shown in Table 4 and Table 5.

Table 4: *Chemicals used in this thesis.*

Chemicals	Short	Purchased
Ethanol	EtOH	Antibac AS, Norway
PBS buffer (10X Dulbecco's) powder	PBS	AppliChem, Germany
PBS Sterile Solution	PBS	Amresco, USA
Sodium Hydroxide pellets	NaOH	Sigma-Aldrich, USA
Glycerol G2025	Glycerol	Sigma-Aldrich, USA
LB Broth with agar (Lennox) L2897	LB broth agar	Sigma-Aldrich, USA
LB Broth, Miller (Luria-Bertani)	LB broth	Fisher Scientific, USA
Agar – A1296	Agar	Sigma-Aldrich, USA
Select Agar – A5054	Agar	Sigma-Aldrich, USA
Select Agar™ powder - 30391023	Agar	Fisher Scientific, USA
MilliQ water	MilliQ water	Merck Millipore, USA
PeqGOLD bacterial DNA kit	DNA kit	VWR, USA
Sodium hypochlorite solution 4% active chlorine	Chlorine	Lilleborg AS, Norway
Crystal violet solution V5265	Crystal violet	Sigma-Aldrich, USA
Agar quick drying silver paint	Silver paint	Agar Scientific, UK
0.2 M Sodium cacodylate	Sodium cacodylate	VWR, USA
25% Glutaraldehyde	Glutaraldehyde	EMS, USA
1, 1, 1, 3, 3, 3-hexamethyldisilazane	HMDS	Sigma-Aldrich, Germany
Osmium tetroxide	Osmium	EMS, USA

Table 5: **Antibiotics used in this thesis.**

Antibiotics	Short	Purchased
Kanamycin disulfate salt from <i>Streptomyces kanamyceticus</i> , aminoglycoside antibiotic	Kanamycin	Sigma-Aldrich, Germany

3.4 Microplastic polymers

A selection of virgin industrially produced resin pellets not exposed to the environment, including HDPS, HDPE, PP, PVC B, and PVC A were obtained from Plastics SA (South Africa). The material was approximate delivered as 4 mm x 4 mm x 0.1 mm particles, as shown in Figure 6, and had some characteristic varieties including: (I) shape [round, square, rectangular]; (II) size [>5 mm $>$]; (III) surface structure [smooth, rough, uneven, cracked]; (IV) density [low-density, high-density]; and (V) colour [white, purple, brown, blank]. Some of these differences, as shape and size, were also present within the same polymer type as shown in Figure 7. For disinfection and to eliminate residual organic matter contamination, the polymers were treated with $<5\%$ chlorine bleach for 20 min, 96% EtOH for 5 min, rinsed with MilliQ water, and exposed to UV-light for 15 min.



Figure 6: **Microplastic polymers used in the thesis.** From left; HDPS, HDPE, PP, PVC B, and PVC A.



Figure 7: **Different characteristics within the same microplastic polymer.** From left; PP, PVC A and PVC B.

3.5 Kanamycin stock solution

Kanamycin stock solutions (50 mg/mL) were made by mixing 0.5 g of kanamycin disulfate with 10 mL of MilliQ water. A 0.2 µm syringe filter was prewet by drawing through 5-10 mL of MilliQ water. The water was discarded, and the kanamycin stock solution was sterilized through the syringe filter. Eppendorf tubes were prepared with 0.5 mL of kanamycin stock solution and stored at -20°C for further use.

3.6 Culture media

3.6.1 Liquid culture media

Liquid media were made by mixing 25 g LB powder (10 g of tryptone, 5 g of yeast extract, 10 g of NaCl) with 1L MilliQ water. The pH was adjusted to 7.5 with NaOH before autoclaving. The medium was stored at 4°C. For selective cultivation of *A. baylyi* strains that contains genes conferring kanamycin resistance, the growth medium was supplemented with 10 µL/mL of premade kanamycin solutions.

3.6.2 Solid culture media

LB agar plates were made by mixing 25 g LB powder (10 g of tryptone, 5 g of yeast extract, 10 g of NaCl) with 15 g agar (A1296), and 1L of MilliQ water. The pH was adjusted to 7.5 with NaOH before autoclaving. The medium was cooled to ~55°C and poured into sterile Petri dishes in a sterile Laminar flow cabinet (ESCO Scientific, Singapore), and stored at 4°C for further use. For selective cultivation of *A. baylyi* strains that contains genes conferring kanamycin resistance, the growth medium was supplemented with 10 µL/mL of premade kanamycin solutions.

3.7 DNA extraction with the peqGOLD bacterial DNA kit

DNA containing the kanamycin resistant marker (*nptII*) from JV31 was isolated using the peqGOLD bacterial DNA kit. Bacteria were inoculated in LB media to log-phase, and 3 mL culture was centrifuged at 4,000 x g for 10 min. The supernatant was discarded, and 100 µL TE Buffer was added and the sample was vortexed to completely resuspend the pellet. Hence, 10 µL Lysozyme resuspended with Elution buffer was added and incubated at 37°C for 10 min, and then 100 µL TL Buffer and 20 µL Proteinase K solution was added and incubated with shaking at 55°C for 1 h. Then 5 µL RNase A was added and mixed at room temperature for 5 min, followed by centrifugation at 10,000 x g for 2 min to pellet any undigested material. The supernatant was transferred to a new microcentrifuge tube without disrupting the pellet, and

220 μL BL Buffer was added and mixed and incubated at 65°C for 10 min. Further, 220 μL of 100% EtOH was added and vortexed for 20 sec at maximum speed. The peqGOLD DNA mini column was inserted into the collection tube, and the sample was transferred to the mini column. The samples were centrifuged at 10,000 x g for 1 min and the filtrate, and the collection tube was discarded. The mini column was transferred into a new collection tube, and 500 μL HBC Buffer diluted with 100% isopropanol was added and centrifuged at 10,000 x g for 1 min. The filtrate was discarded, and 700 μL DNA Wash Buffer diluted with 100% EtOH was added and centrifuged at 10,000 x g for 1 min. The washing steps were repeated, and the empty mini column was centrifuged at maximum speed for 2 min to dry the column. The mini column was then inserted into a new microcentrifuge tube, and 100 μL Elution Buffer heated to 65°C was added for 5 min, and the sample was centrifuged at 10,000 x g for 1 min to elute the DNA twice.

3.8 Measuring DNA concentrations with NanoDrop

The eluated DNA was quantified using the Nano Drop™ 2000 spectrophotometer (Thermo Fisher Scientific, USA). The DNA concentrations were determined by measuring the absorbance at 260 nm wavelength (A260) and 280 nm wavelength (A280), and the purity was determined by the ratio of absorbance at 260 nm and the absorbance at 280 nm (A260/A280). The spectrophotometer was blanked with Elution Buffer before measuring the DNA samples and washed with MilliQ water between measures to prevent cross-contamination of the DNA products. The eluated DNA was stored in Eppendorf tubes at -20°C for further use.

3.9 Transformation of *A. baylyi* in the presence of MP polymers

Overnight culture (2.5 mL) incubated for 16 h of naturally competent *A. baylyi* JV26 was mixed with 7.5 mL of LB broth and 100 ng ml⁻¹ of isolated DNA containing the kanamycin resistant marker from JV31. Four individual transformation assays with respectively 0, 10, 50 and 200 MP polymers were performed with the sterile polymers HDPE, HDPS, PP, PVC A, and PVC B. The transformations were incubated at 30°C with shaking (100 rpm) for 90 min and plated in triplicates in appropriate dilutions with PBS on LB medium (recipient titer) and LB with 10 mg ml⁻¹ kanamycin (transformant titer). The colonies formed on the agar plates were counted after incubating 16-40 h at 30°C, and the transformation frequencies were calculated with Equation 1:

$$\text{Transformation frequency} = \frac{\text{Transformant titer}}{\text{Recipient titer}} \quad (\text{Eqn. 1})$$

3.10 Quantification of biofilm formation on MP surfaces

Overnight culture (100 μ L) incubated for 16 h of JV26 was mixed with 50 mL of LB broth and the sterile MP polymers HDPE, HDPS, PVC B, PVC A, and PP for respectively 24, 48, 72 and 96 h. The samples were incubated at 30°C with shaking (200 rpm), and the LB broth medium was changed every other day to maintain bacterial growth. After incubation, the MP polymers were washed gently with PBS to remove free-living bacteria, and then dried 1 h at 60°C for biofilm fixation. The polymers were stained with 0.3% (w/v) crystal violet for 15 min in a 96 well plate, and the excess stain were removed by washing the wells 4 x with MilliQ water. To detach the crystal violet stain, 200 μ L of 95% EtOH was added for 10 min. The solubilized crystal violet stain was then measured with a FLUOstar OPTIMA microplate reader (BMG Labtech) at OD_{595nm}, and 95% EtOH was used as blank.

3.11 Bacterial biofilm detachment methods

A Branson 1510 ultrasonic cleaner operated at its maximum power output of 80W and a Heidolph REAX top vortex operated at maximum speed was compared to investigate the best biofilm detachment output. Test samples were ultrasoned for respectively 30, 60, 120, 180 and 240 seconds, and vortexed for respectively 10, 30, 60, 90 and 120 seconds, and then plated in triplicates in appropriate dilutions with PBS on LB agar. Number of colonies were counted after incubating at 30°C.

3.12 Transformation of *A. baylyi* biofilms on MP polymers

Overnight cultures (100 μ L) incubated for 16 h of JV26 was mixed with 50 mL of LB broth. Three individual transformation assays with the sterile MP polymers PVC B, PVC A and PP were incubated at 30°C with shaking (200 rpm) for 96 h. The LB broth medium was changed every other day to maintain bacterial growth. After 96 h, the MP polymers were gently washed with PBS to remove free-living bacteria. Further, 5 MP polymers of each polymer type were added to 5 mL of LB broth and 100 ng ml⁻¹ of isolated DNA from JV31, and the transformation was performed as described earlier. A Branson 1510 ultrasonic cleaner operated at its maximum power output of 80W for 4 min was used to detach the bacterial biofilms. The dilution series, plating, and transformation frequency calculations were performed as described earlier.

3.13 Characterization of MP surface morphology and bacterial biofilm formation with SEM

Overnight culture (100 μ L) incubated for 16 h of JV26 was mixed with 50 mL of LB broth and the sterile MP polymers PVC B, PVC A and PP for respectively 24, 48, 72 and 96 h. The samples were incubated at 30°C with shaking (200 rpm), and the LB broth medium was changed every other day to maintain bacterial growth. The polymers containing biofilm were washed gently with PBS and fixated in 10 mL 3% glutaraldehyde in 0.1 M sodium cacodylate buffer for 24 h. The fixation liquid was then diluted 1:10 with cacodylate buffer for longer storage. The samples were post-fixed with and without 1% osmium tetroxide and then exposed to an EtOH dehydration series of 50, 60, 70, 80, 90, and 2 x 100% (v/v) EtOH, followed by a chemical dehydration series of 100% EtOH + HMDS at 50, 60, 70, 80, 90, and 2 x 100% (v/v), for 5 min at each concentration. All of the polymers with and without biological material were attached to SEM specimen stubs with silver paint and dried overnight. Hence, the samples were coated with gold in a Polaron SC7640, and the images were obtained from a Zeiss Gemini 300 SEM (Germany) at the Advanced Microscopy Core Facility (AMCF) at UiT. The samples were mounted according to the manufactures protocol, and the immersion lens (In-Lens) detector was used. To obtain clear pictures the focus, brightness and contrast were adjusted, and the scanning speed were set to 9. Multiple images were taken at 20, 40, 100, and 200 μ m across 3 different regions on the polymer surfaces.

3.14 Statistical analysis

All statistical analyses on the raw data were performed in Microsoft Office Excel (2016 version). The data were presented as mean \pm standard deviation of means using the data analysis ToolPak with customized scripts. Outliers and all of the transformant and recipient titers containing less than 30 colonies and more than 300 colonies were removed from the raw data due to the acceptance of 30 to 300 colonies as the most suitable number of colonies on plates for counting (Tomasiewicz et al., 1980).

4 Results

The transformation frequency and efficiency of the natural competent bacteria *A. baylyi* was studied to investigate if DNA uptake alters in the presence and absence of microplastic polymers that can be found as plastic pollution in nature. The study also includes the use of SEM and OD to investigate and quantify the early biofilm formation on the MP polymers. Also, SEM was used to investigate the morphology differences of virgin and aged polymers.

4.1 DNA concentrations and purity

The donor DNA containing the kanamycin resistance marker (*nptII*) was isolated from the JV31 mutant, and the DNA concentration results are shown in Table 6. The NanoDrop curve shown in Figure 8 contains a peak at 260 nm, a slope passing through 280 nm, followed by a flat line above 300 nm for both of the measurements. The results of the concentrations and the 260/280 OD-ratio indicate that the quality of the DNA is suitable for further analysis.

Table 6: The NanoDrop results which shows the DNA concentration and purity of JV31.

Sample ID	Nucleic Acid	Unit	A260 (Abs)	A280 (Abs)	260/280	260/230
1	191.6	ng/ μ L	3.831	2.072	1.85	2.19
2	203.8	ng/ μ L	4.076	2.213	1.84	2.12

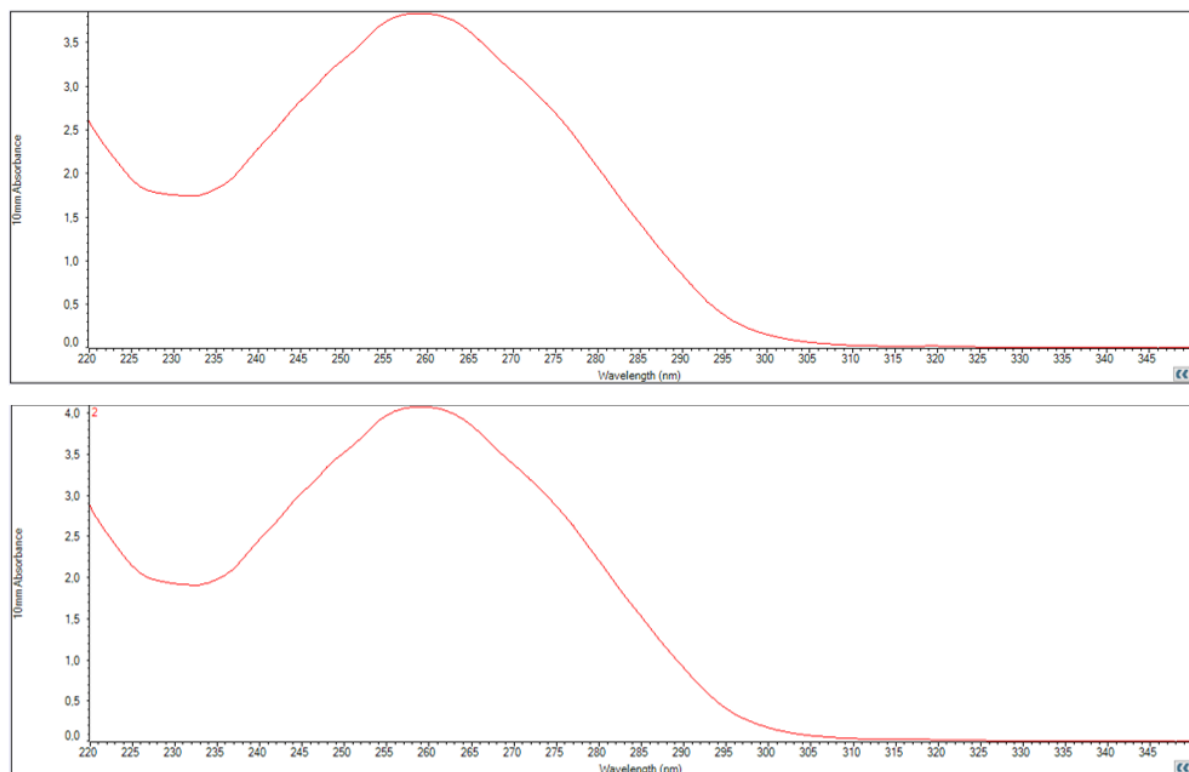


Figure 8: The NanoDrop curve.

4.2 Natural transformation and twitching motility

The results were in the beginning of the study affected by twitching motility, as shown in Figure 9. The twitching made it difficult or almost impossible to detect the formed colonies on the agar plates. In Figure 9, half of the agar plates contained clear colonies while the other half contained diffuse spread of surface translocation of *A. baylyi*.

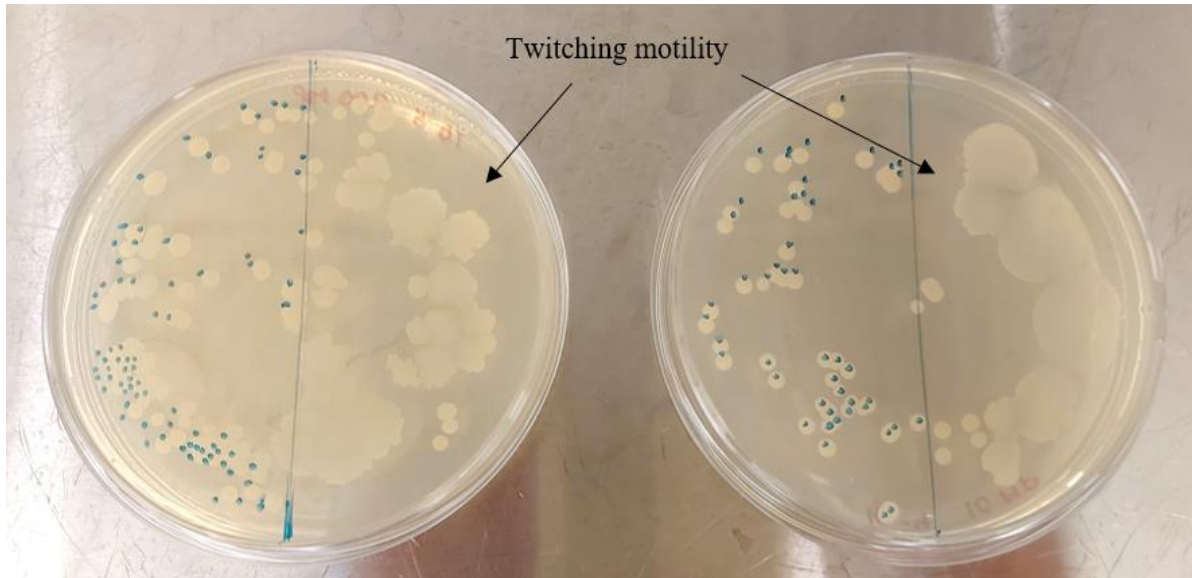


Figure 9: Twitching motility of *A. baylyi* JV26 on LB broth agar plates.

4.3 Natural transformation of *A. baylyi* under influence of different concentrations of microplastic polymers

The natural transformation efficiency of *A. baylyi* was investigated when it was under influence of different concentrations (0, 10, 50 and 200 MP) of MP polymers. All of the transformation results are the mean value of multiple transformation setups with at least 3 technical and 3 biological replicates, and all of the raw data can be found in Appendix B – Natural transformation raw data. The transformation frequency results, shown in Figure 10, revealed that the recipient strain JV26 acquired the *nptII* marker from the donor strain JV31. The results revealed that the DNA uptake alters in the presence of different concentrations and types of polymers. The DNA uptake efficiency decreased or were unfaceted for HDPS, PP, PVC A and PVC B when the concentration of polymers increased, while the DNA uptake efficiency increased for HDPE when the concentration of polymers increased. The negative control (no addition of any MP) does have a higher transformation frequency than HDPE, HDPS and PVC A, while PP and PVC B do have a higher transformation frequency than without any MP. The standard deviation indicates that some of the data points are more spread and less concentrated around the mean than others, for instance with no MP, and PP 10 and 50 MP.

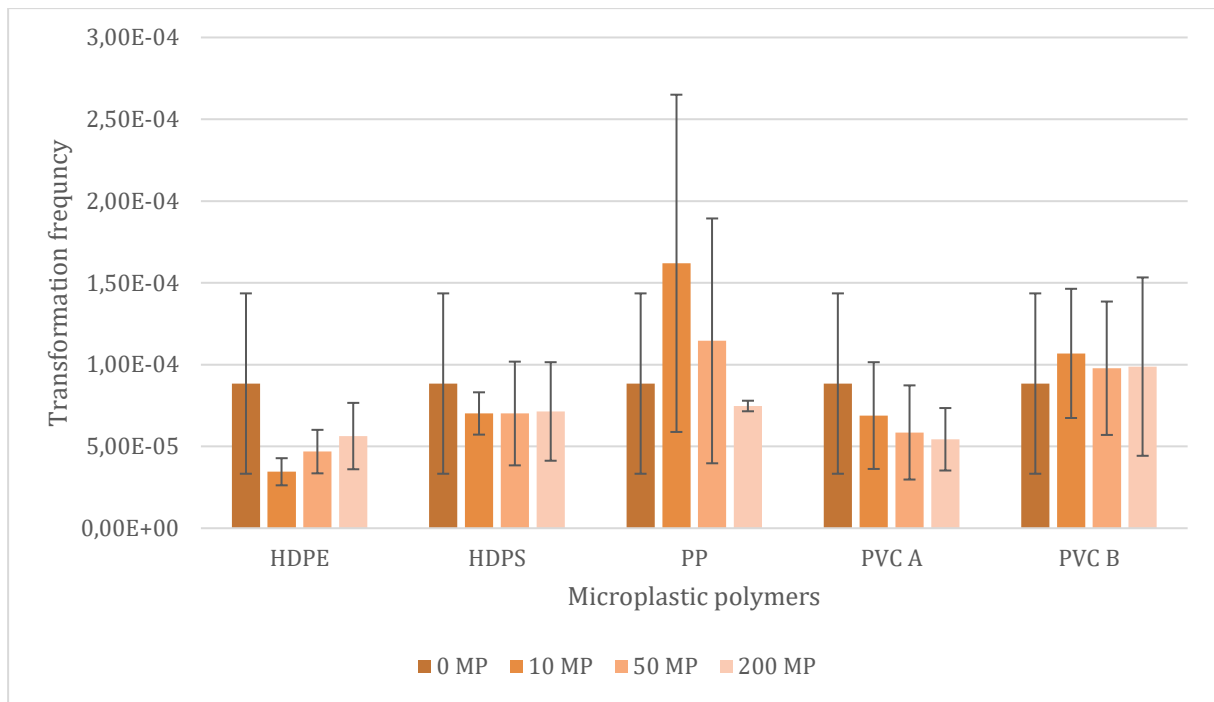


Figure 10: The mean transformation frequency results of *A. baylyi* for HDPE, HDPS, PP, PVC A and PVC B under influence of different concentrations of MP polymers (0, 10, 50 and 200 MP). The data is the mean transformation frequency given with standard deviation. In all the transformation assays performed, no MP added was used as negative control.

4.4 The early biofilm formation of *A. baylyi* on MP polymers

The early biofilm formation at 24, 48, 72 and 96 h of *A. baylyi* on HDPE, HDPS, PP, PVC A, and PVC B was investigated with optical density at 595 nm. All of the raw data can be found in the Appendix A – OD measurements raw data. The OD results, shown in Figure 11, revealed that the colonization speed varied for all the different MP polymers, and that the biofilm formation had a steadily increase for PVC A, PVC B and PP in the beginning, while the biofilm formation was close to zero for the MP polymers HDPE and HDPS. Glass beads which were used as a negative control also had an optical density close to zero for all the different time points, indicating no biofilm formation. PVC B and PVC A do have a rapid increase until 48 h, and then the curve flattens more out after this timepoint. PP increases in line with the PVCs until 24 h, but has a drop at 48 h before it starts increasing again. At 96 h, PVC A had the most accumulated amount of biofilm followed by PVC B, PP, HDPE and HDPS.

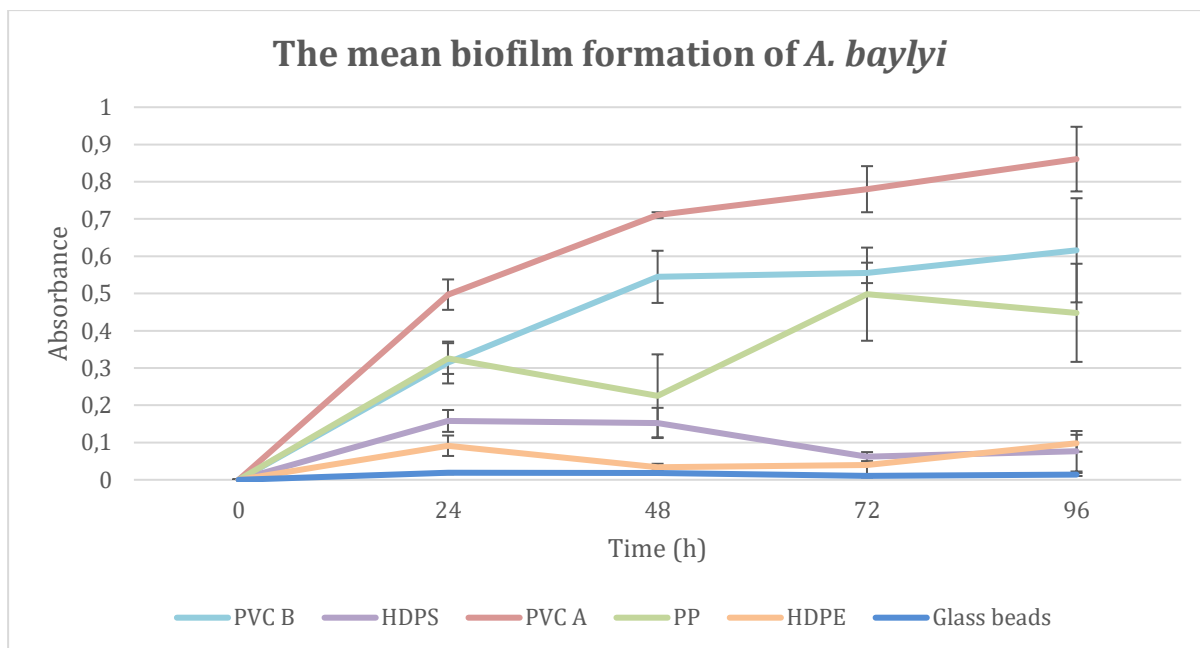


Figure 11: **Growth curves of the early biofilm formation (24, 48, 72 and 96 h) of *A. baylyi* on PVC B, PVC A, PP, HDPS, HDPE.** The number of cells at each specific time point was assessed by measuring the optical density absorption at 595 nm. The data is the mean absorbance given with standard deviation. Glass beads were used as negative control.

4.5 Natural transformation of *A. baylyi* biofilms grown on microplastic polymers for 96 h

The natural transformation of *A. baylyi* biofilms grown on microplastic polymers for 96 h was investigated. A Branson 1510 ultrasonic cleaner operated at its maximum power output of 80 W and a Heidolph REAX top vortex operated at maximum speed was compared to investigate the best biofilm detachment output when comparing methods, and the results revealed that the ultrasonic bath operated at a maximum power for 4 min gave the best detachment output and were therefore used further in this study. The transformation frequency results of biofilms grown on the MP polymers PVC B, PVC A and PP for 96 h, shown in Figure 12, revealed that the DNA uptake of the kanamycin resistance marker was the highest for PP. The MP polymers PVC B, PVC A, and PP was selected for the natural transformation setup based on the results obtained from the optical density measurements, due to the most bacterial biofilm formation on these polymers. All of the transformation frequency results are the mean value of multiple transformation setups with at least 3 technical and 3 biological replicates, and all of the raw data can be found in Appendix B – Natural transformation raw data. The standard deviation for PVC A is more spread and less concentrated around the mean than the standard deviations for PVC B and PP.

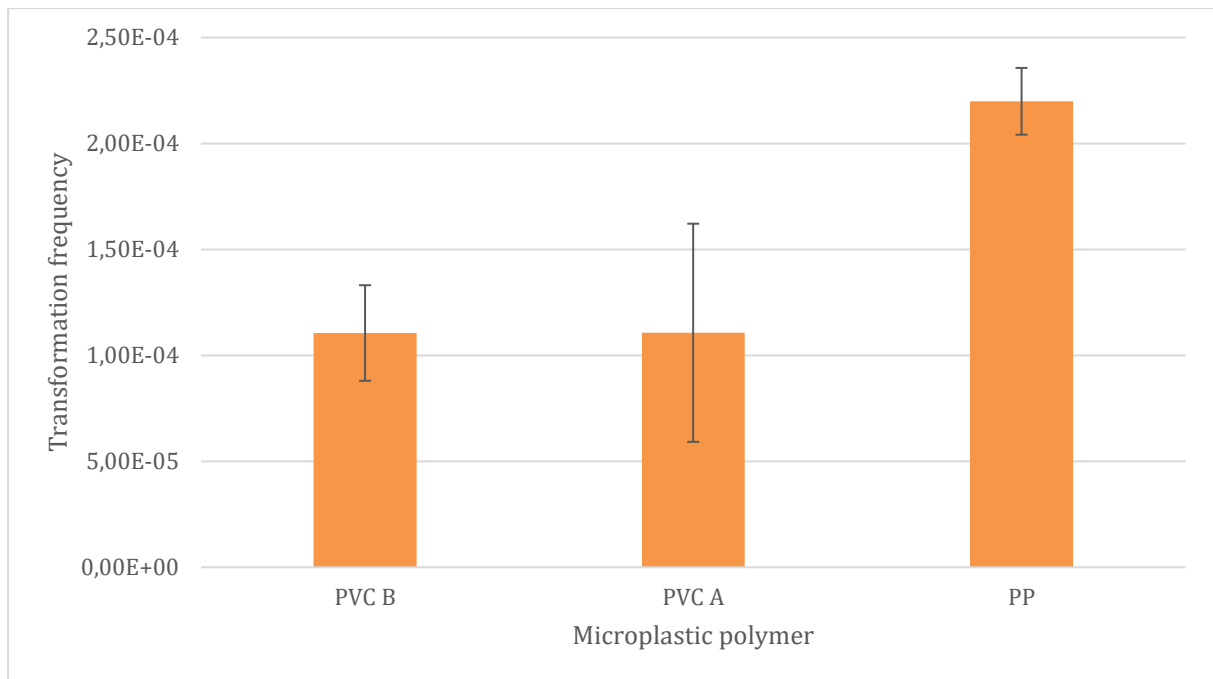


Figure 12: The transformation frequency results of biofilms of *A. baylyi* grown on the MP polymers PVC B, PVC A and PP for 96 h. The data is the mean transformation frequency given with standard deviation.

4.6 Morphology characteristics of virgin and aged microplastic polymers with SEM

The virgin and aged microplastic polymers HDPE, HDPS, PP, PVC A, and PVC B were studied with SEM to investigate if the exposure to UV irradiation and chemicals affects the surface morphology. The SEM images revealed different surface roughness, showing that the MPs have complex surface topography characteristics generally characterized as smooth, rough, uneven, porous, or cracked. Several areas on the MP surfaces were inspected to investigate if there were any alterations within the same surface. As shown in Figure 13, the virgin polymers contain more or less a smooth and uniform surface morphology, but also microscopic flaws, such as small grooves and cracks, inadvertently introduced during manufacturing. The aged MPs revealed that the exposure to environmental conditions expands these flaws, and that the aged MP polymers contains more fragmentation and formation of cracks, resulting in open structures, as well as an increase in the surface roughness. Aged PP has especially visible surface changes with formation of more uneven surface structure and longer and deeper cracks. Aged PVC A and PVC B do also have surface changes with an increasing number of small grooves and roughness, and HDPE and HDPS with a not that clear difference compared to the others, with just a slightly increase in surface roughness.

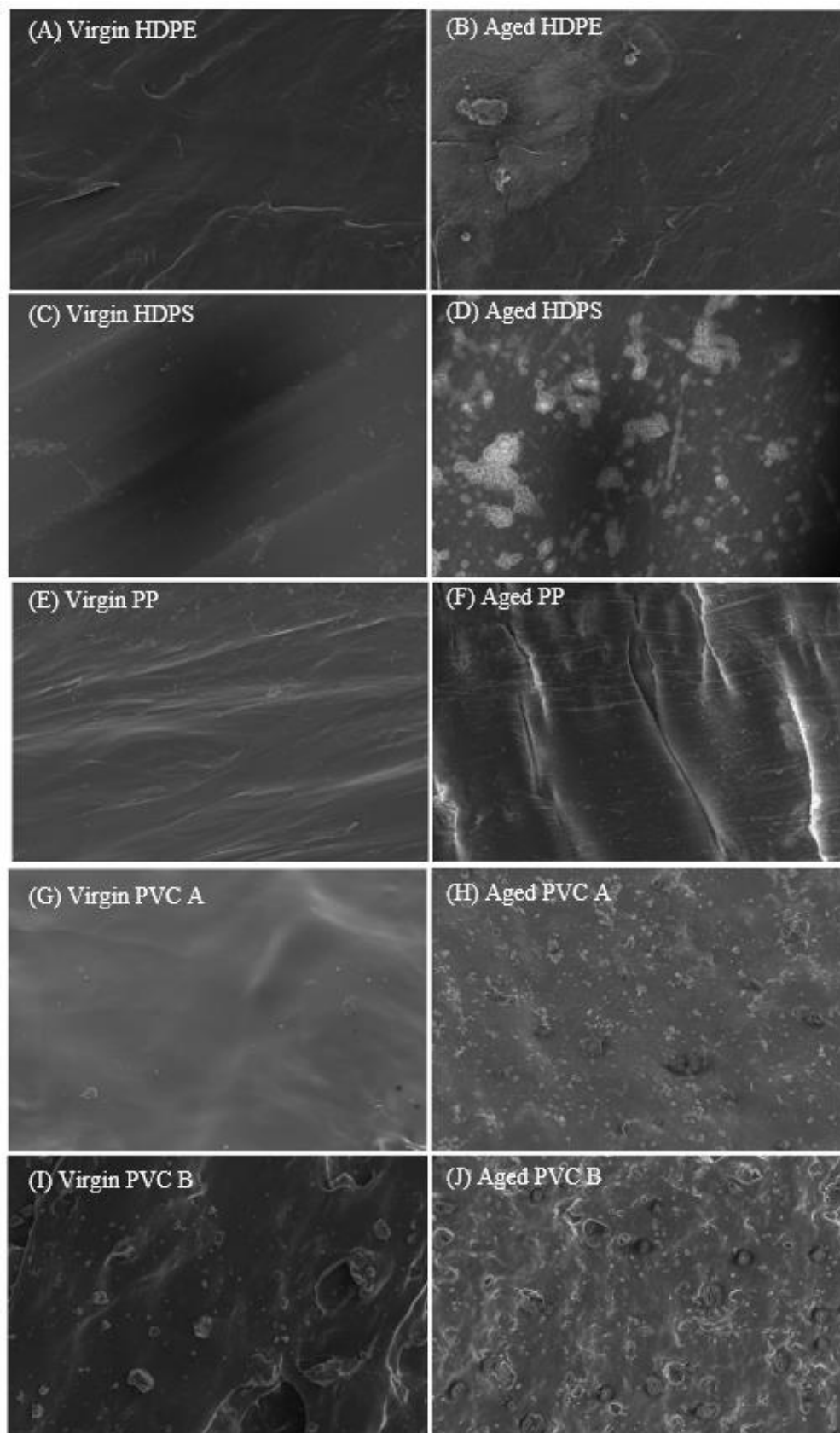


Figure 13: High-resolution SEM images of the surface of HDPE, HDPS, PP, PVC A, and PVC B before and after exposure to UV irradiation, ethanol and chlorine. (A) Virgin HDPE, (B) aged HDPE, (C) virgin HDPS, (D) aged HDPS, (E) virgin PP, (F) aged PP, (G) virgin PVC A, (H) aged PVC A, (I) virgin PVC B, and (J) aged PVC B. All images were captured at 20.0 k x magnification.

Some of the deep cracks formed on the microplastic surface of aged PP contains remnants of bacterial biofilm and residual organic matter of *A. baylyi* from earlier experimental setups performed in this study, and the aged surface of HDPE and HDPS contains remnants of different chemicals as shown in Figure 14.

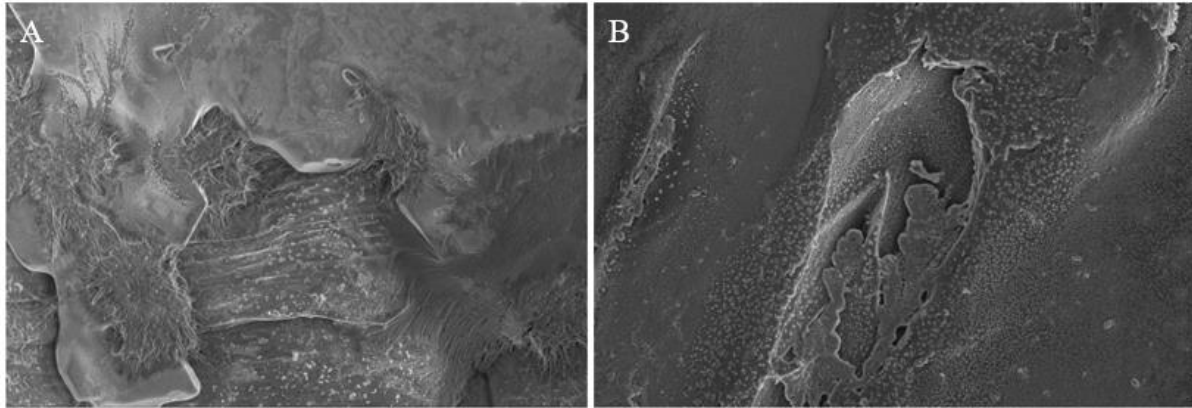
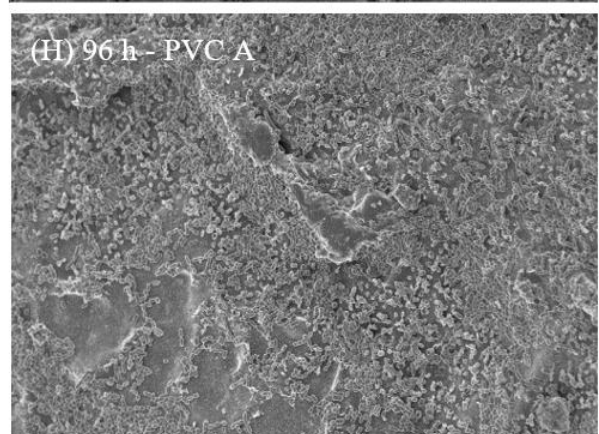
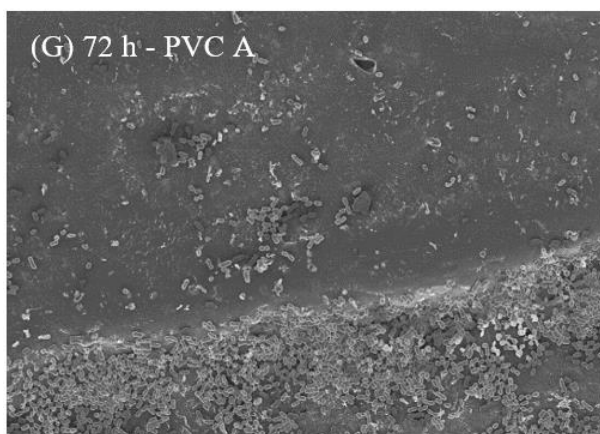
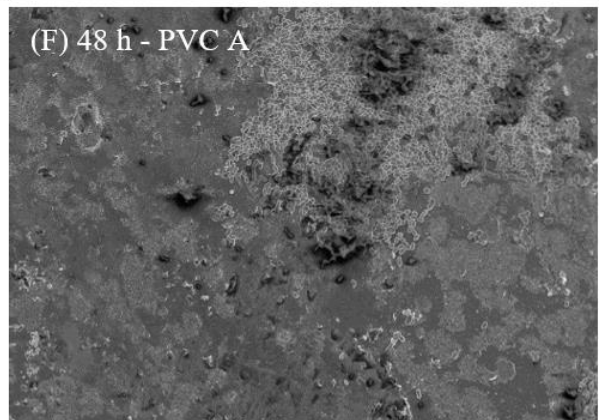
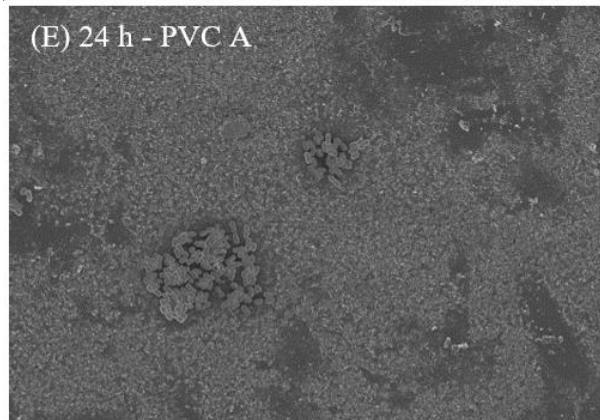
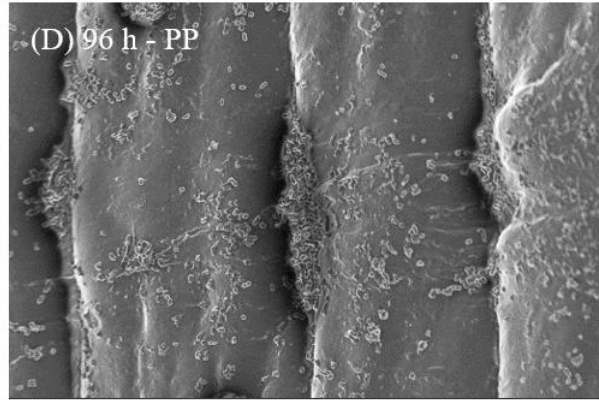
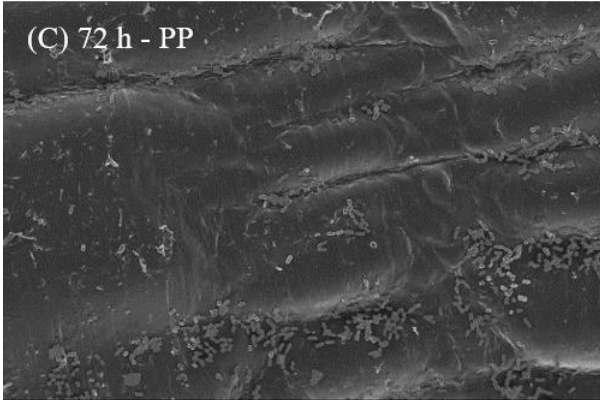
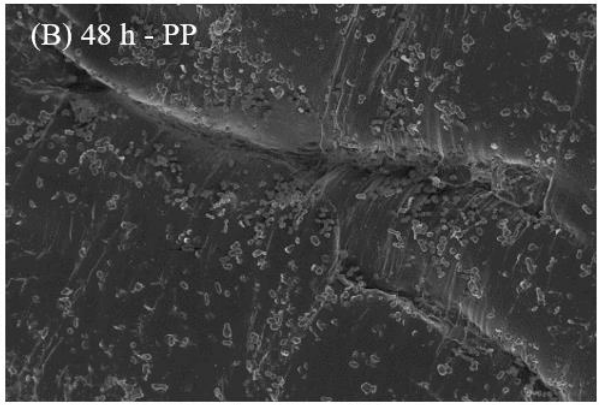
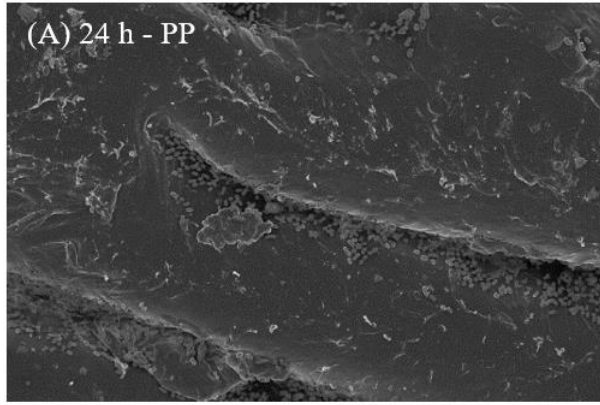


Figure 14: **High-resolution SEM images of remnants on the surface of aged MPs.** Remnants of bacterial biofilm and residual organic matter of *A. baylyi* on the surface of aged PP (A), and remnants of different chemicals on the surface of aged HDPS (B). Both of the images were captured at 20.0 k x magnification.

4.7 Characterization of early biofilm formation of *A. baylyi* on microplastic polymers with SEM

The 4 days biofilm formation of *A. baylyi* on aged PP, PVC A, and PVC B were studied with SEM. The SEM images, shown in Figure 15, revealed distinct amount of colonization of *A. baylyi* at 24, 48, 72 and 96 h, and differences in the colonization pattern depending on the polymer type. Several areas on the MP surface were inspected to investigate if there were any alterations in colonization within the same surface, and for all of the polymers, the surface areas characterized as rough, uneven, porous or cracked contained more biofilm and individual cells of *A. baylyi* than the smooth and even surfaces. The results also revealed that there was an increasing number of individual bacteria cells and biofilm with increasing incubation time. The images showed that *A. baylyi* is colonizing the different MP surfaces at different speeds, where the MP polymer containing the most biofilm and individual cells was the following order: PVC B > PVC A > PP. The results for PP and PVC B at 24 h displays that *A. baylyi* starts to colonize the formed cracks, and at 96 h the colonization are more firmly attached in the cracks, forming more dense microbial communities. The SEM results for PVC A at 24 h revealed that the MP surface contains small patches with bacterial colonization and big areas containing no bacteria, but these patches with bacteria becomes bigger with increased incubation time. For both PVC A and PVC B at 96 h, the bacterial communities was stretching outward to form regular and irregular structures, and the MP surface was hard to spot due to the dense bacterial communities.



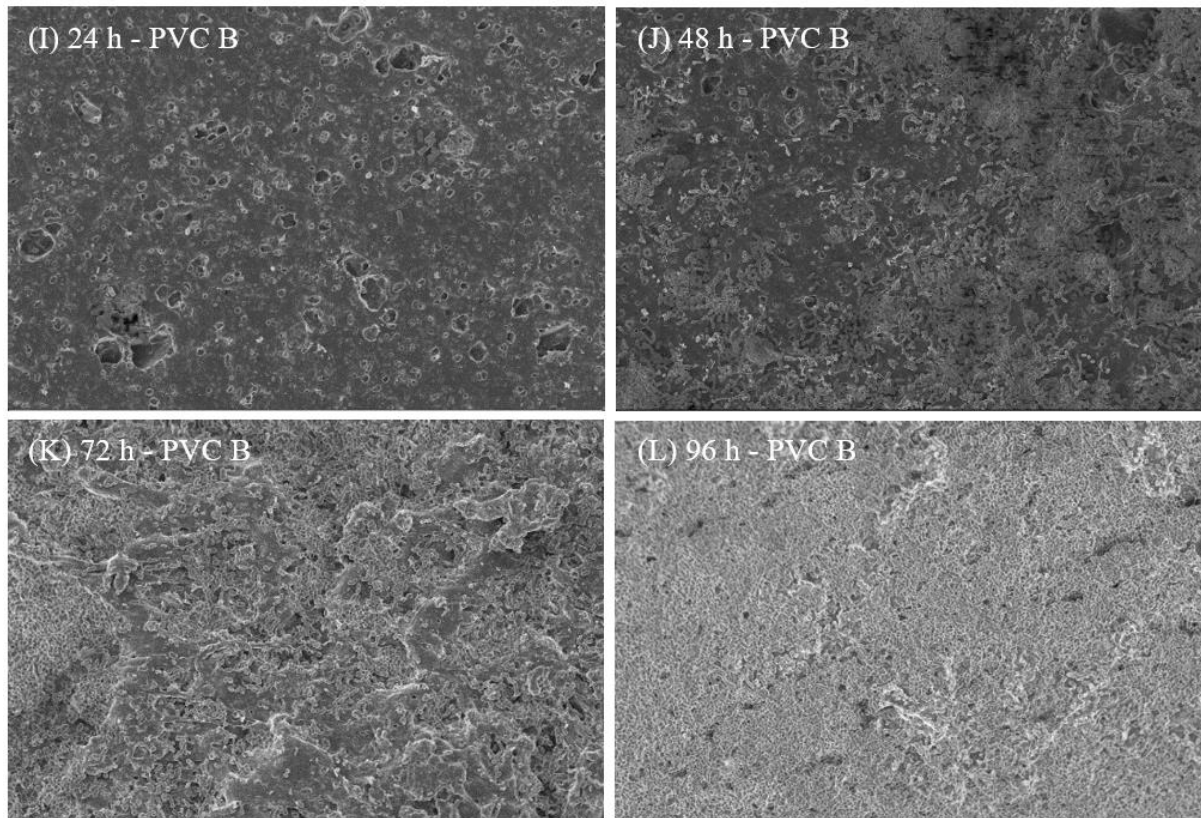


Figure 15: High-resolution SEM images of biofilm of *A. baylyi* on HDPE, HDPS, PP, PVC A, and PVC B. (A) 24 h biofilm on PP, (B) 48 h biofilm on PP, (C) 72 h biofilm on PP, and (D) 96 h biofilm on PP, (E) 24 h biofilm on PVC A, (F) 48 h biofilm on PVC A, (G) 72 h biofilm on PVC A, and (H) 96 h biofilm on PVC A, (I) 24 h biofilm on PVC B, (J) 48 h biofilm on PVC B, (K) 72 h biofilm on PVC B, and (L) 96 h biofilm on PVC B. All images were captured at 20.0 k x magnification.

5 Discussion

Microplastic pollution is a big and rapidly increasing environmental problem, and although the direct effects of MP pollution are increasingly studied the indirect effects are hardly investigated, especially in the context of spreading ARGs. The focus of this study aimed to provide new insight in evaluating the risks caused by plastic wastes in the aquatic environment, and thereby lay the foundation for further investigations of the interactions between MPs associated with ARGs. The main goal was to evaluate how the presence of different types of MP polymers affects the potential for DNA uptake via natural transformation in the naturally competent bacteria *A. baylyi*, to obtain a better understanding of HGT of ARGs within MP-associated communities in natural environments. Important subgoals was to investigate the natural transformation efficiency of biofilms grown on MPs for 96 h, the effect of weathering processes on the MP surface, and the early biofilm formation on different MPs. The overall results provided new insight in evaluating the risk caused by plastic waste in the environment as the presence of different MPs affects the natural transformation efficiency and biofilm formation of *A. baylyi*. In addition, the results confirms that weathering processes changes the surface structure of virgin MPs.

5.1 Use *A. baylyi* as a model organism

A. baylyi was selected as the model organism in this study due to its powerful genetic opportunities afforded by its transformation and recombination capabilities. By mixing active growing *A. baylyi* cultures with DNA, transformation in the laboratory is easily accomplished, and the bacterium has an efficient molecular machinery for the uptake and incorporation of exogenous DNA due to its natural competence (Elliott and Neidle, 2011). In addition, it is favourable to laboratory exploration because it is nutritionally versatile, fast growing, easily cultured, well characterized, and low-pathogenic (Wilharm et al., 2013). The strains JV26 (the recipient strain) and JV31 (the donor strain) were obtained from the Department of Pharmacy, UiT , and both of the mutants were therefore readily available for laboratory explorations. The strains are near-isogenic, and do therefore have good incorporation of DNA from the donor cell into the genome of the recipient cell via homologous recombination (de Vries et al., 2003, Overballe-Petersen et al., 2013). In this study, a single bacterial strain was used as the model in contrast to natural environments. This is in contrast to microbial nature of polymer surfaces that mostly comprises multiple bacterial species, where interspecies interactions can shape the development, structure and function of the communities developed. A natural model system

would be very complex to study and draw conclusions from. Although a single strain was used in this study, the understanding and evaluation of the bacterial and MP connection can be of help to simulate the fate of ARGs in nature, and the impact on natural transformation.

5.1.1 Twitching motility of *A. baylyi*

The transformations were affected by twitching motility when using LB broth containing low salt concentrations, which made it difficult or almost impossible to count the colonies formed. McQueary et al. (2012) and De Silva and Kumar (2018) have studied the surface-associated motility in *A. baumannii* when strains were subjected to different salt concentrations, and the results revealed that reduced salinity enhanced twitching significantly, and therefore the growth media was changed to LB broth containing higher salt concentrations. In addition, a study by Henrichsen (1972) concluded that twitching on solid agar is normally dependent on the availability of a surface film of liquid, and therefore the agar plates were dried before usage to ensure that the agar surface were dry. Also, expired Milli-Q 0.22 µm membrane filter for particulate-free and bacteria-free water, Q-Gard® T1 Purification Cartridge, and Quantum® TEX Polishing Cartridge designed to remove trace levels of organics and ions were changed, since the Milli-Q water that was used may have contained contaminating substances that could have provoked twitching. After all those alterations, the twitching problem were almost solved, but still the phenomenon was observed in experiments performed later in the study, but to a lesser extent than before.

A study by Leong et al. (2017) identified transformation and twitching genes and their operons in *A. baylyi*, and the results revealed that both transformation and twitching utilize the same core type IV pilus proteins. The results also showed that proteins not needed for both competence and twitching, were instead found to specialize in one or the other. Some of the pilins studied were found to be required for both twitching and transformation, and some were found to be specialized for transformation and some for twitching motility. A study by Wilharm et al. (2013) revealed that competence and twitching are physiologically linked in *A. baumannii*, which means that many isolates are naturally transformable only while they are twitching along wet surfaces. One hypothesis could be that twitching motility and competence is linked in *A. baylyi* in similar ways as in *A. baumannii*.

5.2 Effect of selected microplastic polymers

Considering that ~70% of the global production of plastics is concentrated in 6 major polymer types (Geyer et al., 2017), a selection of these MPs, including HDPE, HDPS, PP, PVC A, and PVC B were selected as the target plastics in this study. Although there is a big variation in shape and size for the MPs obtained from the aquatic environment, laboratory-based MP research have infrequently considered these variations in MPs. The most often used MPs in MP research are industrially produced resin pellets, designed to obtain a specific particle size with desired properties made of pure polymers (Rozman et al., 2021). Although resin pellets represent MPs and are easily obtained, there is also other environmentally relevant plastic particles in forms of fragments, films and fibers, but in this study resin pellets were chosen to study the interactions between MPs and ARGs due to the advantage of similar particles containing equal size and shape rather than random particles.

The resin pellets selected had some characteristic varieties including: (I) polymer type; (II) shape; (III) size; (IV) surface structure; (V) density; and (VI) colour, and some of these differences were also present within the same polymer type. As seen in Figure 7, PP, PVC A and PVC B have some characteristic variations in size and shape, where some of the polymers have larger surface structure for bacterial attachment and colonization. These morphological differences affect the results obtained in this thesis, especially when using optical density as a measurement for the amount of biofilm formed on the MP surfaces. In this cases, the MP polymers with a larger surface tend to have a higher OD/absorbance because of more surface area for bacterial colonization. All of these differences in characteristics are important to consider when discussing the results, and if the experiments should have been repeated, the polymers with approximately same size and shape should have been selected, or the MPs should have been chosen based on weight.

5.3 Natural transformation

5.3.1 Natural transformation of *A. baylyi* with microplastic polymers

The natural transformation efficiency of *A. baylyi* under influence of different concentrations (0-, 10-, 50- and 200 number of MP particles) of MP polymers were investigated. The results revealed that the recipient strain JV26 acquired the kanamycin resistant gene (*nptII*) obtained from the donor strain JV31. This is as expected, since *A. baylyi* is highly competent for natural transformation and has the potential for uptake and chromosomal incorporation of DNA (Barbe et al., 2004). In the genus *Acinetobacter*, maximum competence is reached during exponential

growth-phase, and under optimal condition up to 25% of all cells in a competent *A. baylyi* culture are transformed (Palmen and Hellingwerf, 1997), and therefore, the transformations were performed in this phase. As described earlier, all of the transformant and recipient titers containing less than 30 colonies and more than 300 colonies were removed from the raw data due to the acceptance of 30 to 300 colonies as the most suitable number of colonies for counting (Tomasiewicz et al., 1980). By implementing this, the number of experiments in this study were reduced.

The transformation frequency results indicate a statistically significant difference when comparing HDPE to the rest of the MP polymers. The transformation frequency for HDPE increases when the concentration of MP polymers increases, while the transformation frequency for the rest of the polymers decreases when the concentration of MP polymers increases. The results indicate small effects, but the trend is however clear. Natural transformation is less efficient in *A. baylyi* in the presence of HDPE, HDPS and PVC A, than for PP and PVC B. PP and PVC B have an increased potential for DNA acquisition, but when the concentration of these polymers increases (to 50 and 200 MP particles), the transformation frequency decreases. The standard deviation for almost all of the transformation frequencies were approximately +/- half of the value. This is expected for transformation data, except for some data points that had a very small standard deviation, such as PP (200 MP particles), and some that had a large standard deviation, such as PP (10 and 50 MP particles). By looking at the raw data for these data points, the transformant and recipient titers differs within the same concentration of MP polymers. One of the experimental setups for PP (10 MP) has a tripling of the number of transformants/total CFU, which is presumably the reason for the big standard deviation for this data point.

The natural transformation assay was performed for 90 min, because by use of 100 ng DNA, the transformation is reaching a plateau and remains stable for the next 24 h. To investigate how the transformation frequency alters during the 90 min, and if it is a speed uptake difference, the transformation frequency could have been measured during different time points during the time from 0 to 90 min. Hence, the idea could have been to stop the transformation assay earlier with DNase to investigate if the trends are clearer before the transformation reach saturation at 90 min. A study by Bonifácio et al. (2021) evaluated the kinetics of natural transformation using 1 µg of isogenic gDNA at 30°C, and the results showed that natural transformation occurred shortly after 15 min of incubation with the donor genetic material, and that transformants were obtained at all the tested time points. A slow increase in transformation frequency was observed

in the time frame from 15 min to 5 h raising from $(2.4 \pm 1.9) \times 10^{-7}$ to $(3.4 \pm 2.0) \times 10^{-6}$ transformants/total CFU. Another solution to obtain more clear trends could have been the use of minimal growth medium instead of rich LB broth, so the bacterial growth is slowed down. Also it could have been an idea to re-streak the transformants on minimal media with rifampicin to make sure they are transformant cells, not mutant ones. The characterizing of transformants is normally a standard procedure, however, resistance against 10 mg/l kanamycin is a very strong phenotype in ADP1, that have over the last 20 years shown to not form by spontaneous mutation (K. Harms, personal information).

The natural transformation assays were in the beginning performed with virgin MP polymers, but due to many failed attempts because of twitching motility, all of the MP polymers used later in the experimental setups were partly aged, because of the disinfection with UV irradiation and washing with chlorine and ethanol. This could be one reason for the alterations of the transformation frequencies. The aging of the MP polymers has shown to have higher sorption capacity than virgin MPs, due to the increase in surface areas, hydrophilic properties at the surface, and higher contents of oxygen-containing groups (Agboola and Benson, 2021). For further analysis, the MP polymers used in this study should have undergone the same artificial aging process, since aged MPs show different morphology and chemical properties from virgin MPs and are suggested to promote the formation of biofilms on MPs and uptake of free DNA.

5.4 A. *baylyi* biofilm formation on microplastic polymers studied with optical density

The early biofilm formation of *A. baylyi* on HDPE, HDPS, PP, PVC A, and PVC B was investigated with optical density at 595 nm. The samples were diluted with EtOH before measuring the OD of crystal violet, because if a sample has an OD greater than 3, it means that only 1 photon of light out of 1.000 will be measured by the detector, and this small amount of light is hard to accurately detect above the background noise (Dell, 2012). Therefore, OD measurements above 3 will have greater error and be less accurate. The results from the OD measurements indicates that the colonization speed differs for the different polymers. The biofilm formation increases for the polymers PVC B, PVC A and PP, while the biofilm formation is closer to zero for HDPE and HDPS, including the negative control glass. In addition, by visual inspection of the stained MP polymers, PVC B, PVC A and PP contained more crystal violet stain than the rest of the polymers, which correlates with the results obtained from the OD measurements.

By looking at the raw data, the OD measurements varies within the same polymer type because the polymers are random picked and they have variations in size, shape and aging, but the trend is still clear; PVC A has the most rapid increase in OD (biofilm) for all of the timepoints, which indicates that *A. baylyi* colonize PVC A most efficiently. The amount of biofilm is thus followed on what is detected on PVC B, PP, HDPS and HDPE. The OD measurements of biofilms were performed with aged MP polymers, which had been used in earlier experimental setups with transformation assay and thus disinfected several times. The SEM images for aged PP revealed that some of the deep cracks formed on the polymer surface contained remnants of bacterial biofilm and residual organic matter of *A. baylyi* from earlier experimental setups performed in this study, which were not fully removed with the sterilization and washing steps. If the residual organic matter is not removed from the MP surface, this debris will affect the OD measurement results when the MP polymers are stained with crystal violet, since this method cannot distinguish the living status of cells. This could also be one reason for the variations of the OD measurements of biofilms that was obtained.

5.4.1 Natural transformation of *A. baylyi* biofilm grown on microplastic polymers for 96 h

The natural transformation of *A. baylyi* biofilms grown on the MP polymers PVC B, PVC A and PP for 96 h was investigated. In this experimental setup, a Branson 1510 ultrasonic cleaner operated at its maximum power output of 80 W, was used to detach the bacteria from the MP polymers. It is not verified or analysed if all of the bacteria on the MP polymer surfaces are detached with this method. The transformation frequency results after 96 h indicates a reduced number of transformant and recipient titers, which is expected due to limited special growing on the MP polymers compared to the earlier transformations performed. However, the transformation frequency at 96 h is higher than earlier transformation setups. In liquid cultures the transformation frequencies were mostly around 10^{-5} and some at 10^{-4} . However, for this transformation setups, all of the transformation frequencies were at 10^{-4} for both PVC B, PVC A and PP. The transformation frequency for *A. baylyi* biofilms indicates that the colonization of PP is the most efficient.

5.5 Scanning electron microscopy

5.5.1 Virgin and aged microplastic polymers characteristics

The virgin and aged polymers HDPE, HDPS, PP, PVC A, and PVC B were studied with scanning electron microscopy to investigate if the exposure to UV irradiation and chemicals affects the surface morphology. The exposure of plastics to environmental conditions is expected to result in mechanical alteration of the surface morphology, and over time the surface area of plastics which is available for microbial colonization increases (Tu et al., 2020, Fotopoulou et al., 2014). The SEM images confirmed that UV irradiation and chemicals caused fragmentation and formation of cracks and unevenness, resulting in open structures, as well as an increase in surface roughness. These physico-chemical properties of surfaces are known to influence the attachment of bacterial biofilm development, and the hydrophobicity has been shown to determine bacterial attachment, with bacteria preferentially attaching to more hydrophilic surfaces. Since the surface hydrophobicity was not measured, it cannot be excluded that it might have influenced the biofilm formation.

All of these morphologic changes observed on the surface of the aged polymers can improve their susceptibility to liquid penetration and provide preferential areas for foreign substances or organisms to become lodged in the particles, increasing their potential as transport vectors for co-occurring pollutants and microorganisms in the environment. This liquid penetration is clear on the surface of aged PP, shown in Figure 14, where some of the deep cracks formed contains remnants of bacterial biofilm and residual organic matter of *A. baylyi* from earlier experimental setups performed in this thesis. In addition to surface alterations, the aged surface of HDPE and HDPS contains remnants of different chemicals, most likely chlorine which is used in the disinfection and washing steps of the polymers, which also indicates that the rinsing with MilliQ water was not fully successful to eliminate residual salt.

5.5.2 Early *A. baylyi* biofilm formation on microplastic polymers

The 4 days early-stage biofilm formation on the aged polymers PP, PVC A, and PVC B was studied with SEM. The samples were pre-fixed with and without 1% osmium tetroxide to determine if this post-fixation step improved imaging. The results revealed that the preparation method without osmium conducted useful images, which requires less time and costs, and is therefore suitable for bacterial biofilm studies studied with SEM. Although only one particle from each polymer type were studied, not allowing a more thorough statistical analysis, a consistent difference between PVC B, PVC A and PP was obvious throughout the entire

incubation period. The SEM results after 4 days of incubation, shown in Figure 15, revealed that the development and colonization of *A. baylyi* on the PVC B surface exhibited a larger area covered by a biofilm matrix and individual cells followed by PVC A and PP. The same trend was shown in a study by Pinto et al. (2019). The study determined the development and colonization of bacterial communities on the MP polymers PP and PVC under ambient and sim light conditions in the coastal Northern Adriatic over the course of two months using SEM. The results revealed that after one week of incubation, the surface of PVCs exhibited a larger area of their surface covered by a biofilm matrix and individual cells in both the ambient and dim light treatment compared to PP. Another study by Xu et al. (2019) investigated the successional stages of microbial communities attached to PP and PVC microplastics exposed for one year in the coastal seawater of China, and the SEM analysis in this study also revealed that PVC favored microbial adhesion compared to PP.

The relatively large differences in biofilm formation and composition after 4 days of incubation might be an indication that differences in the chemical composition and surface structure play a significant role in the attachment of bacterial populations. The differences between the surface morphologies of PVC and PP may be determined by their specific properties, and thus, the physical and chemical properties of different materials should be considered in evaluation the development and colonization of bacterial communities on the MP surfaces. By looking at the chemical properties, the Cl atom in PVC occupies a greater space than the methyl group in PP, and the PVC monomers are further away than the PP monomers. Furthermore, the Cl atom is a strong electron-withdrawing group, and the electron cloud is attracted to the C-Cl bond, thereby decreasing the electron density of the C-C bond and thus causing lower bond energy, making it vulnerable to attack and breakage. Therefore, PVC is more susceptible to biological attack, for instance by bacteria, than PP (Xu et al., 2019, Crawford and Quinn, 2017).

5.6 Further studies

The first experimental step after this study would be to achieve some more data on natural transformation of *A. baylyi* in the presence and absence of the different microplastic polymers, and on natural transformation of *A. baylyi* biofilms grown on MPs. In addition, it would be interesting to observe and verify this model in a natural system, by for instance using ocean or wastewater. Since this study only focuses on the impact of natural transformation on MPs with a model organism it is necessary and important to figure out how this works in the real and complicated environment.

6 Conclusion

This project provides new insight into evaluating the risks caused by microplastic waste and the interactions between MPs and ARGs in the aquatic environment. The main conclusion of this study is that the presence and absence of the MP polymers HDPS, HDPE, PP, PVC A, and PVC B affects the potential for DNA uptake via natural transformation in the naturally competent bacteria *A. baylyi*. Further, the transformation frequency of the kanamycin resistance marker (*nptII*) alters depending on the presence and absence of different concentrations of MP polymers. The effects are small, but the trend is clear; the DNA uptake is the highest in the presence of PP and PVC B. Weathering processes were confirmed to change the surface morphology of virgin plastics, with an increase in surface roughness, pores and cracks. The early bacterial accumulation of *A. baylyi* on the different MP polymers were found to differ, where the OD measurements revealed that most bacterial accumulation was found on the polymers PVC A, PVC B and PP. The SEM images revealed that the bacterial colonization of *A. baylyi* started in the formed cracks and wells before colonizing the smooth MP surfaces. These results are laying the foundation for further investigations of natural transformation associated with MPs in the aquatic environment, and it is necessary to further examine the interactions between MPs and ARGs related to environmental implications to better understand the environmental and health impact and fate of both of the contaminants.

7 References

- AGBOOLA, O. D. & BENSON, N. U. 2021. Physisorption and Chemisorption Mechanisms Influencing Micro (Nano) Plastics-Organic Chemical Contaminants Interactions: A Review. *Frontiers in Environmental Science*, 9.
- AL-WAILI, N., SALOM, K., AL-GHAMDI, A. & ANSARI, M. J. 2012. Antibiotic, pesticide, and microbial contaminants of honey: human health hazards. *TheScientificWorldJournal*, 2012, 930849-930849.
- AMARAL-ZETTLER, L. A., ZETTLER, E. R. & MINCER, T. J. 2020. Ecology of the plastisphere. *Nature Reviews Microbiology*, 18, 139-151.
- AMINOV, R. I. 2010. A brief history of the antibiotic era: lessons learned and challenges for the future. *Frontiers in microbiology*, 1, 134-134.
- ANDAM, C. P., FOURNIER, G. P. & GOGARTEN, J. P. 2011. Multilevel populations and the evolution of antibiotic resistance through horizontal gene transfer. *FEMS Microbiology Reviews*, 35, 756-767.
- ARIAS-ANDRES, M., KLÜMPER, U., ROJAS-JIMENEZ, K. & GROSSART, H.-P. 2018. Microplastic pollution increases gene exchange in aquatic ecosystems. *Environmental Pollution*, 237, 253-261.
- ATUGODA, T., VITHANAGE, M., WIJESEKARA, H., BOLAN, N., SARMAH, A. K., BANK, M. S., YOU, S. & OK, Y. S. 2021. Interactions between microplastics, pharmaceuticals and personal care products: Implications for vector transport. *Environment International*, 149, 106367.
- BARBE, V., VALLENET, D., FONKNECHTEN, N., KREIMEYER, A., OZTAS, S., LABARRE, L., CRUVEILLER, S., ROBERT, C., DUPRAT, S., WINCKER, P., ORNSTON, L. N., WEISSENBACH, J., MARLIÈRE, P., COHEN, G. N. & MÉDIGUE, C. 2004. Unique features revealed by the genome sequence of *Acinetobacter* sp. ADP1, a versatile and naturally transformation competent bacterium. *Nucleic Acids Res*, 32, 5766-79.
- BEN, Y., FU, C., HU, M., LIU, L., WONG, M. H. & ZHENG, C. 2019. Human health risk assessment of antibiotic resistance associated with antibiotic residues in the environment: A review. *Environmental Research*, 169, 483-493.
- BONIFÁCIO, M., MATEUS, C., ALVES, A. R., MALDONADO, E., DUARTE, A. P., DOMINGUES, F., OLEASTRO, M. & FERREIRA, S. 2021. Natural Transformation as a Mechanism of Horizontal Gene Transfer in *Aliarcobacter butzleri*. *Pathogens*, 10, 909.
- BONNET, M., LAGIER, J. C., RAOULT, D. & KHELAIPIA, S. 2019. Bacterial culture through selective and non-selective conditions: the evolution of culture media in clinical microbiology. *New microbes and new infections*, 34, 100622-100622.
- BOUCHER, J. & FRIOT, D. 2017. *Primary Microplastics in the Oceans: A Global Evaluation of Sources*.
- BURMEISTER, A. R. 2015. Horizontal Gene Transfer. *Evolution, medicine, and public health*, 2015, 193-194.
- CLARDY, J., FISCHBACH, M. A. & CURRIE, C. R. 2009. The natural history of antibiotics. *Current biology : CB*, 19, R437-R441.
- CLEMMER, K. M., BONOMO, R. A. & RATHER, P. N. 2011. Genetic analysis of surface motility in *Acinetobacter baumannii*. *Microbiology (Reading, England)*, 157, 2534-2544.
- CORRAL, J., PÉREZ-VARELA, M., SÁNCHEZ-OSUNA, M., CORTÉS, P., BARBÉ, J. & ARANDA, J. 2021. Importance of twitching and surface-associated motility in the virulence of *Acinetobacter baumannii*. *Virulence*, 12, 2201-2213.

- COSTA, J. P. D., ROCHA-SANTOS, T. & DUARTE, A. C. The environmental impacts of plastics and micro-plastics use, waste and pollution: EU and national measures. 2020.
- CRAWFORD, C. B. & QUINN, B. 2017. 4 - Physiochemical properties and degradation. In: CRAWFORD, C. B. & QUINN, B. (eds.) *Microplastic Pollutants*. Elsevier.
- CRESPY, D., BOZONNET, M. & MEIER, M. 2008. 100 Years of Bakelite, the Material of a 1000 Uses. *Angewandte Chemie International Edition*, 47, 3322-3328.
- DAVIES, J. & DAVIES, D. 2010. Origins and evolution of antibiotic resistance. *Microbiology and molecular biology reviews : MMBR*, 74, 417-433.
- DE SILVA, P. M. & KUMAR, A. 2018. Effect of Sodium Chloride on Surface-Associated Motility of *Acinetobacter baumannii* and the Role of AdeRS Two-Component System. *The Journal of Membrane Biology*, 251, 5-13.
- DE VRIES, J., HEINE, M., HARMS, K. & WACKERNAGEL, W. 2003. Spread of recombinant DNA by roots and pollen of transgenic potato plants, identified by highly specific biomonitoring using natural transformation of an *Acinetobacter* sp. *Applied and environmental microbiology*, 69, 4455-4462.
- DELL, E. 2012. Optical Density for Absorbance Measurements. *BMG Labtech*.
- DONG, H., CHEN, Y., WANG, J., ZHANG, Y., ZHANG, P., LI, X., ZOU, J. & ZHOU, A. 2021. Interactions of microplastics and antibiotic resistance genes and their effects on the aquaculture environments. *Journal of Hazardous Materials*, 403, 123961.
- EBERT, C., TUCHSCHERR, L., UNGER, N., PÖLLATH, C., GLADIGAU, F., POPP, J., LÖFFLER, B. & NEUGEBAUER, U. 2021. Correlation of crystal violet biofilm test results of *Staphylococcus aureus* clinical isolates with Raman spectroscopic read-out. *Journal of Raman Spectroscopy*, n/a.
- ELLIOTT, K. T. & NEIDLE, E. L. 2011. *Acinetobacter baylyi* ADP1: Transforming the choice of model organism. *IUBMB Life*, 63, 1075-1080.
- EMAMALIPOUR, M., SEIDI, K., ZUNUNI VAHED, S., JAHANBAN-ESFAHLAN, A., JAYMAND, M., MAJDI, H., AMOOZGAR, Z., CHITKUSHEV, L. T., JAVAHERI, T., JAHANBAN-ESFAHLAN, R. & ZARE, P. 2020. Horizontal Gene Transfer: From Evolutionary Flexibility to Disease Progression. *Frontiers in Cell and Developmental Biology*, 8.
- ERIKSEN, M., LEBRETON, L. C. M., CARSON, H. S., THIEL, M., MOORE, C. J., BORRERO, J. C., GALGANI, F., RYAN, P. G. & REISSER, J. 2014. Plastic Pollution in the World's Oceans: More than 5 Trillion Plastic Pieces Weighing over 250,000 Tons Afloat at Sea. *PLOS ONE*, 9, e111913.
- ERNI-CASSOLA, G., ZADJELOVIC, V., GIBSON, M. I. & CHRISTIE-OLEZA, J. A. 2019. Distribution of plastic polymer types in the marine environment; A meta-analysis. *Journal of Hazardous Materials*, 369, 691-698.
- FOTOPOULOU, K., VAKROS, J. & KARAPANAGIOTI, H. 2014. *Surface properties of marine microplastics that affect their interaction with pollutants and microbes*.
- GEYER, R., JAMBECK, J. R. & LAW, K. L. 2017. Production, use, and fate of all plastics ever made. *Science advances*, 3, e1700782-e1700782.
- GOMES, L. C. & MERGULHÃO, F. J. 2017. SEM Analysis of Surface Impact on Biofilm Antibiotic Treatment. *Scanning*, 2017, 2960194-2960194.
- GRIN, I., SCHWARZ, H. & LINKE, D. 2011. Electron microscopy techniques to study bacterial adhesion. *Adv Exp Med Biol*, 715, 257-69.
- GUO, X.-P., SUN, X.-L., CHEN, Y.-R., HOU, L., LIU, M. & YANG, Y. 2020. Antibiotic resistance genes in biofilms on plastic wastes in an estuarine environment. *Science of The Total Environment*, 745, 140916.
- GUO, X., PANG, J., CHEN, S. & JIA, H. 2018. Sorption properties of tylosin on four different microplastics. *Chemosphere*, 209, 240-245.

- GUPTA, N. 2019. DNA Extraction and Polymerase Chain Reaction. *Journal of cytology*, 36, 116-117.
- HENRICHSEN, J. 1972. Bacterial surface translocation: a survey and a classification. *Bacteriological reviews*, 36, 478-503.
- HENRICHSEN, J. 1983. TWITCHING MOTILITY. *Annual Review of Microbiology*, 37, 81-93.
- HUTCHINGS, M. I., TRUMAN, A. W. & WILKINSON, B. 2019. Antibiotics: past, present and future. *Current Opinion in Microbiology*, 51, 72-80.
- HÜLTER, N., SØRUM, V., BORCH-PEDERSEN, K., LILJEGREN, M. M., UTNES, A. L. G., PRIMICERIO, R., HARMS, K. & JOHNSEN, P. J. 2017. Costs and benefits of natural transformation in *Acinetobacter baylyi*. *BMC Microbiology*, 17, 34.
- IVAR DO SUL, J. A. & COSTA, M. F. 2014. The present and future of microplastic pollution in the marine environment. *Environmental Pollution*, 185, 352-364.
- KANNISTO, M., AHO, T., KARP, M. & SANTALA, V. 2014. Metabolic engineering of *Acinetobacter baylyi* ADP1 for improved growth on gluconate and glucose. *Applied and environmental microbiology*, 80, 7021-7027.
- KIM, S.-K. 2021. Sampling the sea to find ways of tracing the origins of microplastic pollution. *Reinforced Plastics*.
- KOSTAKIOTI, M., HADJIFRANGISKOU, M. & HULTGREN, S. J. 2013. Bacterial biofilms: development, dispersal, and therapeutic strategies in the dawn of the postantibiotic era. *Cold Spring Harbor perspectives in medicine*, 3, a010306-a010306.
- LAW, K. & THOMPSON, R. 2014. Oceans. Microplastics in the seas. *Science (New York, N.Y.)*, 345, 144-5.
- LEONG, C. G., BLOOMFIELD, R. A., BOYD, C. A., DORNBUSCH, A. J., LIEBER, L., LIU, F., OWEN, A., SLAY, E., LANG, K. M. & LOSTROH, C. P. 2017. The role of core and accessory type IV pilus genes in natural transformation and twitching motility in the bacterium *Acinetobacter baylyi*. *PloS one*, 12, e0182139-e0182139.
- LI, J., ZHANG, K. & ZHANG, H. 2018. Adsorption of antibiotics on microplastics. *Environmental Pollution*, 237, 460-467.
- LIU, G., ZHU, Z., YANG, Y., SUN, Y., YU, F. & MA, J. 2019. Sorption behavior and mechanism of hydrophilic organic chemicals to virgin and aged microplastics in freshwater and seawater. *Environmental Pollution*, 246, 26-33.
- LIU, Y., LIU, W., YANG, X., WANG, J., LIN, H. & YANG, Y. 2021. Microplastics are a hotspot for antibiotic resistance genes: Progress and perspective. *Science of The Total Environment*, 773, 145643.
- LU, X.-M., LU, P.-Z. & LIU, X.-P. 2020. Fate and abundance of antibiotic resistance genes on microplastics in facility vegetable soil. *Science of The Total Environment*, 709, 136276.
- MANN, A., NEHRA, K., RANA, J. S. & DAHIYA, T. 2021. Antibiotic resistance in agriculture: Perspectives on upcoming strategies to overcome upsurge in resistance. *Current Research in Microbial Sciences*, 2, 100030.
- MARATHE, N. P. & BANK, M. S. 2022. The Microplastic-Antibiotic Resistance Connection. In: BANK, M. S. (ed.) *Microplastic in the Environment: Pattern and Process*. Cham: Springer International Publishing.
- MARTÍNEZ-CAMPOS, S., GONZÁLEZ-PLEITER, M., FERNÁNDEZ-PIÑAS, F., ROSAL, R. & LEGANÉS, F. 2021. Early and differential bacterial colonization on microplastics deployed into the effluents of wastewater treatment plants. *Science of The Total Environment*, 757, 143832.

- MCCORMICK, A., HOELLEIN, T. J., MASON, S. A., SCHLUEP, J. & KELLY, J. J. 2014. Microplastic is an Abundant and Distinct Microbial Habitat in an Urban River. *Environmental Science & Technology*, 48, 11863-11871.
- MCQUEARY, C. N., KIRKUP, B. C., SI, Y., BARLOW, M., ACTIS, L. A., CRAFT, D. W. & ZURAWSKI, D. V. 2012. Extracellular stress and lipopolysaccharide modulate *Acinetobacter baumannii* surface-associated motility. *Journal of Microbiology*, 50, 434-443.
- MEEK, R. W., VYAS, H. & PIDDOCK, L. J. V. 2015. Nonmedical Uses of Antibiotics: Time to Restrict Their Use? *PLoS biology*, 13, e1002266-e1002266.
- MUHAMMAD, M. H., IDRIS, A. L., FAN, X., GUO, Y., YU, Y., JIN, X., QIU, J., GUAN, X. & HUANG, T. 2020. Beyond Risk: Bacterial Biofilms and Their Regulating Approaches. *Frontiers in Microbiology*, 11.
- MUNITA, J. M. & ARIAS, C. A. 2016. Mechanisms of Antibiotic Resistance. *Microbiology spectrum*, 4, 10.1128/microbiolspec.VMBF-0016-2015.
- NERLAND, I. L., HALSBAND, C., ALLAN, I. & THOMAS, K. V. 2014. Microplastics in marine environments: Occurrence, distribution and effects. <http://hdl.handle.net/11250/283879>: Norwegian Institute for Waster Research
- OVERBALLE-PETERSEN, S., HARMS, K., ORLANDO, L. A. A., MAYAR, J. V. M., RASMUSSEN, S., DAHL, T. W., ROSING, M. T., POOLE, A. M., SICHERITZ-PONTEN, T., BRUNAK, S., INSELMANN, S., VRIES, J. D., WACKERNAGEL, W., PYBUS, O. G., NIELSEN, R., JOHNSEN, P. J., NIELSEN, K. M. & WILLERSLEV, E. 2013. Bacterial natural transformation by highly fragmented and damaged DNA. *Proceedings of the National Academy of Sciences*, 110, 19860-19865.
- PALMEN, R. & HELLINGWERF, K. J. 1997. Uptake and processing of DNA by *Acinetobacter calcoaceticus*--a review. *Gene*, 192, 179-90.
- PHAM, D. N., CLARK, L. & LI, M. 2021. Microplastics as hubs enriching antibiotic-resistant bacteria and pathogens in municipal activated sludge. *Journal of Hazardous Materials Letters*, 2, 100014.
- PINTO, M., LANGER, T. M., HÜFFER, T., HOFMANN, T. & HERNDL, G. J. 2019. The composition of bacterial communities associated with plastic biofilms differs between different polymers and stages of biofilm succession. *PloS one*, 14, e0217165-e0217165.
- RABIN, N., ZHENG, Y., OPOKU-TEMENG, C., DU, Y., BONSU, E. & SINTIM, H. O. 2015. Biofilm formation mechanisms and targets for developing antibiofilm agents. *Future Medicinal Chemistry*, 7, 493-512.
- REISSER, J., SHAW, J., HALLEGRAEFF, G., PROIETTI, M., BARNES, D. K. A., THUMS, M., WILCOX, C., HARDESTY, B. D. & PATTIARATCHI, C. 2014. Millimeter-Sized Marine Plastics: A New Pelagic Habitat for Microorganisms and Invertebrates. *PLOS ONE*, 9, e100289.
- ROCHMAN, C., ANDRADY, A., DUDAS, S., FABRES, J., GALGANI, F., LEAD, D., HIDALGO-RUZ, V., HONG, S., KERSHAW, P., LEBRETON, L., LUSHER, A., NARAYAN, R., PAHL, S., POTE MRA, J., ROCHMAN, C., SHERIF, S., SEAGER, J., SHIM, W., SOBRAL, P. & AMARAL-ZETTLER, L. 2016. *SOURCES, FATE AND EFFECTS OF MICROPLASTICS IN THE MARINE ENVIRONMENT: PART 2 OF A GLOBAL ASSESSMENT*.
- ROZMAN, U., TURK, T., SKALAR, T., ZUPANČIČ, M., ČELAN KOROŠIN, N., MARINŠEK, M., OLIVERO-VERBEL, J. & KALČIKOVÁ, G. 2021. An extensive characterization of various environmentally relevant microplastics – Material properties, leaching and ecotoxicity testing. *Science of The Total Environment*, 773, 145576.

- SANTALA, S. & SANTALA, V. 2021. Acinetobacter baylyi ADP1—naturally competent for synthetic biology. *Essays in Biochemistry*, 65, 309-318.
- SEBILLE, E., SPATHI, C. & GILBERT, A. 2016. *The ocean plastic pollution challenge: towards solutions in the UK*.
- SU, Y., ZHANG, Z., ZHU, J., SHI, J., WEI, H., XIE, B. & SHI, H. 2021. Microplastics act as vectors for antibiotic resistance genes in landfill leachate: The enhanced roles of the long-term aging process. *Environmental Pollution*, 270, 116278.
- SUN, D. 2018. Pull in and Push Out: Mechanisms of Horizontal Gene Transfer in Bacteria. *Frontiers in Microbiology*, 9.
- SUN, D., JEANNOT, K., XIAO, Y. & KNAPP, C. W. 2019. Editorial: Horizontal Gene Transfer Mediated Bacterial Antibiotic Resistance. *Frontiers in Microbiology*, 10.
- TACCONELLI, E., CARRARA, E., SAVOLDI, A., HARBARTH, S., MENDELSON, M., MONNET, D. L., PULCINI, C., KAHLMETER, G., KLUYTMANS, J., CARMELI, Y., OUELLETTE, M., OUTTERSON, K., PATEL, J., CAVALERI, M., COX, E. M., TALEBI BEZMIN ABADI, A., RIZVANOV, A. A., HAERTLÉ, T. & BLATT, N. L. 2019. World Health Organization Report: Current Crisis of Antibiotic Resistance. *BioNanoScience*, 9, 778-788.
- TAN, S. C. & YIAP, B. C. 2009. DNA, RNA, and Protein Extraction: The Past and The Present. *Journal of Biomedicine and Biotechnology*, 2009, 574398.
- THOMAS, C. M. & NIELSEN, K. M. 2005. Mechanisms of, and Barriers to, Horizontal Gene Transfer between Bacteria. *Nature Reviews Microbiology*, 3, 711-721.
- THOMPSON, R., OLSEN, Y., MITCHELL, R., DAVIS, A., ROWLAND, S., JOHN, A., MCGONIGLE, D. F. & RUSSELL, A. 2004. Lost at Sea: Where Is All the Plastic? *Science (New York, N.Y.)*, 304, 838.
- THOMPSON, R. C., SWAN, S. H., MOORE, C. J. & VOM SAAL, F. S. 2009. Our plastic age. *Philos Trans R Soc Lond B Biol Sci*, 364, 1973-6.
- TOMASIEWICZ, D. M., HOTCHKISS, D. K., REINBOLD, G. W., READ, R. B., JR. & HARTMAN, P. A. 1980. The Most Suitable Number of Colonies on Plates for Counting (1). *J Food Prot*, 43, 282-286.
- TU, C., ZHOU, Q., ZHANG, C., LIU, Y. & LUO, Y. 2020. Biofilms of Microplastics.
- ULUSEKER, C., KASTER, K. M., THORSEN, K., BASIRY, D., SHOBANA, S., JAIN, M., KUMAR, G., KOMMEDAL, R. & PALA-OZKOK, I. 2021. A Review on Occurrence and Spread of Antibiotic Resistance in Wastewaters and in Wastewater Treatment Plants: Mechanisms and Perspectives. *Frontiers in Microbiology*, 12.
- UTNES, A. L. G., SØRUM, V., HÜLTER, N., PRIMICERIO, R., HEGSTAD, J., KLOOS, J., NIELSEN, K. M. & JOHNSEN, P. J. 2015. Growth phase-specific evolutionary benefits of natural transformation in *Acinetobacter baylyi*. *The ISME Journal*, 9, 2221-2231.
- VAN CAUWENBERGHE, L., VANREUSEL, A., MEES, J. & JANSSEN, C. R. 2013. Microplastic pollution in deep-sea sediments. *Environmental Pollution*, 182, 495-499.
- VERNIKOS, G. & MEDINI, D. 2014. Horizontal Gene Transfer and the Role of Restriction-Modification Systems in Bacterial Population Dynamics.
- WELCH, K., CAI, Y. & STRØMME, M. 2012. A method for quantitative determination of biofilm viability. *Journal of functional biomaterials*, 3, 418-431.
- WILHARM, G., PIESKER, J., LAUE, M. & SKIEBE, E. 2013. DNA Uptake by the Nosocomial Pathogen *Acinetobacter baumannii* Occurs during Movement along Wet Surfaces. *Journal of Bacteriology*, 195, 4146-4153.
- WILLEY, J. M. S. L. W. C. J. P. L. M. 2017. *Prescott's Microbiology*.

- WRIGHT, M. H., ADELSKOV, J. & GREENE, A. C. 2017. Bacterial DNA Extraction Using Individual Enzymes and Phenol/Chloroform Separation. *Journal of microbiology & biology education*, 18, 18.2.48.
- XU, X., WANG, S., GAO, F., LI, J., ZHENG, L., SUN, C., HE, C., WANG, Z. & QU, L. 2019. Marine microplastic-associated bacterial community succession in response to geography, exposure time, and plastic type in China's coastal seawaters. *Marine Pollution Bulletin*, 145, 278-286.
- YANG, K., CHEN, Q.-L., CHEN, M.-L., LI, H.-Z., LIAO, H., PU, Q., ZHU, Y.-G. & CUI, L. 2020a. Temporal Dynamics of Antibiotic Resistome in the Plasticsphere during Microbial Colonization. *Environmental Science & Technology*, 54, 11322-11332.
- YANG, Y., LIU, G., SONG, W., YE, C., LIN, H., LI, Z. & LIU, W. 2019. Plastics in the marine environment are reservoirs for antibiotic and metal resistance genes. *Environment International*, 123, 79-86.
- YANG, Y., LIU, W., ZHANG, Z., GROSSART, H.-P. & GADD, G. M. 2020b. Microplastics provide new microbial niches in aquatic environments. *Applied Microbiology and Biotechnology*, 104, 6501-6511.
- YIN, W., WANG, Y., LIU, L. & HE, J. 2019. Biofilms: The Microbial "Protective Clothing" in Extreme Environments. *International journal of molecular sciences*, 20, 3423.
- YUAN, Q., SUN, R., YU, P., CHENG, Y., WU, W., BAO, J. & ALVAREZ, P. J. J. 2022. UV-aging of microplastics increases proximal ARG donor-recipient adsorption and leaching of chemicals that synergistically enhance antibiotic resistance propagation. *Journal of Hazardous Materials*, 427, 127895.
- ZAMANI DAHAJ, S. A. 2015. *A phylogenetic model to predict the patterns of presence and absence of genes in bacterial genomes and estimate the frequency of horizontal gene transfer.*
- ZEIDLER, S. & MÜLLER, V. 2019. Coping with low water activities and osmotic stress in *Acinetobacter baumannii*: significance, current status and perspectives. *Environmental Microbiology*, 21, 2212-2230.
- ZETTLER, E. R., MINCER, T. J. & AMARAL-ZETTLER, L. A. 2013. Life in the "Plasticsphere": Microbial Communities on Plastic Marine Debris. *Environmental Science & Technology*, 47, 7137-7146.
- ZHANG, J. X. J. & HOSHINO, K. 2014. Chapter 5 - Optical Transducers: Optical Molecular Sensors and Optical Spectroscopy. *In: ZHANG, J. X. J. & HOSHINO, K. (eds.) Molecular Sensors and Nanodevices.* Oxford: William Andrew Publishing.

Appendix

Appendix A – OD measurements raw data

The raw data for the early accumulation of *A. baylyi* on microplastic polymers by optical density can be found in Figure A 1, and the mean and standard deviation in Figure A 2.

24 h	PVC B	HDPS	PVC A	PP	HDPE	Glass	48 h	PVC B	HDPS	PVC A	PP	HDPE	Glass
		0,108		0,283	0,105	0,017		0,567	0,132	0,715	0,312	0,035	0,013
	0,375	0,159	0,517	0,386	0,132	0,020		0,461	0,113		0,162	0,020	0,025
	0,242	0,184	0,532	0,315	0,084	0,019		0,627	0,220	0,709	0,108	0,039	0,013
	0,336	0,172	0,500	0,346	0,071	0,028			0,148	0,701	0,173	0,032	0,023
	0,306	0,167	0,439	0,297	0,065	0,010		0,524	0,150	0,718	0,372	0,044	0,018
	0,315	0,158	0,497	0,325	0,091	0,019		0,545	0,153	0,711	0,225	0,034	0,018
72 h	PVC B	HDPS	PVC A	PP	HDPE	Glass	96 h	PVC B	HDPS	PVC A	PP	HDPE	Glass
	0,552	0,076	0,704	0,621	0,018	0,012		0,553	0,046	0,717	0,291	0,109	0,014
	0,568	0,057	0,762	0,562	0,036	0,011		0,596	0,153	0,853	0,356	0,122	0,023
	0,537	0,055		0,561	0,027	0,008		0,505	0,063	0,939	0,580	0,082	0,009
	0,525	0,049	0,849	0,438	0,031	0,010		0,859	0,107	0,881	0,584	0,110	0,011
	0,595	0,074	0,805	0,309	0,085	0,015		0,567	0,014	0,914	0,430	0,067	0,012
	0,555	0,062	0,780	0,498	0,039	0,011		0,616	0,077	0,861	0,448	0,098	0,014

Figure A 1: The raw data for the early accumulation of *A. baylyi* on PVC B, HDPS, PVC A, PP, HDPE, and glass.

Mean	PVC B	HDPS	PVC A	PP	HDPE	Glass
0 h	0,000	0,000	0,000	0,000	0,000	0,000
24 h	0,315	0,158	0,497	0,325	0,091	0,019
48 h	0,545	0,153	0,711	0,225	0,034	0,018
72 h	0,555	0,062	0,780	0,498	0,039	0,010
96 h	0,616	0,077	0,861	0,448	0,098	0,014
St.Dev	PVC B	HDPS	PVC A	PP	HDPE	Glass
0 h	0,000	0,000	0,000	0,000	0,000	0,000
24 h	0,056	0,029	0,041	0,041	0,027	0,006
48 h	0,070	0,041	0,008	0,111	0,009	0,006
72 h	0,027	0,012	0,062	0,125	0,026	0,003
96 h	0,140	0,054	0,087	0,132	0,023	0,005

Figure A 2: The mean and standard deviation for the early accumulation of *A. baylyi* on PVC B, HDPS, PVC A, PP, HDPE, and glass.

Appendix B – Natural transformation raw data

The raw data for the natural transformation of *A. baylyi* under influence of different concentrations of microplastic polymers and the natural transformation of *A. baylyi* biofilms grown on microplastic polymers for 96 h can be seen in the following chapter. Natural transformation raw data for HDPE can be seen in Figure A 3, for HDPS in Figure A 4, for PP in Figure A 5, for PVC B in Figure A 6, and for PVC A in Figure A 7. The mean and standard deviation in shown in Figure A 9. Natural transformation raw data for the biofilm grown on MP polymers for 96 h can be seen in Figure A 8, and mean and standard deviation in Figure A 10.

Transformants (0 MP)	10 ⁻¹ = 51	51 x 50 x 10 ¹	2,55E+04	10 ⁻¹ = 43	43 x 50 x 10 ¹	2,15E+04	10 ⁻¹ = 8	8 x 50 x 10 ¹		10 ⁻¹ = 36	36 x 10 ²	3,60E+03	10 ⁻¹ = 54	54 x 10 ²	5,40E+03
	10 ⁻¹ = 32	32 x 50 x 10 ¹	1,60E+04	10 ⁻¹ = 111	111 x 50 x 10 ¹	5,55E+04	10 ⁻¹ = 31	31 x 50 x 10 ¹	1,55E+04	10 ⁻¹ = 42	42 x 10 ²	4,20E+03	10 ⁻¹ = 43	43 x 10 ²	4,30E+03
	10 ⁻¹ = 30	30 x 50 x 10 ¹	1,50E+04	10 ⁻¹ = 73	73 x 50 x 10 ¹	3,65E+04	10 ⁻¹ = 33	33 x 50 x 10 ¹	1,65E+04	10 ⁻¹ = 41	41 x 10 ²	4,10E+03	10 ⁻¹ = 49	49 x 10 ²	4,90E+03
			1,88E+04			3,78E+04			1,60E+04			3,97E+03			4,87E+03
Recipients (0 MP)	10 ⁻⁵ = 59	59 x 50 x 10 ⁵	2,95E+08	10 ⁻⁵ = 158	158 x 50 x 10 ⁵	7,90E+08	10 ⁻⁵ = 42	42 x 50 x 10 ⁵	2,10E+08	10 ⁻⁵ = 182	182 x 10 ⁶	1,82E+08	10 ⁻⁵ = 103	102 x 10 ⁶	1,03E+08
	10 ⁻⁵ = 91	91 x 50 x 10 ⁵	4,55E+08	10 ⁻⁵ = 192	192 x 50 x 10 ⁵	9,60E+08	10 ⁻⁵ = 44	44 x 50 x 10 ⁵	2,20E+08	10 ⁻⁵ = 171	171 x 10 ⁶	1,71E+08	10 ⁻⁵ = 95	95 x 10 ⁶	9,50E+07
	10 ⁻⁵ = 70	70 x 50 x 10 ⁵	3,50E+08	10 ⁻⁵ = 207	207 x 50 x 10 ⁵	1,04E+09	10 ⁻⁵ = 92	92 x 50 x 10 ⁵	4,60E+08	10 ⁻⁵ = 169	169 x 10 ⁶	1,69E+08	10 ⁻⁵ = 89	89 x 10 ⁶	8,90E+07
			3,67E+08			9,28E+08			2,97E+08		1,74E+08			9,57E+07	
Transformation frequency	T titer		1,88E+04	T titer		3,78E+04	T titer		1,60E+04	T titer		3,97E+03	T titer		4,87E+03
	R titer		3,67E+08	R titer		9,28E+08	R titer		2,97E+08	R titer		1,74E+08	R titer		9,57E+07
			5,14E-05			4,08E-05			5,39E-05			2,28E-05			5,09E-05
Transformants (10 MP)	10 ⁻¹ = 30	30 x 50 x 10 ¹	1,50E+04	10 ⁻¹ = 30	30 x 50 x 10 ¹	1,50E+04	10 ⁻¹ = 30	30 x 50 x 10 ¹	1,50E+04	10 ⁻¹ = 41	41 x 10 ²	4,10E+03	10 ⁻¹ = 34	34 x 10 ²	3,40E+03
	10 ⁻¹ = 59	59 x 50 x 10 ¹	2,95E+04	10 ⁻¹ = 42	42 x 50 x 10 ¹	2,10E+04	10 ⁻¹ = 42	42 x 50 x 10 ¹	2,10E+04	10 ⁻¹ = 53	53 x 10 ²	5,30E+03	10 ⁻¹ = 35	35 x 10 ²	3,50E+03
	10 ⁻¹ = 39	39 x 50 x 10 ¹	1,95E+04	10 ⁻¹ = 26	26 x 50 x 10 ¹		10 ⁻¹ = 26	26 x 50 x 10 ¹		10 ⁻¹ = 55	55 x 10 ²	5,50E+03	10 ⁻¹ = 41	41 x 10 ²	4,10E+03
			2,13E+04			1,80E+04			1,80E+04		4,97E+03			3,67E+03	
Recipients (10 MP)	10 ⁻⁵ = 95	95 x 50 x 10 ⁵	4,75E+08	10 ⁻⁵ = 45	45 x 50 x 10 ⁵	2,25E+08	10 ⁻⁵ = 45	45 x 50 x 10 ⁵	2,25E+08	10 ⁻⁵ = 142	142 x 10 ⁶	1,42E+08	10 ⁻⁵ = 126	126 x 10 ⁶	1,26E+08
	10 ⁻⁵ = 156	156 x 50 x 10 ⁵	7,80E+08	10 ⁻⁵ = 114	114 x 50 x 10 ⁵	5,70E+08	10 ⁻⁵ = 114	114 x 50 x 10 ⁵	5,70E+08	10 ⁻⁵ = 120	120 x 10 ⁶	1,20E+08	10 ⁻⁵ = 118	118 x 10 ⁶	1,18E+08
	10 ⁻⁵ = 179	179 x 50 x 10 ⁵	8,95E+08	10 ⁻⁵ = 69	69 x 50 x 10 ⁵	3,45E+08	10 ⁻⁵ = 69	69 x 50 x 10 ⁵	3,45E+08	10 ⁻⁵ = 127	127 x 10 ⁶	1,27E+08	10 ⁻⁵ = 131	131 x 10 ⁶	1,31E+08
			7,17E+08			3,80E+08			3,80E+08		1,30E+08			1,25E+08	
Transformation frequency	T titer		2,13E+04	T titer		1,80E+04	T titer		1,80E+04	T titer		4,97E+03	T titer		3,67E+03
	R titer		7,17E+08	R titer		3,80E+08	R titer		3,80E+08	R titer		1,30E+08	R titer		1,25E+08
			2,98E-05			4,74E-05			4,74E-05			3,83E-05			2,93E-05
Transformants (50 MP)	10 ⁻¹ = 21	21 x 50 x 10 ¹		10 ⁻¹ = 19	19 x 50 x 10 ¹		10 ⁻¹ = 57	57 x 50 x 10 ¹	2,85E+04	10 ⁻¹ = 34	34 x 10 ²	3,40E+03	10 ⁻¹ = 45	45 x 10 ²	4,50E+03
	10 ⁻¹ = 44	44 x 50 x 10 ¹	2,20E+04	10 ⁻¹ = 54	54 x 50 x 10 ¹	2,70E+04	10 ⁻¹ = 42	42 x 50 x 10 ¹	2,10E+04	10 ⁻¹ = 29	29 x 10 ²		10 ⁻¹ = 29	29 x 10 ²	
	10 ⁻¹ = 51	51 x 50 x 10 ¹	2,55E+04	10 ⁻¹ = 76	76 x 50 x 10 ¹	3,80E+04	10 ⁻¹ = 50	50 x 50 x 10 ¹	2,50E+04	10 ⁻¹ = 41	41 x 10 ²	4,10E+03	10 ⁻¹ = 39	39 x 10 ²	3,90E+03
			2,38E+04			3,25E+04			2,48E+04		3,75E+03			4,20E+03	
Recipients (50 MP)	10 ⁻⁵ = 55	55 x 50 x 10 ⁵	2,75E+08	10 ⁻⁵ = 130	130 x 50 x 10 ⁵	6,50E+08	10 ⁻⁵ = 59	59 x 50 x 10 ⁵	2,95E+08	10 ⁻⁵ = 121	121 x 10 ⁶	1,21E+08	10 ⁻⁵ = 125	125 x 10 ⁶	1,25E+08
	10 ⁻⁵ = 79	79 x 50 x 10 ⁵	3,95E+08	10 ⁻⁵ = 164	164 x 50 x 10 ⁵	8,20E+08	10 ⁻⁵ = 77	77 x 50 x 10 ⁵	3,85E+08	10 ⁻⁵ = 98	98 x 10 ⁶	9,80E+07	10 ⁻⁵ = 103	103 x 10 ⁶	1,03E+08
	10 ⁻⁵ = 72	72 x 50 x 10 ⁵	3,60E+08	10 ⁻⁵ = 173	173 x 50 x 10 ⁵	8,65E+08	10 ⁻⁵ = 172	172 x 50 x 10 ⁵	8,60E+08	10 ⁻⁵ = 91	91 x 10 ⁶	9,10E+07	10 ⁻⁵ = 99	99 x 10 ⁶	9,90E+07
			3,43E+08			7,78E+08			5,13E+08		1,03E+08			1,09E+08	
Transformation frequency	T titer		2,38E+04	T titer		3,25E+04	T titer		2,48E+04	T titer		3,75E+03	T titer		4,20E+03
	R titer		3,43E+08	R titer		7,78E+08	R titer		5,13E+08	R titer		1,03E+08	R titer		1,09E+08
			6,92E-05			4,18E-05			4,84E-05			3,63E-05			3,85E-05
Transformants (200 MP)	10 ⁻¹ = 53	53 x 50 x 10 ¹	2,65E+04	10 ⁻¹ = 49	49 x 50 x 10 ¹	2,45E+04	10 ⁻¹ = 6	6 x 50 x 10 ¹		10 ⁻¹ = 46	46 x 10 ²	4,60E+03	10 ⁻¹ = 43	43 x 10 ²	4,30E+03
	10 ⁻¹ = 63	63 x 50 x 10 ¹	3,15E+04	10 ⁻¹ = 133	133 x 50 x 10 ¹	6,65E+04	10 ⁻¹ = 34	34 x 50 x 10 ¹	1,70E+04	10 ⁻¹ = 34	34 x 10 ²	3,40E+03	10 ⁻¹ = 35	35 x 10 ²	3,50E+03
	10 ⁻¹ = 54	54 x 50 x 10 ¹	2,70E+04	10 ⁻¹ = 67	67 x 50 x 10 ¹	3,35E+04	10 ⁻¹ = 5	5 x 50 x 10 ¹		10 ⁻¹ = 33	33 x 10 ²	3,30E+03	10 ⁻¹ = 59	59 x 10 ²	5,90E+03
			2,83E+04			4,15E+04			1,70E+04		3,77E+03			4,57E+03	
Recipients (200 MP)	10 ⁻⁵ = 48	48 x 50 x 10 ⁵	2,40E+08	10 ⁻⁵ = 279	279 x 50 x 10 ⁵	1,40E+09	10 ⁻⁵ = 26	26 x 50 x 10 ⁵		10 ⁻⁵ = 93	93 x 10 ⁶	9,30E+07	10 ⁻⁵ = 91	91 x 10 ⁶	9,10E+07
	10 ⁻⁵ = 67	67 x 50 x 10 ⁵	3,35E+08	10 ⁻⁵ = 221	221 x 50 x 10 ⁵	1,11E+09	10 ⁻⁵ = 22	22 x 50 x 10 ⁵		10 ⁻⁵ = 72	72 x 10 ⁶	7,20E+07	10 ⁻⁵ = 93	93 x 10 ⁶	9,30E+07
	10 ⁻⁵ = 77	77 x 50 x 10 ⁵	3,85E+08	10 ⁻⁵ = 253	253 x 50 x 10 ⁵	1,27E+09	10 ⁻⁵ = 61	61 x 50 x 10 ⁵	3,05E+08	10 ⁻⁵ = 70	70 x 10 ⁶	7,00E+07	10 ⁻⁵ = 60	60 x 10 ⁶	6,00E+07
			3,20E+08			1,26E+09			3,05E+08		7,83E+07			8,13E+07	
Transformation frequency	T titer		2,83E+04	T titer		4,15E+04	T titer		1,70E+04	T titer		3,77E+03	T titer		4,57E+03
	R titer		3,20E+08	R titer		1,26E+09	R titer		3,05E+08	R titer		7,83E+07	R titer		8,13E+07
			8,85E-05			3,31E-05			5,57E-05			4,81E-05			5,61E-05

Figure A 3: Raw data for the natural transformation of *A. baylyi* on the microplastic polymer HDPE. The green colour indicates the use of 20 μ L of sample, and the red colour indicates the use of 100 μ L of sample. Transformant and recipient titers containing less than 30 and more than 300 colonies were removed from the raw data.

Transformants (0 MP)	10 ⁻¹ = 48	48 x 50 x 10 ¹	2,40E+04	10 ⁻¹ = 36	36 x 10 ²	3,60E+03	10 ⁻¹ = 54	54 x 10 ²	5,40E+03
	10 ⁻¹ = 11	11 x 50 x 10 ¹		10 ⁻¹ = 42	42 x 10 ²	4,20E+03	10 ⁻¹ = 43	43 x 10 ²	4,30E+03
	10 ⁻¹ = 63	63 x 50 x 10 ¹	3,15E+04	10 ⁻¹ = 41	41 x 10 ²	4,10E+03	10 ⁻¹ = 49	49 x 10 ²	4,90E+03
			2,78E+04			3,97E+03			4,87E+03
Recipients (0 MP)	10 ⁻⁵ = 39	39 x 50 x 10 ⁵	1,95E+08	10 ⁻⁵ = 182	182 x 10 ⁶	1,82E+08	10 ⁻⁵ = 103	102 x 10 ⁶	1,03E+08
	10 ⁻⁵ = 50	50 x 50 x 10 ⁵	2,50E+08	10 ⁻⁵ = 171	171 x 10 ⁶	1,71E+08	10 ⁻⁵ = 95	95 x 10 ⁶	9,50E+07
	10 ⁻⁵ = 29	29 x 50 x 10 ⁵		10 ⁻⁵ = 169	169 x 10 ⁶	1,69E+08	10 ⁻⁵ = 89	89 x 10 ⁶	8,90E+07
			2,23E+08			1,74E+08			9,57E+07
Transformation frequency	T titer		2,78E+04	T titer		3,97E+03	T titer		4,87E+03
	R titer		2,23E+08	R titer		1,74E+08	R titer		9,57E+07
			1,25E-04			2,28E-05			5,09E-05
Transformants (10 MP)	10 ⁻¹ = 16	16 x 50 x 10 ¹		10 ⁻¹ = 39	39 x 10 ²	3,90E+03	10 ⁻¹ = 41	41 x 10 ²	4,10E+03
	10 ⁻¹ = 59	59 x 50 x 10 ¹	2,95E+04	10 ⁻¹ = 46	46 x 10 ²	4,60E+03	10 ⁻¹ = 37	37 x 10 ²	3,70E+03
	10 ⁻¹ = 48	48 x 50 x 10 ¹	2,40E+04	10 ⁻¹ = 46	46 x 10 ²	4,60E+03	10 ⁻¹ = 33	33 x 10 ²	3,30E+03
			2,68E+04			4,37E+03			3,70E+03
Recipients (10 MP)	10 ⁻⁵ = 84	84 x 50 x 10 ⁵	4,20E+08	10 ⁻⁵ = 88	88 x 10 ⁶	8,80E+07	10 ⁻⁵ = 51	51 x 10 ⁶	5,10E+07
	10 ⁻⁵ = 70	70 x 50 x 10 ⁵	3,50E+08	10 ⁻⁵ = 71	71 x 10 ⁶	7,10E+07	10 ⁻⁵ = 43	43 x 10 ⁶	4,30E+07
	10 ⁻⁵ = 56	56 x 50 x 10 ⁵	2,80E+08	10 ⁻⁵ = 78	78 x 10 ⁶	7,80E+07	10 ⁻⁵ = 47	47 x 10 ⁶	4,70E+07
			3,50E+08			7,90E+07			4,70E+07
Transformation frequency	T titer		2,68E+04	T titer		4,37E+03	T titer		3,70E+03
	R titer		3,50E+08	R titer		7,90E+07	R titer		4,70E+07
			7,64E-05			5,53E-05			7,87E-05
Transformants (50 MP)	10 ⁻¹ = 43	43 x 50 x 10 ¹	2,15E+04	10 ⁻¹ = 55	55 x 10 ²	5,50E+03	10 ⁻¹ = 38	38 x 10 ²	3,80E+03
	10 ⁻¹ = 41	41 x 50 x 10 ¹	2,05E+04	10 ⁻¹ = 51	51 x 10 ²	5,10E+03	10 ⁻¹ = 47	47 x 10 ²	4,70E+03
	10 ⁻¹ = 49	49 x 50 x 10 ¹	2,45E+04	10 ⁻¹ = 43	43 x 10 ²	4,30E+03	10 ⁻¹ = 41	41 x 10 ²	4,10E+03
			2,22E+04			4,97E+03			4,20E+03
Recipients (50 MP)	10 ⁻⁵ = 48	48 x 50 x 10 ⁵	2,40E+08	10 ⁻⁵ = 99	99 x 10 ⁶	9,90E+07	10 ⁻⁵ = 78	78 x 10 ⁶	7,80E+07
	10 ⁻⁵ = 42	42 x 50 x 10 ⁵	2,10E+08	10 ⁻⁵ = 83	83 x 10 ⁶	8,30E+07	10 ⁻⁵ = 101	101 x 10 ⁶	1,01E+08
	10 ⁻⁵ = 35	35 x 50 x 10 ⁵	1,75E+08	10 ⁻⁵ = 83	83 x 10 ⁶	8,30E+07	10 ⁻⁵ = 85	85 x 10 ⁶	8,50E+07
			2,08E+08			8,83E+07			8,80E+07
Transformation frequency	T titer		2,22E+04	T titer		4,97E+03	T titer		4,20E+03
	R titer		2,08E+08	R titer		8,83E+07	R titer		8,80E+07
			1,06E-04			5,62E-05			4,77E-05
Transformants (200 MP)	10 ⁻¹ = 53	53 x 50 x 10 ¹	2,65E+04	10 ⁻¹ = 55	55 x 10 ²	5,50E+03	10 ⁻¹ = 47	47 x 10 ²	4,70E+03
	10 ⁻¹ = 59	59 x 50 x 10 ¹	2,95E+04	10 ⁻¹ = 90	90 x 10 ²	9,00E+03	10 ⁻¹ = 58	58 x 10 ²	5,80E+03
	10 ⁻¹ = 94	94 x 50 x 10 ¹	4,70E+04	10 ⁻¹ = 78	78 x 10 ²	7,80E+03	10 ⁻¹ = 47	47 x 10 ²	4,70E+03
			3,43E+04			7,43E+03			5,07E+03
Recipients (200 MP)	10 ⁻⁵ = 34	34 x 50 x 10 ⁵	1,70E+08	10 ⁻⁵ = 112	112 x 10 ⁶	1,12E+08	10 ⁻⁵ = 103	103 x 10 ⁶	1,03E+08
	10 ⁻⁵ = 78	78 x 50 x 10 ⁵	3,90E+08	10 ⁻⁵ = 95	95 x 10 ⁶	9,50E+07	10 ⁻⁵ = 126	126 x 10 ⁶	1,26E+08
	10 ⁻⁵ = 87	87 x 50 x 10 ⁵	4,35E+08	10 ⁻⁵ = 127	127 x 10 ⁶	1,27E+08	10 ⁻⁵ = 118	118 x 10 ⁶	1,18E+08
			3,32E+08			1,11E+08			1,16E+08
Transformation frequency	T titer		3,43E+04	T titer		7,43E+03	T titer		5,07E+03
	R titer		3,32E+08	R titer		1,11E+08	R titer		1,16E+08
			1,04E-04			6,68E-05			4,38E-05

Figure A 4: Raw data for the natural transformation of *A. baylii* on the microplastic polymer HDPS. The green colour indicates the use of 20 μ L of sample, and the red colour indicates the use of 100 μ L of sample. Transformant and recipient titers containing less than 30 and more than 300 colonies were removed from the raw data.

Transformants (0 MP)	10 ⁻¹ = 85	85 x 50 x 10 ¹	4,25E+04	10 ⁻¹ = 52	52 x 50 x 10 ¹	2,60E+04	10 ⁻¹ = 36	36 x 10 ²	3,60E+03	10 ⁻¹ = 54	54 x 10 ²	5,40E+03				
	10 ⁻¹ = 81	81 x 50 x 10 ¹	4,05E+04	10 ⁻¹ = 91	91 x 50 x 10 ¹	4,55E+04	10 ⁻¹ = 42	42 x 10 ²	4,20E+03	10 ⁻¹ = 43	43 x 10 ²	4,30E+03				
	10 ⁻¹ = 91	91 x 50 x 10 ¹	4,55E+04	10 ⁻¹ = 114	114 x 50 x 10 ¹	5,70E+04	10 ⁻¹ = 41	41 x 10 ²	4,10E+03	10 ⁻¹ = 49	49 x 10 ²	4,90E+03				
			4,28E+04			4,28E+04			3,97E+03			4,87E+03				
Recipients (0 MP)	10 ⁻⁵ = 117	117 x 50 x 10 ⁵	5,85E+08	10 ⁻⁵ = 32	32 x 50 x 10 ⁵	1,60E+08	10 ⁻⁵ = 182	182 x 10 ⁶	1,82E+08	10 ⁻⁵ = 103	103 x 10 ⁶	1,03E+08				
	10 ⁻⁵ = 121	121 x 50 x 10 ⁵	6,05E+08	10 ⁻⁵ = 51	51 x 50 x 10 ⁵	2,55E+08	10 ⁻⁵ = 171	171 x 10 ⁶	1,71E+08	10 ⁻⁵ = 95	95 x 10 ⁶	9,50E+07				
	10 ⁻⁵ = 130	130 x 50 x 10 ⁵	6,50E+08	10 ⁻⁵ = 61	61 x 50 x 10 ⁵	3,05E+08	10 ⁻⁵ = 169	169 x 10 ⁶	1,69E+08	10 ⁻⁵ = 89	89 x 10 ⁶	8,90E+07				
			6,13E+08			2,40E+08			1,74E+08			9,57E+07				
Transformation frequency	T titer		4,28E+04	T titer		4,28E+04	T titer		3,97E+03	T titer		4,87E+03				
	R titer		6,13E+08	R titer		2,40E+08	R titer		1,74E+08	R titer		9,57E+07				
			6,98E-05			1,78E-04			2,28E-05			5,09E-05				
Transformants (10 MP)	10 ⁻¹ = 88	88 x 50 x 10 ¹	4,40E+04	10 ⁻¹ = 136	136 x 50 x 10 ¹	6,80E+04	10 ⁻¹ = 59	59 x 10 ²	5,90E+03	10 ⁻¹ = 55	55 x 10 ²	5,50E+03				
	10 ⁻¹ = 96	96 x 50 x 10 ¹	4,80E+04	10 ⁻¹ = 163	163 x 50 x 10 ¹	8,15E+04	10 ⁻¹ = 63	63 x 10 ²	6,30E+03	10 ⁻¹ = 46	46 x 10 ²	4,60E+03				
	10 ⁻¹ = 63	63 x 50 x 10 ¹	3,15E+04	10 ⁻¹ = 184	184 x 50 x 10 ¹	9,20E+04	10 ⁻¹ = 52	52 x 10 ²	5,20E+03	10 ⁻¹ = 49	49 x 10 ²	4,90E+03				
			4,12E+04			8,05E+04			5,80E+03			5,00E+03				
Recipients (10 MP)	10 ⁻⁵ = 79	79 x 50 x 10 ⁵	3,95E+08	10 ⁻⁵ = 52	52 x 50 x 10 ⁵	2,60E+08	10 ⁻⁵ = 67	67 x 10 ⁶	6,70E+07	10 ⁻⁵ = 33	33 x 10 ⁶	3,30E+07				
	10 ⁻⁵ = 82	82 x 50 x 10 ⁵	4,10E+08	10 ⁻⁵ = 62	62 x 50 x 10 ⁵	3,10E+08	10 ⁻⁵ = 53	53 x 10 ⁶	5,30E+07	10 ⁻⁵ = 36	36 x 10 ⁶	3,60E+07				
	10 ⁻⁵ = 76	76 x 50 x 10 ⁵	3,80E+08	10 ⁻⁵ = 39	39 x 50 x 10 ⁵	1,95E+08	10 ⁻⁵ = 51	51 x 10 ⁶	5,10E+07	10 ⁻⁵ = 50	50 x 10 ⁶	5,00E+07				
			3,95E+08			2,55E+08			5,70E+07			3,97E+07				
Transformation frequency	T titer		4,12E+04	T titer		8,05E+04	T titer		5,80E+03	T titer		5,00E+03				
	R titer		3,95E+08	R titer		2,55E+08	R titer		5,70E+07	R titer		3,97E+07				
			1,04E-04			3,16E-04			1,02E-04			1,26E-04				
Transformants (50 MP)	10 ⁻¹ = 69	69 x 50 x 10 ¹	3,45E+04	10 ⁻¹ = 84	84 x 50 x 10 ¹	4,20E+04	10 ⁻¹ = 297	297 x 10 ²	2,97E+04	10 ⁻¹ = 23	23 x 10 ²	2,30E+03	10 ⁻¹ = 40	40 x 10 ²	4,00E+03	
	10 ⁻¹ = 95	95 x 50 x 10 ¹	4,75E+04	10 ⁻¹ = 118	118 x 50 x 10 ¹	5,90E+04	10 ⁻¹ = 229	229 x 10 ²	2,29E+04	10 ⁻¹ = 36	36 x 10 ²	3,60E+03	10 ⁻¹ = 48	48 x 10 ²	4,80E+03	
	10 ⁻¹ = 67	67 x 50 x 10 ¹	3,35E+04	10 ⁻¹ = 157	157 x 50 x 10 ¹	7,85E+04	10 ⁻¹ = 233	233 x 10 ²	2,29E+04	10 ⁻¹ = 41	41 x 10 ²	4,10E+03	10 ⁻¹ = 50	50 x 10 ²	5,00E+03	
			3,85E+04			5,98E+04			2,52E+04			3,33E+03			4,60E+03	
Recipients (50 MP)	10 ⁻⁵ = 100	100 x 50 x 10 ⁵	5,00E+08	10 ⁻⁵ = 51	51 x 50 x 10 ⁵	2,55E+08	10 ⁻⁵ = 256	256 x 10 ⁶	2,56E+08	10 ⁻⁵ = 55	55 x 10 ⁶	5,50E+07	10 ⁻⁵ = 49	49 x 10 ⁶	4,90E+07	
	10 ⁻⁵ = 94	94 x 50 x 10 ⁵	4,70E+08	10 ⁻⁵ = 51	51 x 50 x 10 ⁵	2,55E+08	10 ⁻⁵ = 320	320 x 10 ⁶		10 ⁻⁵ = 51	51 x 10 ⁶	5,10E+07	10 ⁻⁵ = 55	55 x 10 ⁶	5,50E+07	
	10 ⁻⁵ = 101	101 x 50 x 10 ⁵	5,05E+08	10 ⁻⁵ = 57	57 x 50 x 10 ⁵	2,85E+08	10 ⁻⁵ = 216	216 x 10 ⁶	2,16E+08	10 ⁻⁵ = 48	48 x 10 ⁶	4,80E+07	10 ⁻⁵ = 51	51 x 10 ⁶	5,10E+07	
			4,92E+08			2,65E+08			2,36E+08			5,13E+07			5,17E+07	
Transformation frequency	T titer		3,85E+04	T titer		5,98E+04	T titer		2,52E+04	T titer		3,33E+03	T titer		4,60E+03	
	R titer		4,92E+08	R titer		2,65E+08	R titer		2,36E+08	R titer		5,13E+07	R titer		5,17E+07	
			7,83E-05			2,26E-04			1,07E-04			6,49E-05			8,90E-05	
Transformants (200 MP)	10 ⁻¹ = 42	42 x 50 x 10 ¹	2,10E+04	10 ⁻¹ = 57	57 x 10 ²	5,70E+03	10 ⁻¹ = 35	35 x 10 ²	3,50E+03	10 ⁻¹ = 35	35 x 10 ²	3,50E+03				
	10 ⁻¹ = 43	43 x 50 x 10 ¹	2,15E+04	10 ⁻¹ = 110	110 x 10 ²	1,10E+04	10 ⁻¹ = 21	21 x 10 ²	2,29E+03	10 ⁻¹ = 42	42 x 10 ²	4,20E+03				
	10 ⁻¹ = 52	52 x 50 x 10 ¹	2,60E+04	10 ⁻¹ = 76	76 x 10 ²	7,60E+03	10 ⁻¹ = 43	43 x 10 ²	4,30E+03	10 ⁻¹ = 27	27 x 10 ²					
			2,28E+04			8,10E+03			3,90E+03			3,85E+03				
Recipients (200 MP)	10 ⁻⁵ = 56	56 x 50 x 10 ⁵	2,80E+08	10 ⁻⁵ = 159	159 x 10 ⁶	1,59E+08	10 ⁻⁵ = 50	50 x 10 ⁶	5,00E+07	10 ⁻⁵ = 53	53 x 10 ⁶	5,30E+07				
	10 ⁻⁵ = 57	57 x 50 x 10 ⁵	2,85E+08	10 ⁻⁵ = 145	145 x 10 ⁶	1,45E+08	10 ⁻⁵ = 41	41 x 10 ⁶	4,10E+07	10 ⁻⁵ = 42	42 x 10 ⁶	4,20E+07				
	10 ⁻⁵ = 69	69 x 50 x 10 ⁵	3,45E+08	10 ⁻⁵ = 182	182 x 10 ⁶	1,82E+08	10 ⁻⁵ = 48	48 x 10 ⁶	4,80E+07	10 ⁻⁵ = 39	39 x 10 ⁶	3,90E+07				
			3,03E+08			1,64E+08			4,63E+07			4,47E+07				
Transformation frequency	T titer		2,28E+04	T titer		8,10E+03	T titer		3,90E+03	T titer		3,85E+03				
	R titer		3,03E+08	R titer		1,64E+08	R titer		4,63E+07	R titer		4,47E+07				
			7,53E-05			4,95E-05			8,42E-05			8,62E-05				

Figure A 5: Raw data for the natural transformation of *A. baylyi* on the microplastic polymer PP. The green colour indicates the use of 20 μ L of sample, and the red colour indicates the use of 100 μ L of sample. Transformant and recipient titers containing less than 30 and more than 300 colonies were removed from the raw data.

Transformants (0 MP)	10 ⁻¹ = 63	63 x 50 x 10 ¹	3,15E+04	10 ⁻¹ = 69	69 x 50 x 10 ¹	3,45E+04	10 ⁻¹ = 36	36 x 10 ²	3,60E+03	10 ⁻¹ = 54	54 x 10 ²	5,40E+03			
	10 ⁻¹ = 54	54 x 50 x 10 ¹	2,70E+04	10 ⁻¹ = 73	73 x 50 x 10 ¹	3,65E+04	10 ⁻¹ = 42	42 x 10 ²	4,20E+03	10 ⁻¹ = 43	43 x 10 ²	4,30E+03			
	10 ⁻¹ = 48	48 x 50 x 10 ¹	2,40E+04	10 ⁻¹ = 70	70 x 50 x 10 ¹	3,50E+04	10 ⁻¹ = 41	41 x 10 ²	4,10E+03	10 ⁻¹ = 49	49 x 10 ²	4,90E+03			
			2,75E+04			3,53E+04			3,97E+03			4,87E+03			
Recipients (0 MP)	10 ⁻⁵ = 64	64 x 50 x 10 ⁵	3,20E+08	10 ⁻⁵ = 57	57 x 50 x 10 ⁵	2,85E+08	10 ⁻⁵ = 182	182 x 10 ⁶	1,82E+08	10 ⁻⁵ = 103	102 x 10 ⁶	1,03E+08			
	10 ⁻⁵ = 53	53 x 50 x 10 ⁵	2,65E+08	10 ⁻⁵ = 38	38 x 50 x 10 ⁵	1,90E+08	10 ⁻⁵ = 171	171 x 10 ⁶	1,71E+08	10 ⁻⁵ = 95	95 x 10 ⁶	9,50E+07			
	10 ⁻⁵ = 55	55 x 50 x 10 ⁵	2,75E+08	10 ⁻⁵ = 52	52 x 50 x 10 ⁵	2,60E+08	10 ⁻⁵ = 169	169 x 10 ⁶	1,69E+08	10 ⁻⁵ = 89	89 x 10 ⁶	8,90E+07			
			2,87E+08			2,45E+08			1,74E+08			9,57E+07			
Transformation frequency	T titer		2,75E+04	T titer		3,53E+04	T titer		3,97E+03	T titer		4,87E+03			
	R titer		2,87E+08	R titer		2,45E+08	R titer		1,74E+08	R titer		9,57E+07			
			9,59E-05			1,44E-04			2,28E-05			5,09E-05			
Transformants (10 MP)	10 ⁻¹ = 142	142 x 50 x 10 ¹	7,10E+04	10 ⁻¹ = 72	72 x 50 x 10 ¹	3,60E+04	10 ⁻¹ = 44	44 x 50 x 10 ¹	2,20E+04	10 ⁻¹ = 115	115 x 10 ²	1,15E+04	10 ⁻¹ = 23	23 x 10 ²	
	10 ⁻¹ = 64	64 x 50 x 10 ¹	3,20E+04	10 ⁻¹ = 70	70 x 50 x 10 ¹	3,50E+04	10 ⁻¹ = 16	16 x 50 x 10 ¹	2,45E+04	10 ⁻¹ = 140	140 x 10 ²	1,40E+04	10 ⁻¹ = 39	39 x 10 ²	3,90E+03
	10 ⁻¹ = 92	92 x 50 x 10 ¹	4,60E+04	10 ⁻¹ = 120	120 x 50 x 10 ¹	6,00E+04	10 ⁻¹ = 49	49 x 50 x 10 ¹	2,33E+04	10 ⁻¹ = 154	154 x 10 ²	1,54E+04	10 ⁻¹ = 42	42 x 10 ²	4,20E+03
			4,97E+04			4,37E+04			2,33E+04			1,36E+04			4,05E+03
Recipients (10 MP)	10 ⁻⁵ = 66	66 x 50 x 10 ⁵	3,30E+08	10 ⁻⁵ = 79	79 x 50 x 10 ⁵	3,95E+08	10 ⁻⁵ = 41	41 x 50 x 10 ⁵	2,05E+08	10 ⁻⁵ = 298	298 x 10 ⁶	2,98E+08	10 ⁻⁵ = 115	115 x 10 ⁶	1,15E+08
	10 ⁻⁵ = 80	80 x 50 x 10 ⁵	4,00E+08	10 ⁻⁵ = 60	60 x 50 x 10 ⁵	3,00E+08	10 ⁻⁵ = 48	48 x 50 x 10 ⁵	2,40E+08	10 ⁻⁵ = 325	325 x 10 ⁶	2,77E+08	10 ⁻⁵ = 93	93 x 10 ⁶	9,30E+07
	10 ⁻⁵ = 82	82 x 50 x 10 ⁵	4,10E+08	10 ⁻⁵ = 62	62 x 50 x 10 ⁵	3,10E+08	10 ⁻⁵ = 51	51 x 50 x 10 ⁵	2,55E+08	10 ⁻⁵ = 277	277 x 10 ⁶	2,77E+08	10 ⁻⁵ = 91	91 x 10 ⁶	9,10E+07
			3,80E+08			3,35E+08			2,33E+08			2,88E+08			9,97E+07
Transformation frequency	T titer		4,97E+04	T titer		4,37E+04	T titer		2,33E+04	T titer		1,36E+04	T titer		4,05E+03
	R titer		3,80E+08	R titer		3,35E+08	R titer		2,33E+08	R titer		2,88E+08	R titer		9,97E+07
			1,31E-04			1,30E-04			9,96E-05			4,74E-05			4,06E-05
Transformants (50 MP)	10 ⁻¹ = 90	90 x 50 x 10 ¹	4,50E+04	10 ⁻¹ = 68	68 x 50 x 10 ¹	3,40E+04	10 ⁻¹ = 35	35 x 50 x 10 ¹	1,75E+04	10 ⁻¹ = 212	212 x 10 ²	2,12E+04	10 ⁻¹ = 40	40 x 10 ²	4,00E+03
	10 ⁻¹ = 99	99 x 50 x 10 ¹	4,95E+04	10 ⁻¹ = 105	105 x 50 x 10 ¹	5,25E+04	10 ⁻¹ = 44	44 x 50 x 10 ¹	2,20E+04	10 ⁻¹ = 186	186 x 10 ²	1,86E+04	10 ⁻¹ = 36	36 x 10 ²	3,60E+03
	10 ⁻¹ = 73	73 x 50 x 10 ¹	3,65E+04	10 ⁻¹ = 107	107 x 50 x 10 ¹	5,35E+04	10 ⁻¹ = 49	49 x 50 x 10 ¹	2,45E+04	10 ⁻¹ = 272	272 x 10 ²	2,72E+04	10 ⁻¹ = 53	53 x 10 ²	5,30E+03
			4,37E+04			4,67E+04			2,13E+04			2,23E+04			4,30E+03
Recipients (50 MP)	10 ⁻⁵ = 96	96 x 50 x 10 ⁵	4,80E+08	10 ⁻⁵ = 66	66 x 50 x 10 ⁵	3,30E+08	10 ⁻⁵ = 53	53 x 50 x 10 ⁵	2,65E+08	10 ⁻⁵ = 287	287 x 10 ⁶	2,87E+08	10 ⁻⁵ = 96	96 x 10 ⁶	9,60E+07
	10 ⁻⁵ = 77	77 x 50 x 10 ⁵	3,85E+08	10 ⁻⁵ = 74	74 x 50 x 10 ⁵	3,70E+08	10 ⁻⁵ = 66	66 x 50 x 10 ⁵	3,30E+08	10 ⁻⁵ = 262	262 x 10 ⁶	2,62E+08	10 ⁻⁵ = 89	89 x 10 ⁶	8,90E+07
	10 ⁻⁵ = 83	83 x 50 x 10 ⁵	4,15E+08	10 ⁻⁵ = 60	60 x 50 x 10 ⁵	3,00E+08	10 ⁻⁵ = 58	58 x 50 x 10 ⁵	2,90E+08	10 ⁻⁵ = 292	292 x 10 ⁶	2,92E+08	10 ⁻⁵ = 118	118 x 10 ⁶	1,18E+08
			4,27E+08			3,33E+08			2,95E+08			2,80E+08			1,01E+08
Transformation frequency	T titer		4,37E+04	T titer		4,67E+04	T titer		2,13E+04	T titer		2,23E+04	T titer		4,30E+03
	R titer		4,27E+08	R titer		3,33E+08	R titer		2,95E+08	R titer		2,80E+08	R titer		1,01E+08
			1,02E-04			1,40E-04			7,23E-05			7,97E-05			4,26E-05
Transformants (200 MP)	10 ⁻¹ = 31	31 x 50 x 10 ¹	1,55E+04	10 ⁻¹ = 88	88 x 50 x 10 ¹	4,40E+04	10 ⁻¹ = 52	52 x 50 x 10 ¹	2,60E+04	10 ⁻¹ = 276	276 x 10 ²	2,76E+04	10 ⁻¹ = 172	172 x 10 ²	1,72E+04
	10 ⁻¹ = 20	20 x 50 x 10 ¹	1,55E+04	10 ⁻¹ = 93	93 x 50 x 10 ¹	4,65E+04	10 ⁻¹ = 30	30 x 50 x 10 ¹	1,50E+04	10 ⁻¹ = 380	380 x 10 ²	3,80E+04	10 ⁻¹ = 158	158 x 10 ²	1,58E+04
	10 ⁻¹ = 34	34 x 50 x 10 ¹	1,70E+04	10 ⁻¹ = 72	72 x 50 x 10 ¹	3,60E+04	10 ⁻¹ = 39	39 x 50 x 10 ¹	1,95E+04	10 ⁻¹ = 412	412 x 10 ²	4,12E+04	10 ⁻¹ = 134	134 x 10 ²	1,34E+04
			1,63E+04			4,22E+04			2,02E+04			2,76E+04			1,55E+04
Recipients (200 MP)	10 ⁻⁵ = 53	53 x 50 x 10 ⁵	2,65E+08	10 ⁻⁵ = 37	37 x 50 x 10 ⁵	1,85E+08	10 ⁻⁵ = 20	20 x 50 x 10 ⁵	1,50E+08	10 ⁻⁵ = 260	260 x 10 ⁶	2,60E+08	10 ⁻⁵ = 229	229 x 10 ⁶	2,29E+08
	10 ⁻⁵ = 68	68 x 50 x 10 ⁵	3,40E+08	10 ⁻⁵ = 41	41 x 50 x 10 ⁵	2,05E+08	10 ⁻⁵ = 39	39 x 50 x 10 ⁵	1,95E+08	10 ⁻⁵ = 284	284 x 10 ⁶	2,84E+08	10 ⁻⁵ = 252	252 x 10 ⁶	2,52E+08
	10 ⁻⁵ = 59	59 x 50 x 10 ⁵	2,95E+08	10 ⁻⁵ = 62	62 x 50 x 10 ⁵	3,10E+08	10 ⁻⁵ = 44	44 x 50 x 10 ⁵	2,20E+08	10 ⁻⁵ = 372	372 x 10 ⁶	3,72E+08	10 ⁻⁵ = 292	292 x 10 ⁶	2,92E+08
			3,00E+08			2,33E+08			2,08E+08			2,72E+08			2,58E+08
Transformation frequency	T titer		1,63E+04	T titer		4,22E+04	T titer		2,02E+04	T titer		2,76E+04	T titer		1,55E+04
	R titer		3,00E+08	R titer		2,33E+08	R titer		2,08E+08	R titer		2,72E+08	R titer		2,58E+08
			5,42E-05			1,81E-04			9,72E-05			1,01E-04			6,00E-05
															4,53E-05

Figure A 6: Raw data for the natural transformation of *A. baylii* on the microplastic polymer PVC B. The green colour indicates the use of 20 μ L of sample, and the red colour indicates the use of 100 μ L of sample. Transformant and recipient titers containing less than 30 and more than 300 colonies were removed from the raw data.

Transformants (0 MP)	10 ⁻¹ = 99	99 x 50 x 10 ¹	4,95E+04	10 ⁻¹ = 10	10 x 50 x 10 ¹		10 ⁻¹ = 36	36 x 10 ²	3,60E+03	10 ⁻¹ = 54	54 x 10 ²	5,40E+03
	10 ⁻¹ = 81	81 x 50 x 10 ¹	4,05E+04	10 ⁻¹ = 13	13 x 50 x 10 ¹		10 ⁻¹ = 42	42 x 10 ²	4,20E+03	10 ⁻¹ = 43	43 x 10 ²	4,30E+03
	10 ⁻¹ = 82	82 x 50 x 10 ¹	4,10E+04	10 ⁻¹ = 33	33 x 50 x 10 ¹	1,65E+04	10 ⁻¹ = 41	41 x 10 ²	4,10E+03	10 ⁻¹ = 49	49 x 10 ²	4,90E+03
			4,37E+04			1,65E+04			3,97E+03			4,87E+03
Recipients (0 MP)	10 ⁻⁵ = 38	38 x 50 x 10 ⁵	1,90E+08	10 ⁻⁵ = 69	69 x 50 x 10 ⁵	3,45E+08	10 ⁻⁵ = 182	182 x 10 ⁶	1,82E+08	10 ⁻⁵ = 103	102 x 10 ⁶	1,03E+08
	10 ⁻⁵ = 82	82 x 50 x 10 ⁵	4,10E+08	10 ⁻⁵ = 114	114 x 50 x 10 ⁵	5,70E+08	10 ⁻⁵ = 171	171 x 10 ⁶	1,71E+08	10 ⁻⁵ = 95	95 x 10 ⁶	9,50E+07
	10 ⁻⁵ = 82	82 x 50 x 10 ⁵	4,10E+08	10 ⁻⁵ = 85	85 x 50 x 10 ⁵	4,25E+08	10 ⁻⁵ = 169	169 x 10 ⁶	1,69E+08	10 ⁻⁵ = 89	89 x 10 ⁶	8,90E+07
			3,37E+08			4,47E+08		1,74E+08				9,57E+07
Transformation frequency	T titer		4,37E+04	T titer		1,65E+04	T titer		3,97E+03	T titer		4,87E+03
	R titer		3,37E+08	R titer		4,47E+08	R titer		1,74E+08	R titer		9,57E+07
			1,30E-04			3,69E-05			2,28E-05			5,09E-05
Transformants (10 MP)	10 ⁻¹ = 49	49 x 50 x 10 ¹	2,45E+04	10 ⁻¹ = 87	87 x 50 x 10 ¹	4,35E+04	10 ⁻¹ = 93	93 x 10 ²	9,30E+03	10 ⁻¹ = 42	42 x 10 ²	4,20E+03
	10 ⁻¹ = 49	49 x 50 x 10 ¹	2,45E+04	10 ⁻¹ = 78	78 x 50 x 10 ¹	3,90E+04	10 ⁻¹ = 38	38 x 10 ²	3,80E+03	10 ⁻¹ = 28	28 x 10 ²	2,80E+03
	10 ⁻¹ = 63	63 x 50 x 10 ¹	3,15E+04	10 ⁻¹ = 90	90 x 50 x 10 ¹	4,50E+04	10 ⁻¹ = 41	41 x 10 ²	4,10E+03	10 ⁻¹ = 38	38 x 10 ²	3,80E+03
			2,68E+04			4,25E+04		5,73E+03				4,00E+03
Recipients (10 MP)	10 ⁻⁵ = 68	68 x 50 x 10 ⁵	3,40E+08	10 ⁻⁵ = 83	83 x 50 x 10 ⁵	4,15E+08	10 ⁻⁵ = 112	112 x 10 ⁶	1,12E+08	10 ⁻⁵ = 91	91 x 10 ⁶	9,10E+07
	10 ⁻⁵ = 80	80 x 50 x 10 ⁵	4,00E+08	10 ⁻⁵ = 80	80 x 50 x 10 ⁵	4,00E+08	10 ⁻⁵ = 136	136 x 10 ⁶	1,36E+08	10 ⁻⁵ = 111	111 x 10 ⁶	1,11E+08
	10 ⁻⁵ = 76	76 x 50 x 10 ⁵	3,80E+08	10 ⁻⁵ = 62	62 x 50 x 10 ⁵	3,10E+08	10 ⁻⁵ = 87	87 x 10 ⁶	8,70E+07	10 ⁻⁵ = 76	76 x 10 ⁶	7,60E+07
			3,73E+08			3,75E+08		1,12E+08				9,27E+07
Transformation frequency	T titer		2,68E+04	T titer		4,25E+04	T titer		5,73E+03	T titer		4,00E+03
	R titer		3,73E+08	R titer		3,75E+08	R titer		1,12E+08	R titer		9,27E+07
			7,19E-05			1,13E-04		5,13E-05				4,32E-05
Transformants (50 MP)	10 ⁻¹ = 25	25 x 50 x 10 ¹		10 ⁻¹ = 33	33 x 50 x 10 ¹	1,65E+04	10 ⁻¹ = 39	32 x 10 ²	3,90E+03	10 ⁻¹ = 39	39 x 10 ²	3,90E+03
	10 ⁻¹ = 39	39 x 50 x 10 ¹	1,95E+04	10 ⁻¹ = 18	18 x 50 x 10 ¹		10 ⁻¹ = 20	20 x 10 ²		10 ⁻¹ = 47	47 x 10 ²	4,70E+03
	10 ⁻¹ = 48	48 x 50 x 10 ¹	2,40E+04	10 ⁻¹ = 92	92 x 50 x 10 ¹	4,60E+04	10 ⁻¹ = 36	36 x 10 ²	3,60E+03	10 ⁻¹ = 50	50 x 10 ²	5,00E+03
			2,18E+04			3,13E+04		3,75E+03				4,53E+03
Recipients (50 MP)	10 ⁻⁵ = 64	64 x 50 x 10 ⁵	3,20E+08	10 ⁻⁵ = 23	23 x 50 x 10 ⁵		10 ⁻⁵ = 91	91 x 10 ⁶	9,10E+07	10 ⁻⁵ = 106	106 x 10 ⁶	1,06E+08
	10 ⁻⁵ = 104	104 x 50 x 10 ⁵	5,20E+08	10 ⁻⁵ = 24	24 x 50 x 10 ⁵		10 ⁻⁵ = 127	127 x 10 ⁶	1,27E+08	10 ⁻⁵ = 93	93 x 10 ⁶	9,30E+07
	10 ⁻⁵ = 83	83 x 50 x 10 ⁵	4,15E+08	10 ⁻⁵ = 62	62 x 50 x 10 ⁵	3,10E+08	10 ⁻⁵ = 80	80 x 10 ⁶	8,00E+07	10 ⁻⁵ = 113	113 x 10 ⁶	1,13E+08
			4,18E+08			3,10E+08		9,93E+07				1,04E+08
Transformation frequency	T titer		2,18E+04 (A)	T titer		3,13E+04	T titer		3,75E+03	T titer		4,53E+03
	R titer		4,18E+08 (B)	R titer		3,10E+08	R titer		9,93E+07	R titer		1,04E+08
			5,20E-05			1,01E-04		3,78E-05				4,36E-05
Transformants (200 MP)	10 ⁻¹ = 22	22 x 50 x 10 ¹		10 ⁻¹ = 47	47 x 10 ²	4,70E+03	10 ⁻¹ = 40	40 x 10 ²	4,00E+03			
	10 ⁻¹ = 47	47 x 50 x 10 ¹	2,35E+04	10 ⁻¹ = 45	45 x 10 ²	4,50E+03	10 ⁻¹ = 21	21 x 10 ²				
	10 ⁻¹ = 54	54 x 50 x 10 ¹	2,70E+04	10 ⁻¹ = 96	96 x 10 ²	9,60E+03	10 ⁻¹ = 44	44 x 10 ²	4,40E+03			
			2,53E+04			6,27E+03		4,20E+03				
Recipients (200 MP)	10 ⁻⁵ = 89	89 x 50 x 10 ⁵	4,45E+08	10 ⁻⁵ = 88	88 x 10 ⁶	8,80E+07	10 ⁻⁵ = 111	111 x 10 ⁶	1,11E+08			
	10 ⁻⁵ = 63	63 x 50 x 10 ⁵	3,15E+08	10 ⁻⁵ = 94	94 x 10 ⁶	9,40E+07	10 ⁻⁵ = 102	102 x 10 ⁶	1,02E+08			
	10 ⁻⁵ = 60	60 x 50 x 10 ⁵	3,00E+08	10 ⁻⁵ = 143	143 x 10 ⁶	1,43E+08	10 ⁻⁵ = 98	98 x 10 ⁶	9,80E+07			
			3,53E+08			1,08E+08		1,04E+08				
Transformation frequency	T titer		2,53E+04	T titer		6,27E+03	T titer		4,20E+03			
	R titer		3,53E+08	R titer		1,08E+08	R titer		1,04E+08			
			7,15E-05			5,78E-05		4,05E-05				

Figure A 7: Raw data for the natural transformation of *A. baylyi* on the microplastic polymer PVC A. The green colour indicates the use of 20 μ L of sample, and the red colour indicates the use of 100 μ L of sample. Transformant and recipient titers containing less than 30 and more than 300 colonies were removed from the raw data.

Transformants (PVC B)	10 ⁰ = 268	(268/2) x 10	1,34E+03	10 ⁰ = 65	(65/2) x 10	3,25E+02	10 ⁰ = 102	(102/2) x 10	5,10E+02	10 ⁰ = 20	(20/2) x 10	1,00E+02	10 ⁰ = 92	(92/2) x 10	4,60E+02
	10 ⁰ = 308	(308/2) x 10		10 ⁰ = 78	(78/2) x 10	3,90E+02	10 ⁰ = 177	(177/2) x 10	8,85E+02	10 ⁰ = 30	(30/2) x 10	1,50E+02	10 ⁰ = 25	(25/2) x 10	
	10 ⁰ = 220	(220/2) x 10	1,10E+03	10 ⁰ = 58	(58/2) x 10	2,90E+02	10 ⁰ = 280	(280/2) x 10	1,40E+03	10 ⁰ = 90	(90/2) x 10	4,50E+02	10 ⁰ = 125	(125/2) x 10	6,25E+02
			1,22E+03			3,35E+02			9,32E+02			3,00E+02			5,43E+02
Recipients (PVC B)	10 ⁻³ = 362	362 x 50 x 10 ³		10 ⁻³ = 62	62 x 50 x 10 ³	3,10E+06	10 ⁻³ = 97	97 x 50 x 10 ³	4,85E+06	10 ⁻³ = 16	16 x 50 x 10 ³		10 ⁻³ = 67	67 x 50 x 10 ³	3,35E+06
	10 ⁻³ = 271	271 x 50 x 10 ³	1,36E+07	10 ⁻³ = 79	79 x 50 x 10 ³	3,95E+06	10 ⁻³ = 118	118 x 50 x 10 ³	5,90E+06	10 ⁻³ = 63	63 x 50 x 10 ³	3,15E+06	10 ⁻³ = 59	59 x 50 x 10 ³	2,95E+06
	10 ⁻³ = 261	261 x 50 x 10 ³	1,31E+07	10 ⁻³ = 82	82 x 50 x 10 ³	4,10E+06	10 ⁻³ = 213	213 x 50 x 10 ³	1,07E+07	10 ⁻³ = 55	55 x 50 x 10 ³	2,75E+06	10 ⁻³ = 109	109 x 50 x 10 ³	5,45E+06
			1,33E+07			3,72E+06			7,13E+06			2,95E+06			3,92E+06
Transformation frequency	T titer		1,22E+03	T titer		3,35E+02	T titer		9,32E+02	T titer		3,00E+02	T titer		5,43E+02
	R titer		1,33E+07	R titer		3,72E+06	R titer		7,13E+06	R titer		2,95E+06	R titer		3,92E+06
			9,17E-05			9,01E-05			1,31E-04			1,02E-04			1,39E-04
Transformants (PVC A)	10 ⁰ = 91	(91 / 2) x 10	4,55E+02	10 ⁰ = 54	(54 / 2) x 10	2,70E+02	10 ⁰ = 107	(107 / 2) x 10	5,35E+02	10 ⁰ = 50	(50/2) x 10	2,50E+02	10 ⁰ = 101	(101/2) x 10	5,05E+02
	10 ⁰ = 118	(118 / 2) x 10	5,90E+02	10 ⁰ = 60	(60 / 2) x 10	3,00E+02	10 ⁰ = 215	(215 / 2) x 10	1,08E+03	10 ⁰ = 88	(88/2) x 10	4,40E+02	10 ⁰ = 112	(112/2) x 10	5,60E+02
	10 ⁰ = 140	(140 / 2) x 10	7,00E+02	10 ⁰ = 57	(57 / 2) x 10	2,85E+02	10 ⁰ = 225	(225 / 2) x 10	1,13E+03	10 ⁰ = 45	(45/2) x 10	2,25E+02	10 ⁰ = 380	(380/2) x 10	
			5,82E+02			2,85E+02			9,12E+02			3,05E+02			5,33E+02
Recipients (PVC A)	10 ⁻³ = 45	45 x 50 x 10 ³	2,25E+06	10 ⁻³ = 34	34 x 50 x 10 ³	1,70E+06	10 ⁻³ = 122	122 x 50 x 10 ³	6,10E+06	10 ⁻³ = 110	110 x 50 x 10 ³	5,50E+06	10 ⁻³ = 170	170 x 50 x 10 ³	8,50E+06
	10 ⁻³ = 104	104 x 50 x 10 ³	5,20E+06	10 ⁻³ = 11	11 x 50 x 10 ³		10 ⁻³ = 250	250 x 50 x 10 ³	1,25E+07	10 ⁻³ = 119	119 x 50 x 10 ³	5,95E+06	10 ⁻³ = 322	322 x 50 x 10 ³	
	10 ⁻³ = 71	71 x 50 x 10 ³	3,55E+06	10 ⁻³ = 32	32 x 50 x 10 ³	1,60E+06	10 ⁻³ = 244	244 x 50 x 10 ³	1,22E+07	10 ⁻³ = 74	74 x 50 x 10 ³	3,70E+06	10 ⁻³ = 123	123 x 50 x 10 ³	6,15E+06
			3,67E+06			1,65E+06			1,03E+07			5,05E+06			7,33E+06
Transformation frequency	T titer		5,82E+02	T titer		2,85E+02	T titer		9,12E+02	T titer		3,05E+02	T titer		5,33E+02
	R titer		3,67E+06	R titer		1,65E+06	R titer		1,03E+07	R titer		5,05E+06	R titer		7,33E+06
			1,59E-04			1,73E-04			8,88E-05			6,04E-05			7,27E-05
Transformants (PP)	10 ⁰ = 17	(17/2) x 10		10 ⁰ = 271	(271/2) x 10	1,36E+03	10 ⁰ = 142	(142 / 2) x 10	7,10E+02						
	10 ⁰ = 39	(39/2) x 10	1,95E+02	10 ⁰ = 442	(442/2) x 10		10 ⁰ = 123	(123 / 2) x 10	6,15E+02						
	10 ⁰ = 33	(33/2) x 10	1,65E+02	10 ⁰ = 270	(270/2) x 10	1,35E+03	10 ⁰ = 189	(189 / 2) x 10	9,45E+02						
			1,80E+02			1,35E+03			7,57E+02						
Recipients (PP)	10 ⁻³ = 31	31 x 50 x 10 ³	1,55E+06	10 ⁻³ = 90	90 x 50 x 10 ³	4,50E+06	10 ⁻³ = 60	60 x 50 x 10 ³	3,00E+06						
	10 ⁻³ = 35	35 x 50 x 10 ³	1,75E+06	10 ⁻³ = 168	168 x 50 x 10 ³	8,40E+06	10 ⁻³ = 73	73 x 50 x 10 ³	3,65E+06						
	10 ⁻³ = 23	23 x 50 x 10 ³		10 ⁻³ = 145	145 x 50 x 10 ³	7,25E+06	10 ⁻³ = 27	27 x 50 x 10 ³							
			1,65E+06			6,72E+06			3,33E+06						
Transformation frequency	T titer		1,80E+02	T titer		1,35E+03	T titer		7,57E+02						
	R titer		1,65E+06	R titer		6,72E+06	R titer		3,33E+06						
			1,09E-04			2,01E-04			2,28E-04						

Figure A 8: Raw data for the natural transformation of *A. baylyi* biofilms grown on microplastic polymers for 96 h. The green colour indicates the use of 20 μ L of sample, and the orange colour indicates the use of 200 μ L of sample. Transformant and recipient titers containing less than 30 and more than 300 colonies were removed from the raw data.

Mean		0 MP	10 MP	50 MP	200 MP
	HDPE	8,84E-05	3,21E-05	5,18E-05	5,63E-05
	HDPS	8,84E-05	7,01E-05	7,01E-05	7,14E-05
	PP	8,84E-05	1,62E-04	1,15E-04	7,47E-05
	PVC A	8,84E-05	6,89E-05	5,85E-05	5,44E-05
	PVC B	8,84E-05	1,07E-04	9,78E-05	9,88E-05
St.dev		0 MP	10 MP	50 MP	200 MP
	HDPE	5,51E-05	2,26E-05	1,78E-05	2,03E-05
	HDPS	5,51E-05	1,29E-05	3,17E-05	3,01E-05
	PP	5,51E-05	1,03E-04	7,48E-05	3,23E-06
	PVC A	5,51E-05	3,26E-05	2,88E-05	1,91E-05
	PVC B	5,51E-05	3,95E-05	4,08E-05	5,45E-05

Figure A 9: The mean and standard deviation for the natural transformation of *A. baylyi* under influence of different concentrations (0, 10, 50 and 200 MP) of the microplastic polymers HDPE, HDPS, PP, PVC A, and PVC B.

	PVC B	PVC A	PP
Mean	1,11E-04	1,11E-04	1,72E-04
St.dev	2,25E-05	5,15E-05	7,43E-05

Figure A 10: The mean and standard deviation of the natural transformation of *A. baylyi* biofilms grown on the microplastic polymers PVC B, PVC A and PP for 96 h.

